GENERATION OF INDEPENDENT COMPLEMENT RECEPTOR 1 AND COMPLEMENT RECEPTOR 2 KNOCKOUT MICE AND DEFINING THE ROLE OF COMPLEMENT RECEPTOR 1 IN HUMORAL IMMUNITY

by

Luke Robert Donius

A dissertation submitted to the faculty of
The University of Utah
in partial fulfillment of the requirements for the degree of

Doctor of Philosophy

in

Microbiology and Immunology

Department of Pathology

The University of Utah

December 2013

The University of Utah Graduate School

STATEMENT OF DISSERTATION APPROVAL

The dissertation of **Luke Robert Donius**

has been approved by the following supervisory committee members:

John H Weis	, Chair	**8/13/2013** Date Approved
Dean Tantin	, Member	**8/19/2013** Date Approved
Gregory S Hageman	, Member	**8/20/2013** Date Approved
Matthew A Mulvey	, Member	**8/19/2013** Date Approved
Gerald J Spangrude	, Member	**8/19/2013** Date Approved

and by **Peter E Jensen** , Chair of

the Department of **Pathology**

and by David B. Kieda, Dean of The Graduate School.

ABSTRACT

Complement receptor (Cr)1 and Cr2 have long been studied in relation to humoral immunity. These receptors are alternative splice variants of the murine *Cr2* gene, and all previous investigations of the effect of Cr1 and Cr2 on humoral immunity have been conducted utilizing mouse models deficient in both Cr1 and Cr2. To date, very little effort has been taken to delineate the functional roles of each receptor. The known molecular differences and independent transcription of Cr1 and Cr2 suggest a functional significance for each of these that should not be ignored. Additionally, I discovered that Cr1 and Cr2 are differentially expressed by follicular dendritic cells (FDCs) and B cells. It is shown here that B cells predominantly express Cr2, while Cr1 is the near exclusive *Cr2* product on FDCs. To investigate the independent roles of Cr1 and Cr2 in the context of an immune response, I generated two new mouse strains: *Cr1KO* and *Cr2KO*. The predominance of Cr1 on FDCs led to the hypothesis that Cr1 primarily functions in FDC promotion of germinal center (GC) reactions, which is likely mediated by the known complement-dependent deposition of immune complexes in follicles. Analysis of these new strains demonstrated that Cr1 and Cr2 have marked differences in their function in humoral immunity. In many cases, the B cell responses which are decreased in the Cr1/2-deficient mouse are unaffected in the Cr1-deficient mouse. It is shown that Cr1-deficiency on FDCs results in a significant reduction in the maintenance of GC B cells

and memory B cell production. Intriguingly, classically GC-independent responses, such as antigen-specific IgM and IgM memory B cells, are also reduced. However, B cell responses that cannot proceed through germinal centers, notably T-independent B cell responses, are not affected by Cr1-deficiency. In total, this work defines the Cr1KO and Cr2KO mouse lines as new models for the study of Cr1 and Cr2 in humoral immunity. In addition to its use in the study of the function of Cr1, the *Cr1KO* mouse is an invaluable tool in the investigation of GC biology.

TABLE OF CONTENTS

LIST OF FIGURES

LIST OF ABBREVIATIONS

Activation-induced cytidine deaminase…….AID

Class-switch recombination……...CSR

Complement component 3 knockout……...*C3KO*

Complement receptor 1 knockout……..*Cr1KO*

Complement receptor 2 knockout……..*Cr2KO*

Complement receptor 1 and 2 knockout…….*Cr1/2KO*

Complement receptor (human)…….CR

Complement receptor (mouse)……..Cr

Dark zone…….DZ

Days post-immunization……..dpi

Follicular dendritic cell……..FDC

Follicular……...FO

Germinal center……GC

Light zone…….LZ

Marginal zone……..MZ

Somatic hypermutation…….SHM

Wildtype……..WT

ACKNOWLEDGMENTS

I would like to thank my advisor John Weis for his mentorship and dedication to teaching me to be a solid scientist and to not be afraid to do experiments. His seemingly limitless ability to conceive questions has been an inspiration to aspire to. His patience with my growth from a novice scientist to a productive independent thinker has been appreciated.

I thank my thesis committee members Jerry Spangrude, Matt Mulvey, Greg Hageman, and Dean Tantin for their helpful guidance and feedback along the way. Their advice on when to maintain the course and when to cut my losses on a slow moving direction were constructive and invaluable.

I thank my girlfriend Mary for her supportive listening and critical feedback.

I thank all the friends that have provided welcome distractions in the form of mountain biking, skiing, football watching, fantasy football, whiskey drinking, and trips around the mountain west. I especially thank Alex my roommate for five years of easy going living conditions and captivating conversation on topics from science and politics to the finer points of music and football.

I would like to thank my parents, Bob and Kim Donius, whose general interest in the world around them instilled in me a desire to understand how things work. I also

thank them for their genes, love, and support that gave me the tools to get this far and guided me through the tougher days.

I also thank the current and past members of the joint Weis labs, the Department of Pathology, and the rest of the Utah community that have helped along the way but are too numerous to mention by name.

CHAPTER 1

INTRODUCTION

Activation of the complement system has long been accepted to bridge the rapid response of the innate immune system to the high specificity of the adaptive immune response (1). Complement activation results in the generation of complement component 3 (C3) products that covalently bond with microorganisms or antigen, effectively marking them as foreign. These tags, known as opsonins, facilitate recognition and phagocytosis by various complement receptors on immune cells. Binding of opsonized proteins in this manner leads to immune effects through complement receptor signaling, display for detection by other receptors, and phagocytic uptake. Utilization and regulation of this system is co-opted by B cells and follicular dendritic cells (FDCs) using complement receptors (Cr) 1 and 2 to enhance humoral immunity (2). Despite extensive work *in vitro* and the use of various *Cr2* null mice to determine the *in vivo* effects of Cr1/2, little is known about the independent roles of Cr1 and Cr2. It is also unknown why the shorter Cr2 form is generated from an alternative splice. Cr1, which is encoded by inclusion of all the exons of *Cr2*, contains all the binding domains that Cr2 also exhibits. To investigate the importance of these receptors independently, we generated two new mouse lines. In the first mutant strain, all the Cr1-specific exons were deleted. In the

second mutant strain, the alternatively spliced exons were fused to remove the alternative splice site required for Cr2.

The Complement Cascade

The complement cascade has many members, effectors, and three modes of initiation. The cascade can be generally simplified into three steps: initiation via foreign molecule recognition, activation of C3, and targeted destruction by membrane attack complex formation. In addition to this last textbook outcome of complement cascade activation, enhancement of many effector functions such as immune cell recruitment, phagocytosis, and humoral immunity occur (3).

Initiation of the complement cascade is achieved in three distinct manners: the classical, mannose-binding lectin, and alternative pathways. The classical pathway is so named because it was the first to be discovered. It is initiated when immunoglobulin binds cells bringing the complement activation domains of immunoglobulins into close proximity where they are able to recruit and form the cascade-activating C1 complex (3).

The C1 complex consists of the subunits C1qC1rC1s. Together these proteins initiate the complement cascade by cleaving C4 into C4b and C4a. C4b then binds with C2a (the major not minor portion of C2) and they become a C3 convertase (4, 5). C3 convertases are enzymatically active complement protein complexes (C3bBb or C4b2a) that cleave C3 into C3a and C3b (Figure 1.1). C3a, like the related molecule C5a, is a potent activation and recruitment molecule, known as an anaphylatoxin (6). C3b forms a covalent thioester bond with cells and antigens at the site of activation and has many functions. C3b itself may form a complex with the factor B protein, Bb, forming a new

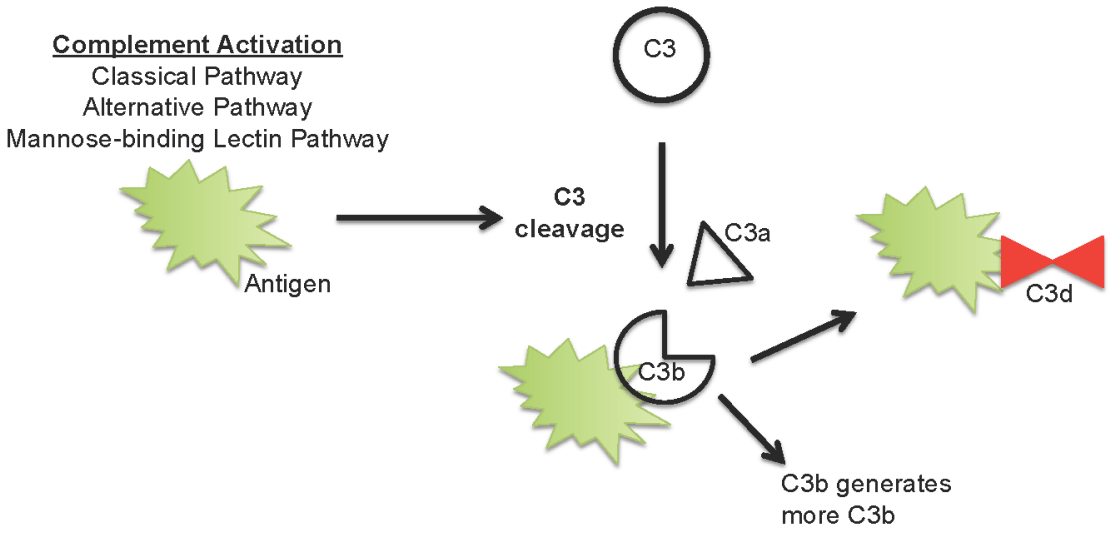

Figure 1.1. Initiation of all three complement pathways results in cleavage of C3 and covalent binding of C3b to the activating antigen. Antigen shown in green can be quickly detected by the complement pathways, resulting in the activation of the complement cascade and the opsonization of antigen by C3b via a thioester bond. Cleavage of the C3 protein also results in the release of the potent anaphylatoxin into the surrounding immune environment. C3b participation in C3 convertases facilitates the generation of more C3a and C3b. Regulatory proteins may further cleave C3d, resulting in inactivation of its C3 convertase activity but not altering its permanent bond with the antigen.

C3 convertase (5). In this way, C3b formation itself may act to begin a positive feedback loop and continuously generate more C3b and C3a. Additionally, C3b may be cleaved by regulatory proteins into iC3b and C3d. Reduction to these fragments abolishes their ability to take part in a C3 convertase complex but makes them available for various receptors: Cr1, Cr2, Cr3, and Cr4. Inclusion of an additional C3b in either C3 convertase complex generates a C5 convertase. C5 convertases generate C5a a potent anaphylatoxin, as well as the membrane attack complex, which is a pore forming complex made of complement proteins C5 through C9. Deposition of the membrane attack complex on cell membranes causes lysis of targeted cells.

The mannose-binding lectin pathway and alternative pathway are similar to the classical pathway after the activation of C3. The mannose-binding lectin pathway is however initiated by detection of the common bacterial cell component mannose, and the alternative pathway is initiated simply by spontaneous deposition and cleavage of C3 on cells and molecules that do not express protective regulatory proteins.

Complement Receptors 1 and 2

Cr1 and Cr2 (Cr will denote murine complement receptors and CR will denote human complement receptors) are capable of binding fragments of C3. Cr1 and Cr2 share a large portion of sequence in common due to their production as alternatively spliced transcripts from the same *Cr2* gene (Figure 1.2) (7). The additional exons included to make Cr1 encode the first six short consensus repeat (SCR) domains of the 21 that make up Cr1 (8). In humans, these exons have become pseudoexons (8); however, humans express a long and short isoform of *CR2*, CR2L and CR2S (9). SCRs 1-6 define Cr1 and

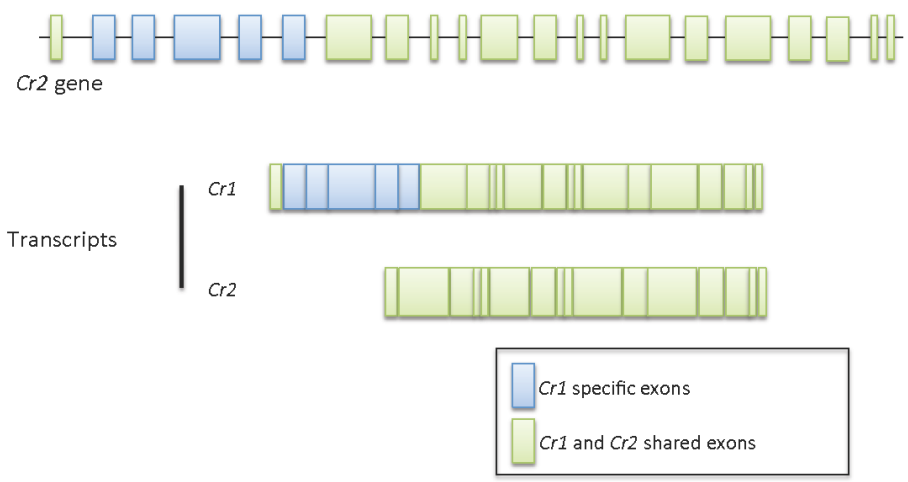

Figure 1.2. The *Cr2* gene encodes two splice variants, Cr1 and Cr2. Splicing of all the exons including those shown in blue into the final transcript generates Cr1. The exons in blue are excluded to generate Cr2.

include sites with binding specificity for C3b (Figure 1.3) as well as for factor I, which is the enzyme that cleaves C3b into iC3b or C3d(g) (10-12). In contrast, Cr2 binds C3d(g) and iC3b (Figure 1.3) (12, 13). To some extent, Cr2 binds C3b as well as C3d(g) and iC3b, but the affinity for the latter two is tremendously greater (13). Cr1 contains all the domains within Cr2 and should bind all the above fragments of C3; however, it has never been tested if any subtle secondary structure differences affect the C3d(g) and iC3b binding affinity of Cr1.

Extensive *in vitro* studies have elucidated the role of Cr2 as the B cell co-receptor (14-17). These studies determined that Cr2 is organized into a signaling complex with CD19 and CD81 and that binding of complement-bound immune complexes by Cr2 enhances the response of B cell receptor stimulation (BCR) (17). Cr2 alone does not initiate an intracellular signaling cascade, but instead when bound by C3d(g) or iC3b (referred to as just C3d from here on) bound antigen initiates signaling via CD19 (18). CD81 and other proteins organize the complex. These members associate and together make up the B cell co-receptor (Figure 1.4). Although direct testing of mouse Cr2 amplification of BCR signaling is less extensive than that shown for human CR2, the parallel function of the two is widely accepted. Amplification has been directly shown by Chakravarty *et al.* 2002 (19) and the close homology of CR2 and CD19 between their respective murine and primate counterparts suggests a conservation of function (7, 20). Additionally, immunoprecipitation of CR2 (human/mouse) or CD19 from transfected immortal A20 mouse B cells co-precipitates the entire CR2-CD19-CD81 B cell co-receptor complex (21).

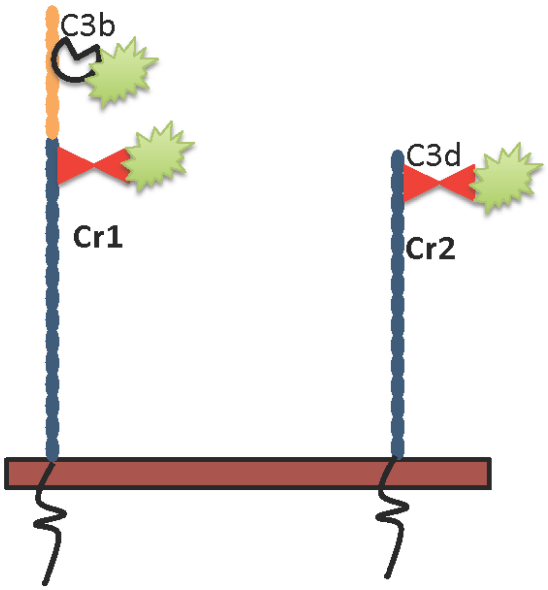

Figure 1.3. Respective C3b and C3d (as well as C3d(g) and iC3b) binding regions on Cr1 and Cr2. Cr1 also binds and acts as a cofactor for the protease factor I which converts C3b to C3d/C3d(g)/iC3b.

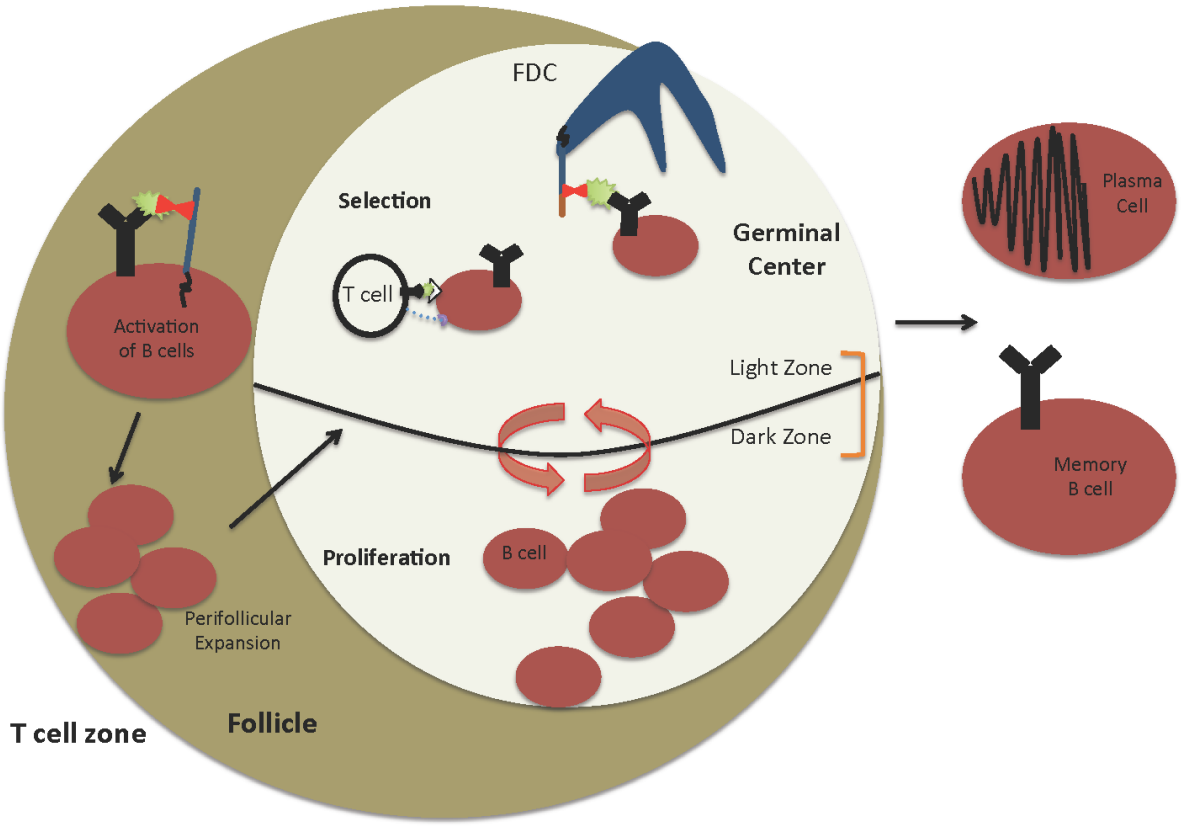

Figure 1.4. Follicle and GC organization. Upon antigen encounter within the B cell follicle, B cells migrate to the perifollicular region at the border of the follicle-T cell zone. These B cells then expand before migrating back to the region around the FDCs and generating a GC. GC B cells then cycle back and forth between periods of proliferation in the dark zone and periods of selection among T cells and FDCs in the light zone. GCs output highly specific often class-switched memory B cells and plasma cells.

Cr1 and Cr2 binding differences are at the root of the general overarching question of this thesis. In light of the fact that all C3 fragments that bind Cr2 also bind Cr1, it is interesting that Cr2 is produced independently of Cr1. The independent nature of Cr1 and Cr2 have generally been ignored by all current research. The few exceptions include the identification of a generally inflamed splenic microenvironment of *Cr1/2KO* mice (22), identification of an excessive cytokine response by *Cr1/2KO* mice following adenovirus infection (23), and a demonstration that transgenic expression of human CR2 in *Cr1/2KO* mice rescues antibody production deficiencies (24). However, these studies did not definitively establish the effects of Cr1- or Cr2-deficiency independently. The first two studies used *Cr1/2KO* mice. The third set of studies were performed on three independent human CR2 transgenic mice that were generated on a *Cr2-/-* background (note the *Cr2-/-* is a *Cr2*-null (25) but not the same as the *Cr1/2KO* (26)). These model mice all had various disadvantages. The first mouse was created by inserting CR2 with its endogenous human CR2 promoter and never produced high levels of CR2 (21). The second mouse transgenically expressed CR2 under the immunoglobulin lambda chain promoter and resulted in premature expression of CR2 during development of B cells. This premature expression caused a partial block in B cell development at the pro-B cell stage (27, 28). A third mouse was successfully generated in which CR2 was expressed at an appropriate stage and in appropriate quantities for mouse and human comparisons (24). As intriguing as these mice are for investigations of human CR2, they, like the original two, do not allow for the definitive study of Cr1-deficiency because human CR2 is not expressed in its autochthonous environment and cannot be assumed to be filling the roles of mouse Cr2. Additionally, a CR1 transgenic mouse, in which CR1 is driven by the

lamda light chain promoter, was created on the *Cr2-/-* mouse strain (29). The expression of CR1 in this mouse line by the lamda chain promoter drives expression in B cells but likely fails to drive expression in FDCs, which is the opposite of Cr1 in mice. Again this is an intriguing model for the study of CR1 in mice, but I would argue it is not truly an analogous replacement of Cr1. In the absence of previous tools or direct studies, we generated the independent Cr1 and Cr2 knockout mice (*Cr1KO* and *Cr2KO*) in order to assess the effects mediated by complement and these receptors on humoral immunity.

B cells and Humoral Immunity

Interest in Cr1 and Cr2 is generated by their selective expression on FDCs and B cells. B cells are the cells that are singularly responsible for the production of antibodies. Each B cell produces antibody, or immunoglobulin, of one specificity. Through a process known as VDJ rearrangement, B cells as a group produce a nearly unlimited number of antigen-specific immunoglobulin possibilities (30). The repertoire of specificities is limited more by the number of cells in an organism than by the repertoire possibilities. B cells that respond to antigen can in some cases undergo a process known as somatic hypermutation (SHM), a process by which mutations are directed to the coding sequences of the immunoglobulin binding regions (31). Targeted SHM is dependent on the mutation-generating enzyme activation-induced cytidine deaminase (AID). SHM provides a B cell with new immunoglobulin specificity that may in fact have a higher affinity than the original immunoglobulin.

There are two main categories of B cells: the innate like B1 cells and the B2 cells that undergo processes in order to produce highly specific and diverse antibodies. B1

cells are an interesting set of B cells that have recently undergone a surge of interest, which has expanded our knowledge of their role in immunity. There are two subsets of B1 cells: B1a and B1b (32). Functionally, B1a cells produce natural antibody (32) and B1b cells are responsible for producing T-independent antigen memory (33, 34). B1a cells are also dependent on Cr2-CD19 signaling for their development. Both reduction and deletion of *Cr2* result in a reduction of the number of B1a cells in mice ((35) and Figure 3.3). The *Cr1/2KO* mouse has been shown to have depressed natural antibody titers and this has been used to explain the *Cr1/2KO* mouse resistance to ischemia reperfusion injury (ischemia reperfusion injury is a disease mediated at least in part by natural antibody targeting of complement activation to apoptotic tissues (36, 37)). However, it has also been suggested that the effect may be due to a non-C3 ligand effect such as desensitization due to CD19 overexpression (38). It was these findings that led us to ask if Cr1 was required for B1a cell development or whether the off target effects of CD19 overexpression alone resulted in B1a loss and natural antibody reduction. The roles of Cr1 and Cr2 in B1 cells and natural antibody production are tested and discussed in Chapter 3.

A subset of B2 cells known as marginal zone (MZ) B cells are found within the spleen. As their name suggests, MZ B cells are found in the MZ of the spleen (39). The MZ is the compartment within the spleen in which blood from arterioles is first delivered. The nature of the MZ is such that cells present there are constantly bathed in any blood-borne antigen. The location of MZ B cells is consistent with their major function of responding with “innate” like quickness to blood borne pathogens. Like B1 cells, MZ B cells have a lower and broader immunoglobulin affinity repertoire. Similar to follicular B

cells (FO B cells), MZ B cells are capable of undergoing extensive class switch recombination (CSR), a process by which immunoglobulin specificity is maintained but the effector region is changed (40). In MZ B cells, CSR predominantly targets switching to IgG3 and some IgG2a (41, 42). MZ B cells are conventionally understood to respond quickly to T-independent antigens, especially repetitive type 2 antigens (TI-2) (39, 43). To a limited extent, MZ B cells are capable of taking part in germinal center reactions (GCs) and undergoing SHM (44). Typical TI-2 antigens, such as polysaccharides, are highly repetitive molecules capable of eliciting massive B cell receptor (BCR) crosslinking on single cells. Another important property of TI-2 antigens is that they are not peptide based and therefore cannot be presented by major histocompatibility-II complexes (MHC-II) to elicit T cell help. A well-documented instance of the importance of the response to TI-2 antigen is the MZ B cell response to polysaccharides, such as those that make up the capsule of the pathogen *Streptococcus pneumoniae* (*S. pneumoniae*) (39, 41). The virulence of *S. pneumoniae* is strongly determined by the polysaccharide capsule, of which nearly 100 variants have been described (45). The importance of MZ B cells and neutralization of the capsule combined with the late formation of the marginal zone in humans (~2 years of age) is likely the reason that young children are particularly susceptible to *S. pneumoniae* infections (39). *Cr1/2KO* mice have been found to exhibit significantly reduced antibody responses to TI-2 antigens and *S. pneumoniae* (26). These mice also survive infection with *S. pneumoniae* at considerably lower rates than wildtype (WT) (26, 46). The marked effects of Cr1/2 deficiency on TI-2 antigens led us to investigate the effect of Cr1-deficiency on these responses using the *Cr1KO* mouse strain (Chapter 3).

FO B cells are highly migratory B cells that conventionally respond to peptide based T-dependent (TD; T cell/Thymus-dependent) antigen, take part in germinal center reactions, and are the precursors of high affinity and long-term memory effectors. They constantly migrate between lymph nodes and the spleen to increase their chances of encountering antigen. The progression from a naïve FO B cell to mature long-term memory B cell or high affinity antibody-producing plasma cell requires antigen recognition, perifollicular expansion of antigen specific B cells, and coordinated expansion and selection in GCs. Fate determination as a memory or plasma cell must also occur and despite its major importance is still a very poorly understood phenomenon.

Antigen recognition by FO B cells

Within any given mouse, antigen-specific B cells are found relatively infrequently (~1000s-10,000s) (47). In order to raise the chances of FO B cell encounter with antigen, the immune system is organized to concentrate antigen in sites where FO B cells are present or frequently visiting. In a snapshot of FO B cell localization, one would find B cells mostly in peripheral immune tissues. However, FO B cells are in fact highly motile and a single mature FO B cell spends only about a day in any given peripheral immune organ (48). Exit from the lymph/blood and trafficking to the follicles is guided by CXCR5 detection of the chemokine CXCL13. Within the follicles, FO B cells may encounter antigen displayed on the surface of subcapsular macrophages, dendritic cells, and FDCs (48). Soluble and small particulate antigen may be captured by dendritic cells or subcapsular macrophages and trafficked to follicles, or it may diffuse into the follicles via conduits (49, 50). Capture, detection, and response to soluble antigens is greatly

enhanced by the presence of antibody, while larger particulate antigens are readily captured and deposited in follicles in the absence of antibody (51). The role of FDCs and Cr as major contributors of antigen display is well established but poorly understood. Use of the *Cr1KO* to ask questions about humoral immunity in the absence of Cr on FDCs is addressed in Chapters 3 and 4.

Perifollicular expansion

In the current model of a B cell response to TD antigen, FO B cells that have been activated by their cognate antigen upregulate the receptors EBI2 and CCR7 and traffic to the follicle perimeter at the border with the adjacent T cell zone (52, 53). It is here that a large pool of clones of antigen-specific B cells is initially generated in conjunction with the help of T cell (Figure 1.4). The expansion of these cells presumably provides "individuals" to select from during the initial stages of the GC reactions. These clones exhibit limited CSR and no SHM before they are recruited to GCs at about four or five days (54).

Germinal centers

GCs are conventionally understood to be the organized sites where B cells undergo SHM after activation by their cognate antigen. Surprisingly, much of the biology of GCs is still poorly understood. A role for GCs that faces little dispute is their importance in affinity maturation. Many studies demonstrate some GC-independent pathways for CSR, large antibody responses, and memory B cell generation. However,

essentially no evidence of affinity maturation in the absence of GCs has been demonstrated (55-57). It is within GCs that GC B cells go through cycles of AID-driven SHM, clonal expansion, and testing of the newly mutated immunoglobulin (55-57). Presumably, this testing occurs against the antigen retained on the FDCs; however, this is an open topic of research (58). These GC B cells consist of the FO B cells initially generated in the perifollicular region. Within the GC, two zones have long been recognized by their visibly two-toned appearance. The light zone (LZ) contains cells that have been classically called centrocytes (55). These GC B cells are in close contact with FDCs and interact frequently with GC T cells (Figure 1.4). In contrast, the dark zone (DZ) is characterized by the presence of B cells, classically termed centroblasts (55). These cells are highly proliferative and endow the dark zone with its darker color due to their high DNA content. Recently, the GC B cells in the light zone and dark zone were demonstrated to be distinguishable by their differential expression of the markers CXCR4, CD83, and CD86 (59). In general, the centrocyte and centroblast terms overlap with the LZ B cell and DZ B cell marker, cell cycle, and AID phenotypes.

Memory B cells and plasma cells

Generally, it has been found that much of the long-term memory and long-lived plasma cell output is through a GC-dependent pathway, and that most of these cells exhibit switched immunoglobulin from IgM to IgG, IgA, or IgE (40). Portions of this model, however, are unknown or are found to be heterogeneous in nature. Recent evidence suggests that even the long held belief that IgM^+ cells are not GC-derived and IgG positive cells are GC-derived is generally true only for the latter. Multiple groups

have shown a collection of both GC-independent and GC-dependent IgM^+ memory B cells (60-62). Furthermore, the mechanisms of memory B cell and plasma cell fate determination are poorly understood. Three possible mechanisms for fate determination have been suggested: inherent B cell receptor signaling differences, environmental differences including T cell/FDC input, and a temporal switch that may shift the output of the GC (63). Experiments investigating the effect of Cr1-deficiency on GC output are discussed in Chapter 4. Additionally, utilization of the *Cr1KO* mouse as a tool to investigate these mechanisms of fate determination is discussed in Chapter 4 as well as in the Summary and Conclusion.

Follicular Dendritic Cells

FDCs are centrally located in B cell follicles and upon formation of GCs take a prominent position in the LZ (64). The current model of FDC function is one in which they define the follicle, concentrate antigen on their surface for surveillance, produce adhesion molecules that enhance B cell interactions, and secrete cytokines to promote B cell survival (Figure 1.4). Recently, the importance of FDCs was demonstrated by deletion of FDCs at the initiation of GCs. This study showed that FDC ablation significantly reduced GCs and resulted in disorganization of both the T zone and follicles (65). Important FDC genes were reduced or lost from peripheral immune tissue after FDC ablation as well. Most notable of these was the B cell recruitment chemokine CXCL13. The importance of FDCs has also been demonstrated by the loss of B cell organization and GC formation in the absence of the stromal produced B cell survival factors lymphotoxin, TNF, or IKK (66, 67).

Antigen retention is one of the major functions of FDCs and its complement dependence makes it of particular interest here. Early studies discovered that iodinated proteins quickly became deposited on cells in follicles and germinal centers (68, 69). Later, the antigen was shown to be deposited on FDCs as immune complexes termed at the time iccosomes (70, 71). This immune complex trapping in primary immune follicles was determined to be dependent on complement and expression of a product of the *Cr2* gene (72). This same study determined that secondary immune follicle trapping of immune complexes could occur in an FcγIIRB receptor-dependent manner. More recently, it was shown that Fc receptors are not prevalent until immunization causes their upregulation (73), highlighting the importance of Cr in the capture of antigen in the primary response. The advent of knockout mouse technology and the engineering of mice with *Cr2* gene mutations led to extensive studies of complement receptors on FDCs just as it had for B cells (2, 74). These studies demonstrated the requirement of Cr for deposition of antigen on FDCs. Chapter 3 defines the novel finding of the Cr1 predominance over Cr2 on FDCs. This prompted the hypothesis tested in Chapter 4 that Cr1 on FDCs is required for the proper maturation of GC B cells and GC-derived effectors.

Summary

The importance of complement as an endogenous adjuvant has been well known for the last 40 years (1). Defining of the Cr1/2 complement-binding domains (11, 13) and the unprecedented mapping of CR2's B cell co-receptor function (15-18) provided a solid foundation for the *in vivo* studies that followed. These *in vivo* studies began with the

generation of multiple *Cr2*$^{-/-}$ mice (25, 26) and a *Cr2* hypomorphic mouse (35) which demonstrated the dramatic influence of both B cell- and FDC-expressed Cr on humoral immunity. I hypothesized, however, that Cr1 and Cr2 have distinct functions in the bridging of complement detection of antigen to humoral immunity. To investigate these independent functions, we engineered two new mouse strains specifically deficient in either Cr2 or Cr1: the *Cr2KO* and *Cr1KO* mice (Chapters 2 and 3/4, respectively). Despite the established role of Cr2 as a member of the B cell co-receptor complex and multiple studies that attributed B cell response deficiencies to Cr2 co-receptor function, it had always been an outstanding question as to why Cr1 could not fill this role by itself. In Chapter 2, I describe the generation and characterization of the *Cr2KO* mouse strain to investigate this question. In Chapter 3, I describe the generation of the *Cr1KO* mouse strain and the previously unappreciated differential expression of Cr1 between B cells and FDCs. The role of Cr1 is tested in relation to B1, MZ B, and FO B cell populations. Previously identified phenotypes in the *Cr1/2KO* and *C3KO* mouse strains are utilized to compare the requirements of Cr1 and Cr2. Humoral immune deficiencies consistent with an FDC-based role for Cr1 are elucidated, which lead to the investigation in Chapter 4 of the requirement for FDC-expressed Cr1 in GC B cell dynamics and memory B cell generation. In this chapter, I elaborate on the extent of the GC deficiencies found in the *Cr1KO* mouse strain. In total, the work described here characterizes two new mouse models that provide strong evidence for the important and independent roles of Cr1 and Cr2, with special attention given to Cr1. Analysis of the *Cr1KO* strain further opens up avenues for research involving the differences of early versus late GC B cells, the importance of antigen retention on affinity, the role for Cr1 on FDC cellular functions,

and the effect of GC B cell numbers on immune outcome. Additionally, these studies uncovered obvious parallels between Cr1 and CR2L and suggest that an understanding of Cr1 functions may uncover mechanisms for targeted enhancement of immunizations.

References

1. Pepys, M. B. 1974. Role of complement in induction of antibody production in vivo. Effect of cobra factor and other C3-reactive agents on thymus-dependent and thymus-independent antibody responses. *J. Exp. Med.* 140: 126–145.

2. Carroll, M. C., and D. E. Isenman. 2012. Regulation of humoral immunity by complement. *Immunity* 37: 199–207.

3. Walport, M. J. 2001. Complement. First of two parts. *N. Engl. J. Med.* 344: 1058–1066.

4. Sjöberg, A. P., L. A. Trouw, and A. M. Blom. 2009. Complement activation and inhibition: a delicate balance. *Trends Immunol.* 30: 83–90.

5. Zipfel, P. F., and C. Skerka. 2009. Complement regulators and inhibitory proteins. *Nat. Rev. Immunol.* 9: 729–740.

6. Guo, R.-F., and P. A. Ward. 2005. Role of C5a in inflammatory responses. *Annu. Rev. Immunol.* 23: 821–852.

7. Kurtz, C. B., M. S. Paul, M. Aegerter, J. J. Weis, and J. Weis. 1989. Murine complement receptor gene family. II. Identification and characterization of the murine homolog (Cr2) to human CR2 and its molecular linkage to Crry. *J. Immunol.* 143: 2058–2067.

8. Holguin, M. H., C. B. Kurtz, C. J. Parker, J. J. Weis, and J. Weis. 1990. Loss of human CR1- and murine Crry-like exons in human CR2 transcripts due to CR2 gene mutations. *J. Immunol.* 145: 1776–1781.

9. Liu, Y. J., J. Xu, O. de Bouteiller, C. L. Parham, G. Grouard, O. Djossou, B. de Saint-Vis, S. Lebecque, J. Banchereau, and K. W. Moore. 1997. Follicular dendritic cells specifically express the long CR2/CD21 isoform. *J. Exp. Med.* 185: 165–170.

10. Kinoshita, T., S. Lavoie, and V. Nussenzweig. 1985. Regulatory proteins for the activated third and fourth components of complement (C3b and C4b) in mice. II. Identification and properties of complement receptor type 1 (CR1). *J. Immunol.* 134: 2564–2570.

11. Molina, H., T. Kinoshita, C. B. Webster, and V. M. Holers. 1994. Analysis of C3b/C3d binding sites and factor I cofactor regions within mouse complement receptors 1 and 2. *J. Immunol.* 153: 789–795.

12. Kalli, K. R., and D. T. Fearon. 1994. Binding of C3b and C4b by the CR1-like site in murine CR1. *J. Immunol.* 152: 2899–2903.

13. Pramoonjago, P., J. Takeda, Y. U. Kim, K. Inoue, and T. Kinoshita. 1993. Ligand specificities of mouse complement receptor types 1 (CR1) and 2 (CR2) purified from spleen cells. *Int. Immunol.* 5: 337–343.

14. Carter, R. H., M. O. Spycher, Y. C. Ng, R. Hoffman, and D. T. Fearon. 1988. Synergistic interaction between complement receptor type 2 and membrane IgM on B lymphocytes. *J. Immunol.* 141: 457–463.

15. Matsumoto, A. K., J. Kopicky-Burd, R. H. Carter, D. A. Tuveson, T. F. Tedder, and D. T. Fearon. 1991. Intersection of the complement and immune systems: a signal transduction complex of the B lymphocyte-containing complement receptor type 2 and CD19. *J. Exp. Med.* 173: 55–64.

16. Matsumoto, A. K., D. R. Martin, R. H. Carter, L. B. Klickstein, J. M. Ahearn, and D. T. Fearon. 1993. Functional dissection of the CD21/CD19/TAPA-1/Leu-13 complex of B lymphocytes. *J. Exp. Med.* 178: 1407–1417.

17. Carter, R. H., and D. T. Fearon. 1992. CD19: lowering the threshold for antigen receptor stimulation of B lymphocytes. *Science* 256: 105–107.

18. Tedder, T. F., M. Inaoki, and S. Sato. 1997. The CD19-CD21 complex regulates signal transduction thresholds governing humoral immunity and autoimmunity. *Immunity* 6: 107–118.

19. Chakravarty, L., M. D. Zabel, J. J. Weis, and J. Weis. 2002. Depletion of Lyn kinase from the BCR complex and inhibition of B cell activation by excess CD21 ligation. *Int. Immunol.* 14: 139–146.

20. Tedder, T. F., and C. M. Isaacs. 1989. Isolation of cDNAs encoding the CD19 antigen of human and mouse B lymphocytes. A new member of the immunoglobulin superfamily. *J. Immunol.* 143: 712–717.

21. Marchbank, K. J., C. C. Watson, D. F. Ritsema, and V. M. Holers. 2000. Expression of human complement receptor 2 (CR2, CD21) in Cr2-/- mice restores humoral immune function. *J. Immunol.* 165: 2354–2361.

22. Jacobson, A. C., J. J. Weis, and J. Weis. 2008. Complement receptors 1 and 2 influence the immune environment in a B cell receptor-independent manner. *J.*

Immunol. 180: 5057–5066.

23. Seregin, S. S., Y. A. Aldhamen, D. M. Appledorn, N. J. Schuldt, A. J. McBride, M. Bujold, S. S. Godbehere, and A. Amalfitano. 2009. CR1/2 is an important suppressor of Adenovirus-induced innate immune responses and is required for induction of neutralizing antibodies. *Gene Ther.* 16: 1245–1259.

24. Kulik, L., K. Chen, B. T. Huber, and V. M. Holers. 2011. Human complement receptor type 2 (CR2/CD21) transgenic mice provide an in vivo model to study immunoregulatory effects of receptor antagonists. *Mol. Immunol.* 48: 883–894.

25. Molina, H., V. M. Holers, B. Li, Y. Fung, S. Mariathasan, J. Goellner, J. Strauss-Schoenberger, R. W. Karr, and D. D. Chaplin. 1996. Markedly impaired humoral immune response in mice deficient in complement receptors 1 and 2. *Proc. Natl. Acad. Sci. USA* 93: 3357–3361.

26. Haas, K. M., M. Hasegawa, D. A. Steeber, J. C. Poe, M. D. Zabel, C. B. Bock, D. R. Karp, D. E. Briles, J. Weis, and T. F. Tedder. 2002. Complement receptors CD21/35 link innate and protective immunity during Streptococcus pneumoniae infection by regulating IgG3 antibody responses. *Immunity* 17: 713–723.

27. Marchbank, K. J., L. Kulik, M. G. Gipson, B. P. Morgan, and V. M. Holers. 2002. Expression of human complement receptor type 2 (CD21) in mice during early B cell development results in a reduction in mature B cells and hypogammaglobulinemia. *J. Immunol.* 169: 3526–3535.

28. Kulik, L., K. J. Marchbank, T. Lyubchenko, K. A. Kuhn, G. A. Liubchenko, C. Haluszczak, M. G. Gipson, M. G. Gibson, S. A. Boackle, and V. M. Holers. 2007. Intrinsic B cell hypo-responsiveness in mice prematurely expressing human CR2/CD21 during B cell development. *Eur. J. Immunol.* 37: 623–633.

29. Pappworth, I. Y., C. Hayes, J. Dimmick, B. P. Morgan, V. M. Holers, and K. J. Marchbank. 2012. Mice expressing human CR1/CD35 have an enhanced humoral immune response to T-dependent antigens but fail to correct the effect of premature human CR2 expression. *Immunobiology* 217: 147–157.

30. Teng, G., and F. N. Papavasiliou. 2007. Immunoglobulin somatic hypermutation. *Annu. Rev. Genet.* 41: 107–120.

31. Maizels, N. 2005. Immunoglobulin gene diversification. *Annu. Rev. Genet.* 39: 23–46.

32. Baumgarth, N. 2011. The double life of a B-1 cell: self-reactivity selects for protective effector functions. *Nat. Rev. Immunol.* 11: 34–46.

33. Haas, K. M., J. C. Poe, D. A. Steeber, and T. F. Tedder. 2005. B-1a and B-1b cells

exhibit distinct developmental requirements and have unique functional roles in innate and adaptive immunity to S. pneumoniae. *Immunity* 23: 7–18.

34. Alugupalli, K. R., J. M. Leong, R. T. Woodland, M. Muramatsu, T. Honjo, and R. M. Gerstein. 2004. B1b lymphocytes confer T cell-independent long-lasting immunity. *Immunity* 21: 379–390.

35. Ahearn, J. M., M. B. Fischer, D. Croix, S. Goerg, M. Ma, J. Xia, X. Zhou, R. G. Howard, T. L. Rothstein, and M. C. Carroll. 1996. Disruption of the Cr2 locus results in a reduction in B-1a cells and in an impaired B cell response to T-dependent antigen. *Immunity* 4: 251–262.

36. Williams, J. P., T. T. Pechet, M. R. Weiser, R. Reid, L. Kobzik, F. D. Moore, M. C. Carroll, and H. B. Hechtman. 1999. Intestinal reperfusion injury is mediated by IgM and complement. *J. Appl. Physiol.* 86: 938–942.

37. Fleming, S. D., T. Shea-Donohue, J. M. Guthridge, L. Kulik, T. J. Waldschmidt, M. G. Gipson, G. C. Tsokos, and V. M. Holers. 2002. Mice deficient in complement receptors 1 and 2 lack a tissue injury-inducing subset of the natural antibody repertoire. *J. Immunol.* 169: 2126–2133.

38. Woods, K. M., M. R. Pope, S. M. Hoffman, and S. D. Fleming. 2011. CR2+ marginal zone B cell production of pathogenic natural antibodies is C3 independent. *J. Immunol.* 186: 1755–1762.

39. Martin, F., and J. F. Kearney. 2002. Marginal-zone B cells. *Nat. Rev. Immunol.* 2: 323–335.

40. Xu, Z., H. Zan, E. J. Pone, T. Mai, and P. Casali. 2012. Immunoglobulin class-switch DNA recombination: induction, targeting and beyond. *Nat. Rev. Immunol.* 12: 517–531.

41. Guinamard, R., M. Okigaki, J. Schlessinger, and J. V. Ravetch. 2000. Absence of marginal zone B cells in Pyk-2-deficient mice defines their role in the humoral response. *Nat. Immunol.* 1: 31–36.

42. Zheng, Y., M. Yu, A. Podd, L. Yuan, D. K. Newman, R. Wen, G. Arepally, and D. Wang. 2013. Critical role for mouse marginal zone B cells in PF4/heparin antibody production. *Blood* 121: 3484–3492.

43. Martin, F., A. M. Oliver, and J. F. Kearney. 2001. Marginal zone and B1 B cells unite in the early response against T-independent blood-borne particulate antigens. *Immunity* 14: 617–629.

44. Phan, T. G., S. Gardam, A. Basten, and R. Brink. 2005. Altered migration, recruitment, and somatic hypermutation in the early response of marginal zone B

cells to T cell-dependent antigen. *J. Immunol.* 174: 4567–4578.

45. Yother, J. 2011. Capsules of Streptococcus pneumoniae and other bacteria: paradigms for polysaccharide biosynthesis and regulation. *Annu. Rev. Microbiol.* 65: 563–581.

46. Haas, K. M., J. C. Poe, and T. F. Tedder. 2009. CD21/35 promotes protective immunity to Streptococcus pneumoniae through a complement-independent but CD19-dependent pathway that regulates PD-1 expression. *J. Immunol.* 183: 3661–3671.

47. Pape, K. A., J. J. Taylor, R. W. Maul, P. J. Gearhart, and M. K. Jenkins. 2011. Different B cell populations mediate early and late memory during an endogenous immune response. *Science* 331: 1203–1207.

48. Cyster, J. G. 2010. B cell follicles and antigen encounters of the third kind. *Nat. Immunol.* 11: 989–996.

49. Roozendaal, R., T. R. Mempel, L. A. Pitcher, S. F. Gonzalez, A. Verschoor, R. E. Mebius, U. H. von Andrian, and M. C. Carroll. 2009. Conduits mediate transport of low-molecular-weight antigen to lymph node follicles. *Immunity* 30: 264–276.

50. Gonzalez, S. F., S. E. Degn, L. A. Pitcher, M. Woodruff, B. A. Heesters, and M. C. Carroll. 2011. Trafficking of B cell antigen in lymph nodes. *Annu. Rev. Immunol.* 29: 215–233.

51. Link, A., F. Zabel, Y. Schnetzler, A. Titz, F. Brombacher, and M. F. Bachmann. 2012. Innate immunity mediates follicular transport of particulate but not soluble protein antigen. *J. Immunol.* 188: 3724–3733.

52. Pereira, J. P., L. M. Kelly, Y. Xu, and J. G. Cyster. 2009. EBI2 mediates B cell segregation between the outer and centre follicle. *Nature* 460: 1122–1126.

53. Green, J. A., and J. G. Cyster. 2012. S1PR2 links germinal center confinement and growth regulation. *Immunol. Rev.* 247: 36–51.

54. Coffey, F., B. Alabyev, and T. Manser. 2009. Initial clonal expansion of germinal center B cells takes place at the perimeter of follicles. *Immunity* 30: 599–609.

55. MacLennan, I. C. 1994. Germinal centers. *Annu. Rev. Immunol.* 12: 117–139.

56. Victora, G. D., and M. C. Nussenzweig. 2012. Germinal centers. *Annu. Rev. Immunol.* 30: 429–457.

57. Shlomchik, M. J., and F. Weisel. 2012. Germinal centers. *Immunol. Rev.* 247: 5–10.

58. Haberman, A. M., and M. J. Shlomchik. 2003. Reassessing the function of immune-complex retention by follicular dendritic cells. *Nat. Rev. Immunol.* 3: 757–764.

59. Victora, G. D., T. A. Schwickert, D. R. Fooksman, A. O. Kamphorst, M. Meyer-Hermann, M. L. Dustin, and M. C. Nussenzweig. 2010. Germinal center dynamics revealed by multiphoton microscopy with a photoactivatable fluorescent reporter. *Cell* 143: 592–605.

60. Dogan, I., B. Bertocci, V. Vilmont, F. Delbos, J. Mégret, S. Storck, C.-A. Reynaud, and J.-C. Weill. 2009. Multiple layers of B cell memory with different effector functions. *Nat. Immunol.* 10: 1292–1299.

61. Taylor, J. J., K. A. Pape, and M. K. Jenkins. 2012. A germinal center-independent pathway generates unswitched memory B cells early in the primary response. *J. Exp. Med.* 209: 597–606.

62. Taylor, J. J., M. K. Jenkins, and K. A. Pape. 2012. Heterogeneity in the differentiation and function of memory B cells. *Trends Immunol.* 33: 590–597.

63. Shlomchik, M. J., and F. Weisel. 2012. Germinal center selection and the development of memory B and plasma cells. *Immunol. Rev.* 247: 52–63.

64. Allen, C. D. C., and J. G. Cyster. 2008. Follicular dendritic cell networks of primary follicles and germinal centers: phenotype and function. *Semin. Immunol.* 20: 14–25.

65. Wang, X., B. Cho, K. Suzuki, Y. Xu, J. A. Green, J. An, and J. G. Cyster. 2011. Follicular dendritic cells help establish follicle identity and promote B cell retention in germinal centers. *J. Exp. Med.* 208: 2497–2510.

66. Fu, Y. X., and D. D. Chaplin. 1999. Development and maturation of secondary lymphoid tissues. *Annu. Rev. Immunol.* 17: 399–433.

67. Victoratos, P., J. Lagnel, S. Tzima, M. B. Alimzhanov, K. Rajewsky, M. Pasparakis, and G. Kollias. 2006. FDC-specific functions of p55TNFR and IKK2 in the development of FDC networks and of antibody responses. *Immunity* 24: 65–77.

68. Nossal, G. J., A. Abbot, J. Mitchell, and Z. Lummus. 1968. Antigens in immunity. XV. Ultrastructural features of antigen capture in primary and secondary lymphoid follicles. *J. Exp. Med.* 127: 277–290.

69. Hanna, M. G., and A. K. Szakal. 1968. Localization of 125I-labeled antigen in germinal centers of mouse spleen: histologic and ultrastructural autoradiographic studies of the secondary immune reaction. *J. Immunol.* 101: 949–962.

70. Tew, J. G., T. E. Mandel, R. P. Phipps, and A. K. Szakal. 1984. Tissue localization and retention of antigen in relation to the immune response. *Am. J. Anat.* 170: 407–

420.

71. Szakal, A. K., M. H. Kosco, and J. G. Tew. 1988. A novel in vivo follicular dendritic cell-dependent iccosome-mediated mechanism for delivery of antigen to antigen-processing cells. *J. Immunol.* 140: 341–353.

72. Yoshida, K., T. K. van den Berg, and C. D. Dijkstra. 1993. Two functionally different follicular dendritic cells in secondary lymphoid follicles of mouse spleen, as revealed by CR1/2 and FcR gamma II-mediated immune-complex trapping. *Immunology* 80: 34–39.

73. Shikh, El, M. E., R. El Sayed, A. K. Szakal, and J. G. Tew. 2006. Follicular dendritic cell (FDC)-FcgammaRIIB engagement via immune complexes induces the activated FDC phenotype associated with secondary follicle development. *Eur. J. Immunol.* 36: 2715–2724.

74. Barrington, R. A., O. Pozdnyakova, M. R. Zafari, C. D. Benjamin, and M. C. Carroll. 2002. B lymphocyte memory: role of stromal cell complement and FcgammaRIIB receptors. *J. Exp. Med.* 196: 1189–1199.

CHAPTER 2

GENERATION OF A NOVEL *Cr2* GENE ALLELE BY HOMOLOGOUS RECOMBINATION THAT ABROGATES PRODUCTION OF Cr2 BUT IS SUFFICIENT FOR EXPRESSION OF Cr1

Luke R Donius, Christopher M Orlando, Janis J Weis, and John H Weis. 2013. Generation of a novel *Cr2* gene allele by homologous recombination that abrogates production of Cr2 but is sufficient for expression of Cr1. *Immunobiology* In Press.

Abstract

The enhancing effects of the complement system for humoral immunity have primarily focused upon the recognition of complement-bound foreign antigens by a co-receptor complex of the antigen-specific B cell receptor (BCR) and complement receptor 2 (Cr2). *In vivo* experiments using *Cr2* gene deficient mice (which lack the expression of

both the Cr1 and Cr2 proteins) do demonstrate depressed humoral responses to immunization but cannot be used to define specific contributions of the singular Cr1 or Cr2 proteins on B cell functions. To study the effect of a Cr2 deficiency in a Cr1 sufficient environment, we created a mouse line in which the alternative splice site required for the expression of the Cr2 isoform was removed. This mouse line, *Cr2KO*, still expressed Cr1 on B cells but was deficient for the full length Cr2 protein. Surprisingly, a new alternative splice within the *Cr2* gene created a truncated product that encoded a novel protein termed iCr2 that was expressed on the surface of the cells. The *Cr2KO* mouse thus provides a new model system for the analysis of Cr1 and Cr2 functions in the immune response of the mouse.

Introduction

The enhancing effects of complement for humoral immunity have been apparent since the foundational studies of Pepys (Pepys, 1974), and the identification of the enhancement of B cell activation through complement receptor (CR) 2 binding of complement-bound antigen (Carter et al., 1988). This well-accepted model of CR2 function relies initially on activation of the complement system by one of the three pathways: classical, alternative, or mannose-binding lectin. All three pathways lead to cleavage and deposition of complement component 3 (C3) fragments on antigen. The iC3b and C3d(g) fragments maintain a covalent bond with the antigen and act to direct the antigen to Cr2/CR2 via the iC3b/C3d(g) binding site on the proteins (Molina et al., 1995; Pramoonjago et al., 1993). (Cr1/Cr2 versus CR1/CR2 will be used here to clearly differentiate the mouse from the human proteins, respectively.) *In vitro* experiments

extensively defined the enhancement of B cell responses by CR2 (Carter et al., 1988; Matsumoto et al., 1993; Matsumoto et al., 1991) and the overlapping binding, co-association, and co-activation characteristics for Cr2 (Krop et al., 1996; Molina et al., 1994).

Cr2 null mouse lines (*Cr1/2KO*) have further supported the hypotheses that *Cr2* gene products expressed by B cells and follicular dendritic cells (FDC) are critical for the detection of antigen and the generation of optimal antibody responses (Haas et al., 2002; Molina et al., 1996). The mouse *Cr2* gene, unlike the human, creates both the Cr1 and Cr2 proteins from a single gene. The same signal sequence – encoding exon is alternatively spliced to either the domain encoding the first short consensus repeat (SCR) domain of the gene (thus generating the 190,000da Cr1 protein) or the exon encoding the seventh and eighth SCR (Figure 2.1a) domains of the *Cr2* gene, which represent the most N-terminal coding sequences of the mature Cr2 protein (145,000da). The sequence of the Cr2 protein is thus fully included within that of the Cr1 protein. Recently, we have found that this alternative splicing pattern is unique to B cells in that murine FDCs express only Cr1 protein from *Cr2* gene transcripts (Donius et al., 2013).

The extensive research on the *Cr1/2KO* mice has not fully discriminated the roles of the Cr1 and Cr2 proteins. The 6 N-terminal SCR domains of the Cr1 protein (which are not included in the Cr2 protein) can act as a co-factor in the regulation of C3 convertase stability and function (Molina et al., 1994), and recent studies have suggested that Cr1 may be important in regulating complement activation in the immune microenvironment (Jacobson et al., 2008; Seregin et al., 2009). To define the functions of the Cr1 protein, we have recently created and described a mouse (*Cr1KO*) that

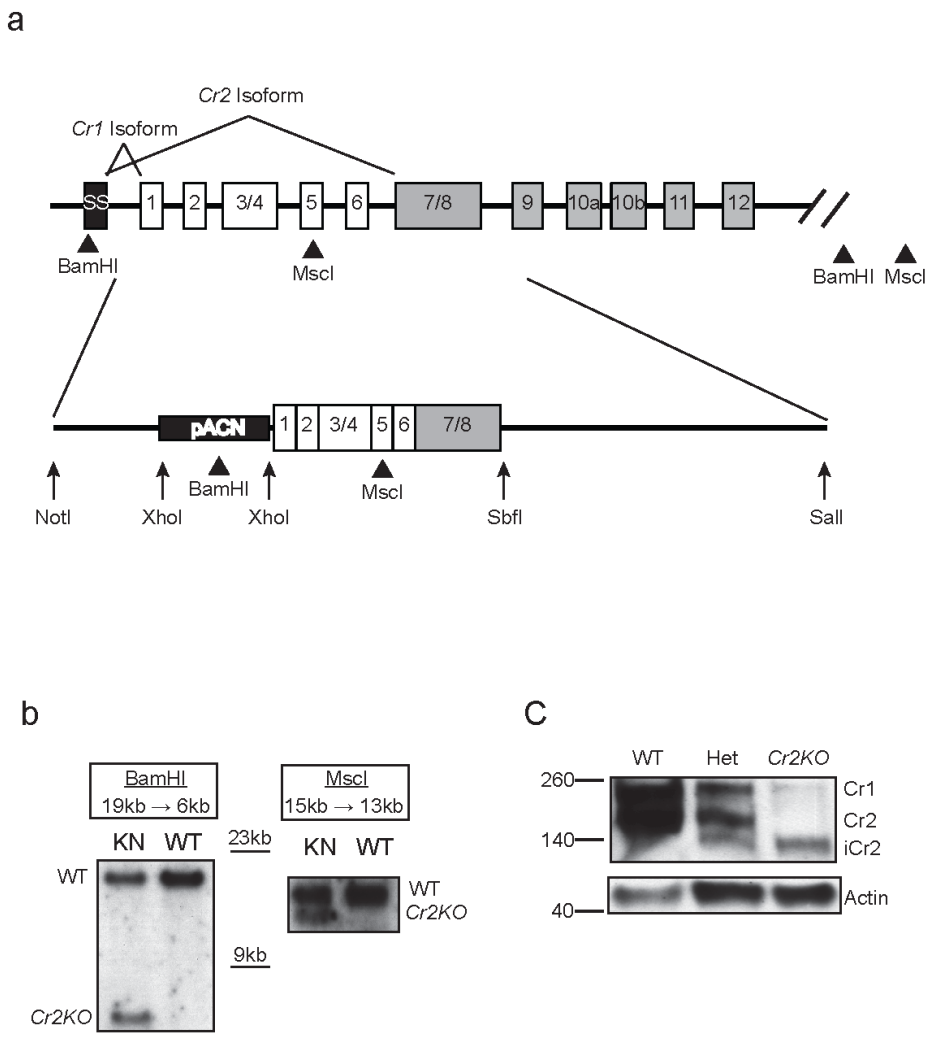

Figure 2.1. Schematic diagram and confirmation of *Cr2* alternative splice site disruption. (a) The exons of the *Cr2* gene are shown with numbers defining the number of the short consensus repeats (SCR) encoded within each. The initial exon denoted SS encodes the signal sequence. The *Cr1* isoform is generated via the inclusion of all exons during splicing while the *Cr2* isoform is generated by alternative splicing that excludes the exons encoding SCRs 1-6. The construct was generated from a cDNA version of the *Cr2* gene with the addition of a pACN neomycin selection marker. Arrows represent the approximate location of restriction sites used for cloning and mapping of homologous sequence used for recombination. Triangles represent the approximate location of BamHI and MscI restriction sites utilized to Southern blot for determination of proper homologous recombination. (b) Representative Southern blots are shown for proper 5' and 3' homologous recombination. BamHI restriction digestion of wild type (WT) genomic DNA exhibits a 19kb band detected by a radiolabeled probe. In the *Cr2KO* condition the fragment is reduced to 6kb. Homologous recombination of the 3' region was determined by probing for a size reduction from 15kb to 13kb. (c) Western blot analysis of *Cr2* gene products from WT and *Cr2KO* mice, as well as mice heterozygous for the *Cr2KO* insertion.

exclusively expresses Cr2 protein on the surface of B cells and lacks expression of either protein on the surface of FDCs.

To define the specific functions of the Cr2 protein in the immune response of the mouse, we created an additional mouse line that specifically lacks the Cr2 protein but still produces Cr1. This mouse, dubbed *Cr2KO*, was created by homologous recombination within the *Cr2* gene with a construct that removed the alternative splice junction utilized in B cells to create the Cr2 protein. Analysis of mice generated from this recombination demonstrated expression of the full length Cr1 protein on B cells but the loss of Cr1 expression (and *Cr2* gene expression) on FDCs, suggesting the disruption of an FDC-specific transcriptional enhancer site within the *Cr2* gene. Intriguingly, the removal of the native alternative splice site in the *Cr2KO* construct resulted in the utilization of an internal cryptic splice site, generating a truncated *Cr2* gene product, termed iCr2, that lacks the iC3b/C3d(g) binding sites present on the normal Cr2 protein. The *Cr2KO* animals thus represent a novel animal model with which to functionally analyze the role of the Cr1 protein on the surface of B cells in the absence of functional Cr2.

Materials and Methods

Generation of the Cr2KO mouse

The pKS+ Bluescript vector was used as a backbone for the creation of the 28kb construct. Using primers (#4151 5'-GTGGTCCTTATTTCTAGGTCAGTGTAAGTTGCTGC-3' and #4152 5'-GTTTTAATTTCCTACTTACCACTCTCACAGACTGGCAG-3'), a 1250bp cDNA version of the exons for SCRs1-8 of *Cr1* was amplified using the long-distance high-

fidelity DNA polymerase Platinum *Pfx* (Invitrogen, Carlsbad, CA). The amplicon was additionally modified by PCR utilizing primers with overhang sequences for the restriction fragments XhoI and SbfI, 5' and 3', respectively. This new SCRs1-8 fragment was cloned and ligated via XhoI and SbfI into the mouse *Cr2* gene NotI-XhoI restriction fragment and 3' to the SbfI-SalI restriction fragment (Figure 2.1a). The XhoI site of the resulting SCR1-8 construct with homology arms was utilized for insertion of the germline self-deleting neomycin resistance construct pACN (Bunting et al., 1999). The entire construct was flanked by the TK1TK2 thymidine kinase-containing negative selection construct. Electroporation of the *Cr2KO* vector into mouse strain 129-derived embryonic stem cells as well as blastocyst injection and implantation for the generation of chimeras was performed by the University of Utah Transgenic and Gene Targeting Mouse Core. Before blastocyst injection mouse embryonic stem cell clones were screened for homologous recombination by Southern blot. Restriction digestion of genomic DNA using BamHI produced a reduction in size from 19kb for wildtype (WT) to 6kb for proper homologous recombination of the 5' homology arm of the vector (Figure 2.1b). The MscI digestion was used to probe for a reduction from 15kb to 13kb upon homologous recombination of the 3' arm. Germline transmission of the *Cr2KO* allele was identified by tail or ear biopsies using PCR to generate a 193bp product (primers: #4934 Fwd 5'-CTCCATGGTTCTGTGCATATAAACACGGGTATCG-3' and #4937 Rev 5'-CCATTGGAGATGGCTGGAGGTGACTCACAAGG-3'). The WT condition was delineated using PCR to identify a 329bp product (primers: #4935 Fwd 5'-GTAAATACAAAAGCACAGTCTCTTTGACTTGC -3' and #4936 Rev 5'-GATACAATACATGTAGCAGACGAGTCACCAA-3'). All *Cr2KO* and WT mice as

well as mice heterozygous between WT and *Cr2KO* were mixed background C57BL/6 and 129 mice. *Cr1/2KO* mice were raised on site and are progeny of the $Cr2^{-/-}$ described previously (Haas et al., 2002). Experiments were performed using 8-16-week-old mice unless otherwise noted. All mice were housed at the Comparative Medicine Center (University of Utah Health Sciences Center) in accordance with the National Institutes of Health Guidelines on the Care and Use of Laboratory Animals.

Follicular dendritic cell preparation

To analyze follicular dendritic cell transcript and protein content, the hematopoietic compartment of mice was ablated via irradiation of mice with 900cGy two days prior to spleen isolation. The stroma of the spleen was isolated by straining the spleen through 100μm nylon mesh. RNA was isolated as previously described (Zabel et al., 1999). Briefly, the splenic stroma from irradiated mice was homogenized in 4M guanidine isocyathionate solution and centrifuged overnight at 30,000rpm on a 5.7M CsCl gradient. The pellet was resuspended in nuclease free water and isolated by ethanol precipitation. The precipitate was resuspended in nuclease free water and cDNA was generated. Protein isolation was performed as described for immunoprecipitation by lysing the stroma in 0.5% NP40 lysis buffer. Lysates were centrifuged for 10 minutes at 14,000 rpm and 4°C to remove nuclei and other insoluble material. Samples were then boiled in SDS-PAGE sample buffer and assayed by western blot.

Western blot analysis

Proteins were separated on TGX SDS-PAGE gels (Bio-Rad, Hercules, CA) and transferred to PVDF membrane. Membranes were blocked in 5% milk 0.2% Tween-20 in 1X TBS. Detection antibodies used were as follows: goat anti-Cr1/2 (Santa Cruz #m-19, Dallas, TX), rabbit anti-actin (Sigma-Aldrich #A2066, St. Louis, MO), rabbit anti-MEK1/2 (ERK1/2)(Cell Signaling #9122S, Danvers, MA), and rabbit anti-CD19 (Santa Cruz Biotechnology #sc-8500-R, Dallas, TX). Actin, ERK1/2, and CD19 were all visualized with HRP-conjugated secondary donkey anti-rabbit IgG (Jackson Immunoresearch #711-035-152, West Grove, PA). The goat anti-Cr1/2 was visualized using an HRP-conjugated bovine anti-goat IgG (Jackson Immunoresearch #805-035-180, West Grove, PA).

Cr1/2 immunoprecipitation

After preparation of single cell suspensions of murine splenocytes and lysis of red blood cells with ACK lysis buffer, live cells were counted by trypan blue and $5.5x10^7$ cells were collected. Cells were resuspended in 1mL NP40 lysis buffer (0.5% NP40, 50mM Tris-HCl (pH 7.5), 150mM NaCl, 0.5mM EDTA, and protease inhibitors (Complete Ultra protease inhibitor cocktail, Roche, Foster City, CA). Cells were incubated in lysis buffer for 30 minutes at 4°C with rotation. Lysates were then precleared by the addition of 60μL of a 10% suspension of protein G agarose beads (P7700, Sigma, St. Louis, MO) in PBS followed by 15-minute incubation at 4°C with rotation, centrifugation at 3,000 rpm for 10 minutes at 4°C, and transfer of the supernatant to a fresh 1.5ml tube. Aliquots containing approximately $5.5x10^6$ cell

equivalents were taken, 1.5µg of antibody for precipitation were added, and samples were incubated overnight at 4°C with rotation. Precipitation of immunoconjugates was accomplished by the addition of 60µL of 10% protein-G agarose bead suspension, incubation for 30 minutes at 4°C with rotation, and centrifugation at 3,000 rpm for 10 minutes. The beads were then washed three times with buffer containing 10mM Tris-HCL buffer (pH 7.5), 0.1mM EDTA, and 0.05% NP40. Pellets were resuspended in 50µL of 2x SDS-PAGE sample buffer and boiled for 5 minutes. Samples were then centrifuged at 14,000 rpm for 5 minutes at 4°C, and supernatant was transferred to a fresh tube and stored at -80°C until western blot analysis.

Immunohistochemistry of splenic cross-sections

Sectioning and immunohistochemistry were performed as described previously (Donius et al., 2013). Briefly, OCT (Sakura Finetek USA, Torrance, CA) embedded spleens were sectioned on a cryostat at 10-12µm. Cr1 was detected using the biotinylated anti-Cr1 antibody clone 8C12 and Cr1/2 were detected using the biotinylated anti-Cr1/2 antibody clone 7E9. Streptavidin conjugated horseradish peroxidase (HRP) was used to detect the antibodies and was visualized using 3, 3'-diaminobenzidine (DAB) (Vector Laboratories, Burlingame, CA).

Biotinylation of cell surface proteins

Total mouse splenocytes were collected and washed three times with PBS (pH 8.0). Cells were then resuspended at $2.5x10^7$ cells/mL in 2.5mM EZ-Link Sulfo-NHS-Biotin (Thermo Scientific, #21217, Waltham, MA) in PBS (pH 8.0) and incubated at 4°

C for one hour with rotation. Unreacted biotinylation reagent was quenched and removed by three washes with 100mM glycine in PBS (pH 8.0). Labeled cells were then lysed at $5.5x10^7$ cells/mL 0.5% NP40 lysis buffer for 30 minutes at 4°C with rotation. For every 1.5mL of cell lysate, 1mL of avidin-sepharose slurry (Protein Mods, #AVG, Madison, WI) was washed three times with 1% NP40 in PBS (pH 7.2). After removal of the last wash, cell lysates were added to settled avidin sepharose gel and incubated at room temperature for 1 hour with rotation. Avidin sepharose gel was transferred to a fresh microcentrifuge tube and washed five times with 1% NP40 in PBS (pH 7.2). Settled avidin sepharose gel was resuspended in a volume of 4X SDS-PAGE sample buffer approximately equal to the volume of gel, boiled for 7 minutes, and placed on ice for 7 minutes. Samples were centrifuged at 14,000 rpm for 10 minutes at 4°C, and supernatant was transferred to a fresh tube and stored at -80°C until western blot analysis. Enrichment for cell-surface proteins was confirmed by blotting for ERK1/2.

Characterization of the iCr2 splice site using ^{32}P-labeled PCR

Detection of small PCR amplicons was achieved by incorporation of ^{32}P-labeled dCTP (Tan and Weis, 1992). Reaction mixes containing 0.01mCi of ^{32}P-labeled dCTP, 0.32mM dNTP, $MgCl_2$ buffer (Biofire, Salt Lake City, UT), 0.5µg each primer, and 0.75 units of Taq polymerase were brought to 10µl with deionized H2O and loaded into glass capillaries. Primer pairs were as follows: primer pair #1, Fwd #43 5'-ATGGGATCCTTGGGTTCGCTC-3' with Rev #4975 5'-GTATGACTTCCATTACGAACAG-3'; primer pair #2, Fwd #43 with Rev #4974 5'-TATGAATCGTTGGAAGTGATGGGC -3'; and primer pair #3, #43 with Rev #45 Rev

#45 5'-GCTAGGTGAACAAGTGTACCT-3' (Figure 2.2a and b). Capillary tube ends were sealed by melting and rapid amplification was performed using an air thermocycler for 16 to 25 cycles. PCR reactions were heated to >95^{o}C in formamide containing loading buffer and immediately loaded onto polyacrylamide sequencing gel under denaturing conditions. The gel was transferred to chromatography paper, dried, and exposed to x-ray film overnight.

Quantitative PCR

Quantitative PCR was done as described previously (Donius et al., 2013). Briefly, cDNA generated from total spleen or spleen stroma from irradiated mice was amplified in a SYBar green (Invitrogen, Carlsbad, CA) containing reaction mix and the measured ΔCt was utilized to generate a transcript number relative to *β-actin* ΔCt. Primers used for *Cr1*, *Cr1/2,* and *β-actin* were as previously described (Debnath et al., 2007; Donius et al., 2013; Roundy et al., 2009).

Flow cytometry

Flow cytometric analysis was performed as previously described (Donius et al., 2013). Briefly, splenocytes were isolated by straining spleens through 100μm nylon mesh into ice cold FACS buffer (0.5% BSA, 2mM EDTA in PBS). Bone marrow from mice was isolated by flushing tibias and femurs with ice cold 0.5% BSA in PBS and straining through a 100um strainer and processed as below. Red blood cells were lysed with ACK buffer and the remaining cells were incubated in antibody mix. Antibodies used were as follows: eBioscience (San Diego, CA) monoclonals anti-B220-PerCP/Cy5.5 (RA3-6B2),

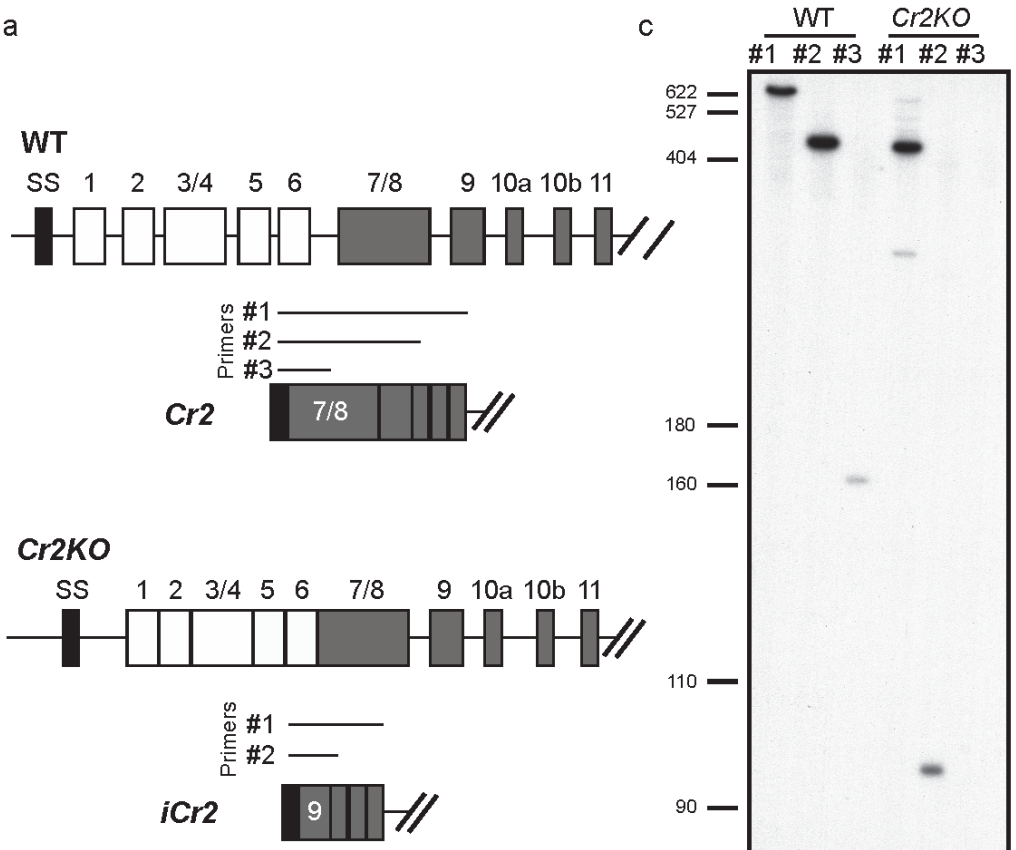

b

Predicted PCR Product Size		
Primer Set	***WT***	***Cr2KO***
#1	866bp	476bp
#2	487bp	97bp
#3	162bp	No product

Figure 2.2. *Cr2KO* mice produce iCr2, an N-terminal truncated version of Cr2. (a) Schematic of PCR products from *Cr2* gene transcripts (WT) and iCr2 transcripts (*Cr2KO*) utilizing a primer specific for the signal sequence (SS) with those from exon sequences encoding SCR 7/8 (primer set #1), SCR 10a (primer set #2), or SCR 11 (primer set #3). Cr1 encoding transcripts would not be identified with these primer sets due to the large size of the product. (b) The primer sets #1, #2, and #3 would predict PCR fragments of 866bp, 487bp, and 162bp fragments, respectively, in WT samples while a PCR fragment of 476bp from primer set #1 and 97bp from primer set #2 would be predicted from *Cr2KO* cDNA samples. No PCR product from primer set #3 would be expected with the *Cr2KO* cDNA samples. (c) Radiographic detection of PCR amplified WT and *Cr2KO* cDNA samples using ^{32}P-labeled dCTP resulted in bands corresponding to the sizes predicted in (a) and (b). Molecular weight markers are noted on the left side of the image.

anti-CD19-PE/Cy7 and PE (clone 1D3), anti-Cr1-biotin (clone 8C12), anti-Cr1/2-PE/Cy7 (clone 8D9), anti-Cr1/2-FITC (clone 7G6), anti-IgM-PE (clone eB121-15F9), and anti-CD40-FITC (clone HM40-3). Additionally, the following BioLegend (San Diego, CA) antibodies were used: anti-IgD-AlexaFluor647 (clone 11-26c.2a), anti-CD23-biotin (cloneB3B4), CD43-PerCP/Cy5.5 clone 1B11 and purified anti-CD16/32 as Fc block. Secondary incubations were performed with streptavidin-APC whenever biotinylated antibodies were used. Final samples were resuspended in 500µl of FACS buffer and stained with 1.5µl 1mM DAPI for live/dead discrimination. All samples were analyzed on a FACSCantoII (BD Biosciences, San Jose, CA) and data were analyzed using FlowJo version 8.8.7 (Tree Star, Inc., Ashland, OR)

Statistical analysis

Statistical analysis and graphs were generated using Prism version 5.0c (GraphPad Software, Inc., San Diego, CA).

Results

Creation of a Cr2- but not Cr1-deficient mouse

A Cr2 deficient, Cr1 sufficient, mouse in which Cr1 is expressed in a cell- and stage-specific manner has long been sought as a model for investigating the role of complement augmentation of B cell responses. The challenge in creating such a mouse was to leave the transcriptional control apparatus intact, but to deprive the *Cr2* gene transcripts of the option to create the Cr2 protein-specific alternative splice. To block the generation of transcripts encoding the Cr2 protein but not those encoding Cr1, we devised

a strategy by which the exons encoding SCR domains 1 through 8 were fused (Figure 2.1a). Normally, B cells process *Cr2* gene transcripts to splice the domain encoding the signal sequence (SS) to the domain encoding SCR1 (and all of the remaining exons) to create the Cr1 protein. The B cell alternative splice of the *Cr2* gene transcript splices the SS-encoding exon to that encoding the SCR7/8 (and all of the remaining exons) to create the Cr2 protein. We proposed that removing this alternative splice site (just upstream of the exon encoding SCR7/8) would block the production of the Cr2 protein and instead force all of the *Cr2* gene transcripts to encode the Cr1 protein. A construct containing a cDNA fusion of the SCRs 1-8 (thus removing the alternative splice junction) was ligated to the testes specific self-deleting pACN neomycin resistance gene and flanked by *Cr2* homologous DNA (Figure 2.1a). To reduce the odds of nonhomologous recombination, a gancyclovir sensitivity gene (thymidine kinase) was also attached. Homologous recombination was utilized to target the construct to the *Cr2* gene of mouse strain 129 embryonic stem (ES) cells. The resulting neomycin resistant and gancyclovir insensitive clones were screened by Southern blot for the predicted insertion of novel BamHI and MscI restriction sites resulting in 19kb to 6kb and 15kb to 13kb size reductions in *Cr2* restriction digest fragments, respectively (Figure 2.1a and b). A single ES line was used to generate the *Cr2KO* mouse line.

To test the validity of our strategy, we obtained protein lysates from splenocytes of our newly generated *Cr2KO* mice, as well as WT and heterozygous littermates. Western blot analysis of these lysates revealed that Cr2 was no longer present in the *Cr2KO* samples and that Cr1 expression was maintained. Surprisingly, *Cr2KO* and heterozygous mice when compared to WT littermates expressed reduced quantities of

Cr1 and produced a new protein that is detected by antibody against Cr1/2 (Figure 2.1c). This new protein, termed incomplete Cr2 (iCr2), was found to be about 15,000da smaller than WT Cr2.

Defining the new iCr2 protein

The splenic lysates from the *Cr2KO* animal demonstrated two proteins, one identical in size to Cr1 and a second (iCr2) that was smaller than the WT Cr2 protein, suggesting that iCr2 could be a new alternatively spliced product from the *Cr2* gene transcripts. The decrease in size of the iCr2 product, compared to WT Cr2 protein, was about that predicted from the loss of two SCR domains. To identify the precise exon order in the *Cr2* gene transcripts that could encode this iCr2 protein, we designed primers embedded within the exons corresponding SCR7/8, SCR10a, and SCR11 to pair with a primer located in the signal sequence (SS) encoding exon (Figure 2.2a). These primer pairs are identified here as #1, #2, and #3, respectively. Primer pair #1, #2, and #3 produce 866bp, 487bp, and 162bp PCR products from WT *Cr2* cDNA (Figure 2.2b). We predicted that if the new *iCr2* product was excluding the 400bp exon encoding SCR7/8 and splicing directly from the SS exon to the SCR9 exon then pair #1 would generate a 476bp product, #2 would generate a 97bp product, and pair #3 would not generate a product (Figure 2.2b). In order to ensure resolution of small PCR products, we performed PCR with ^{32}P-labeled nucleotides and resolved the reactions on polyacrylamide sequencing gels. PCR of cDNA generated from *Cr2KO* splenocyte-derived RNA using these primers revealed products 400bp smaller than those found in WT mice (Figure 2.2c). Predictably, primer pair #3 did not produce a product in *Cr2KO* cDNA. Sanger

sequencing of a product generated from primer pair #2 further demonstrated that splicing exactly joins the SS exon to the exon encoding SCR9 (data not shown). These data indicate that the iCr2 protein consists of sequences including SCR9 and greater. Therefore, this protein would not possess the C3d(g) binding site encoded within the SCR7/8 domains (Molina et al., 1994) but would include those C-terminal sequences required for membrane localization and association with CD19.

Molina et al. previously demonstrated that C3d binds to murine Cr2 within SCR 7/8 and also that the anti-Cr1/2 antibody 7G6 competitively binds to this site (Molina et al., 1994). Another anti-Cr2 antibody, 7E9, binds both Cr1 and Cr2 but does not compete for C3d binding, which suggests that it recognizes an epitope found in SCR9 or greater. Both antibodies also bind to the Cr1 protein while a third antibody, 8C12, is specific for the N-terminal sequences found only in Cr1. These three monoclonal antibodies are all of rat derivation. To evaluate the potential of these antibodies to recognize the iCr2 protein, we performed immunoprecipitations with them followed by western blot using a pan-Cr1/2 reactive goat polyclonal antibody. As shown (Figure 2.3a), the 7E9 antibody can precipitate both the iCr2 and Cr1 proteins from the *Cr2KO* splenic lysates (and the Cr1 and Cr2 proteins from the WT lysate). Additionally, the 8C12 antibody only recognizes the Cr1 protein in both the WT and *Cr2KO* lysates, confirming that the *Cr2KO* line does continue to produce the Cr1 protein. Alternatively, the 7G6 antibody (Figure 2.3b) does not precipitate the iCr2 protein but does precipitate Cr1 and WT Cr2, which supports the transcript/sequence data described above. These data indicate that the iCr2 protein does not possess the sequences encoding SCR7/8 which encode the iC3b/C3d(g) binding site.

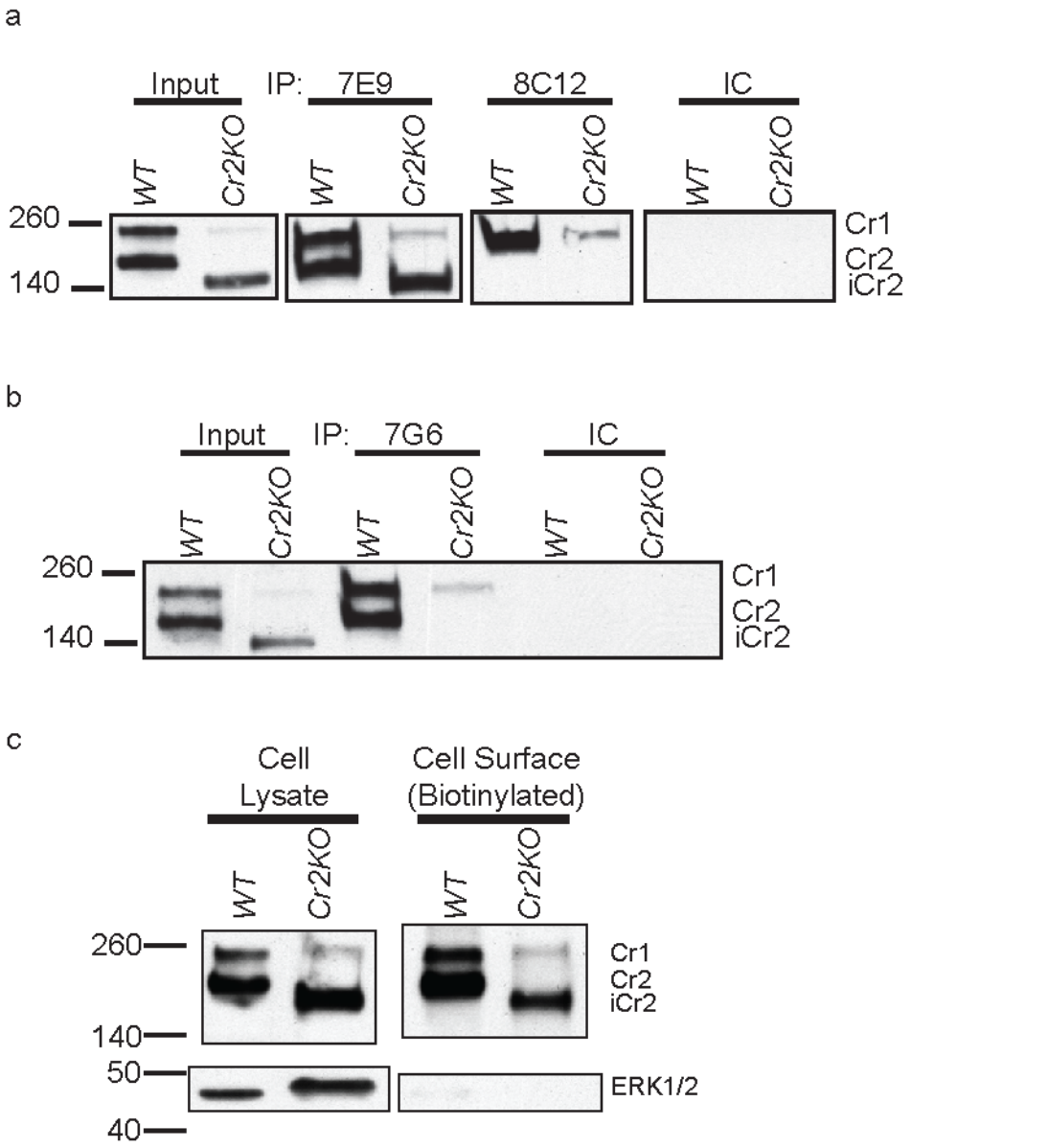

Figure 2.3. Elucidation of structural features of the iCr2 protein by immunoprecipitation and biotin labeling of cell-surface proteins. (a) Western blot analysis of proteins precipitated from strained spleen lysates with antibodies against regions common to Cr1 and Cr2 (7E9) and the cofactor domain unique to Cr1 (8C12). IC, isotype control antibody. (b) Western blot analysis of proteins precipitated from strained spleen lysates with antibody (7G6) against the C3d(g) binding region of Cr1 and Cr2. This region remains in Cr1 produced by the *Cr2KO* mouse but is absent in the iCr2 protein. IC, isotype control antibody. (c) Western blot analysis of cell-surface proteins identified by biotin-labeling and precipitated with avidin-sepharose. Enrichment for cell-surface proteins was confirmed by immunoblotting with antibody against the cytoplasmic protein ERK1/2.

If found on the membrane, the iCr2 protein would be predicted to contain all of the Cr2 protein sequences C-terminal of SCR9 including those sequences that facilitate co-association of the Cr1/Cr2 proteins with CD19. To determine if the iCr2 protein is indeed found at appropriate levels on the cell surface, we preformed surface biotinylation analysis of WT and *Cr2KO* splenocytes. Enrichment of the Cr1 and iCr2 proteins from *Cr2KO* splenocytes was comparable to the identification of Cr1 and Cr2 from WT cells (Figure 2.3c). The intracellular protein ERK1/2 was not detected in the biotinylated fraction when compared to an equivalent exposure of total cell lysate. Additionally, no Cr1, Cr2, or iCr2 was detected in western blot analysis of the nonbiotinylated fractions (data not shown), suggesting that the vast majority of the Cr1, Cr2, and iCr2 proteins are localized on the surface of the expressing cells.

Characterization of B cell protein expression in the Cr2KO animal

Western blot and surface biotinylation analysis described above indicates that splenocytes (i.e., B cells) from the *Cr2KO* animal express both Cr1 and iCr2 on the cell surface. To compare the relative levels of expression of these proteins to Cr1 and Cr2 expression on WT splenic B cells, we isolated splenocytes from WT and *Cr2KO* animals and conducted flow cytometric analysis using antibodies specific for Cr1 (8C12) and for Cr1 and Cr2 (7G6, 8D9). Flow cytometric analysis of $B220^{+}$ (B cells) cells demonstrated that the geometric mean fluorescent intensity (gMFI) of Cr1 expression in the *Cr2KO* animals (identified with the 8C12 and 7G6 antibodies) was lower than Cr1 expressed by WT B cells (defined by 8C12 staining) (Figure 2.4a). The specific binding site of antibody 8D9 on the Cr1/Cr2 proteins is not known. However, staining of the *Cr2KO* B

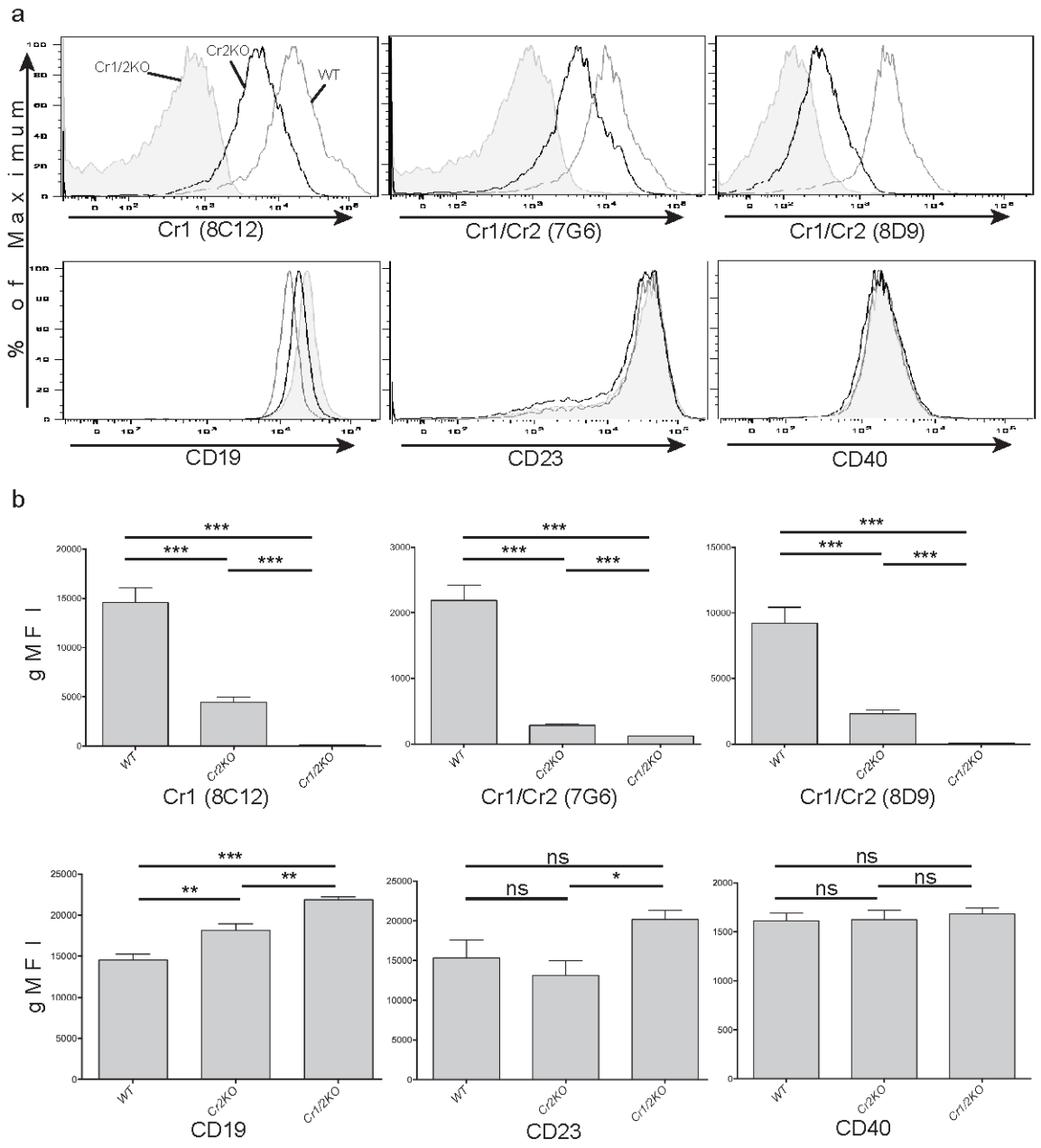

Figure 2.4. Surface expression of Cr1, Cr2, CD19, CD40, and CD23 (FceR2a) on B cells is modulated in *Cr2KO* mice. (a) Representative histograms of Cr1 (antibody clone: 8C12), Cr1/2 (7G6), Cr1/2 (8D9), CD19, CD23, and CD40 expression on $B220^{+}$ cells from the spleens of WT (gray line), *Cr2KO* (black line), and *Cr1/2KO* mice (gray fill). (b) The average geometric mean fluorescent intensity (gMFI) is graphed for $B220^{+}$ cells from WT, *Cr2KO*, and *Cr1/2KO* mice represented in (a). Significance determined by the t-test shown between bars by black lines and denoted by asterisks (*$p<0.05$, **$p<0.01$, ***$p<0.001$, and ns=not significant). Data representative of 2 to 3 independent analyses and n=5-9 for all graphs.

cells with the 8D9 antibody could be predicted to be additive of both Cr1 and iCr2, increasing the gMFI to near WT levels. The 8D9 antibody demonstrated approximately equal staining to that of the 7G6 and 8C12 antibodies (Cr1-specific for the *Cr2KO* cells), suggesting the epitope recognized by 8D9 is also altered by the loss of SCR7/8 in the iCr2 protein. Additional analysis of important receptors on B cells in the *Cr2KO* mice demonstrated identical gMFI staining for CD40 and CD23 (FceR2a) compared to WT. The levels of CD19 expression, however, were slightly elevated compared to WT but intermediate to the *Cr1/2KO* animal as previously described (Haas et al., 2009). The quantified gMFI of multiple similar flow cytometric analyses are shown in Figure 2.4b.

Characterization of marrow and splenic B cell populations
in the Cr2KO animal

To test the effect that Cr2 specific deletion has on B cell development, we assessed the subsets of marrow, splenic, and peritoneal B cells. Pro-B, Pre-B, immature B, and mature B cells from the mature *Cr2KO* animal were compared with those of WT (Figure 2.5a). There were no demonstrable differences in B cell development between WT and *Cr2KO* mice. To determine if the expression of Cr1 by maturing B cells was altered in the *Cr2KO* mice, the cell surface expression of Cr1 was evaluated for the marrow B cell populations (Figure 2.5b). Similar to the WT, the *Cr2KO* mice primarily demonstrated Cr1 expression on the mature B cells within the marrow compartment with a lesser level of expression on the immature B cells, again similar to that seen in WT mice. Therefore, the stage specific expression of Cr1 was not altered from that of WT in the *Cr2KO* animal.

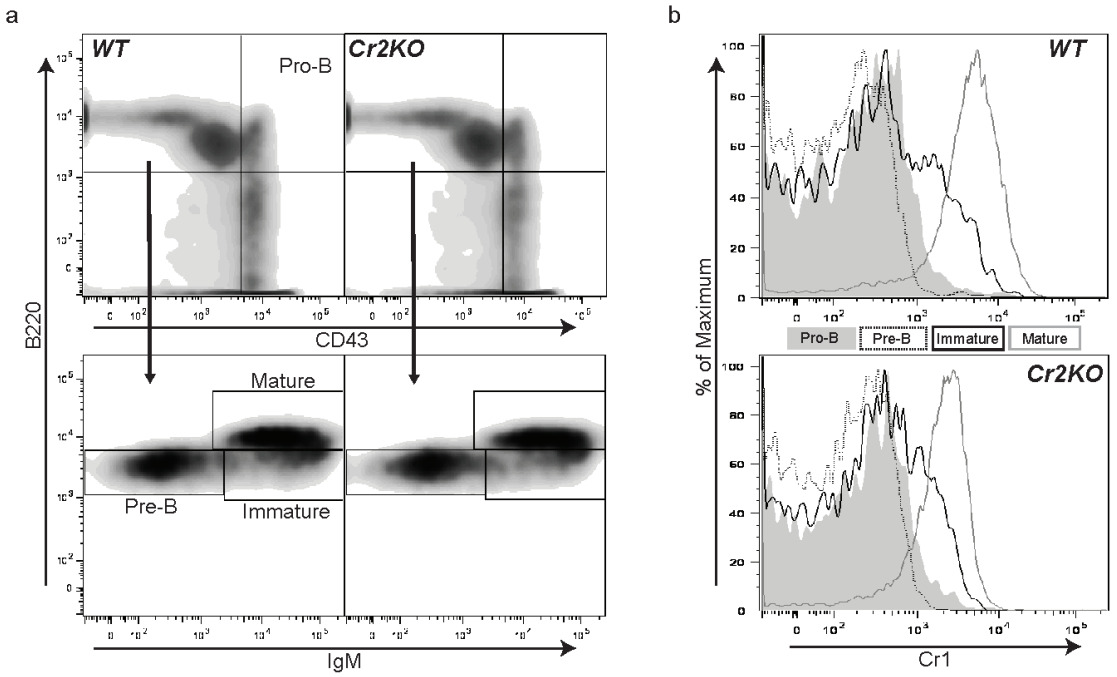

Figure 2.5. Progression of marrow B cell development in the *Cr2KO* animal. (a) Cell surface staining strategy for identifying Pro-B, Pre-B, immature B, and mature B cells in adult WT and *Cr2KO* animals. Pro-B cells are identified as $CD43^{hi}$ and $B220^{+}$ (a, top panel) and the $CD43^{lo/-}$ subset was further delineated by expression of IgM and B220. Pre-B cells IgM^{lo} $B220^{lo}$, immature B cells IgM^{hi} $B220^{lo}$, and mature B cells IgM^{hi} $B220^{hi}$ are shown (a, bottom panel). No marked differences were identified between the bone marrow B cell subsets of *Cr2KO* mice compared to WT bone marrow B cell subsets. (b) Cr1 expression in maturing and mature marrow B cells from WT and *Cr2KO* animals was determined using the sorting gates shown in (a). Both *Cr2KO* and WT mice exhibit the same timing of expression of Cr1 at the immature B cell stage with all mature B cells expressing Cr1. Cr1 expression in the *Cr2KO* is reduced compared to WT. Data representative of n=3 littermates.

Peritoneal B1 populations have been shown to be altered in the *Cr1/2KO* animals but not in the *Cr1KO* mouse (Ahearn et al., 1996; Donius et al., 2013). We examined B1a and B1b populations in the *Cr2KO* mice and found that they were not significantly different than WT (data not shown). Similarly, Cr1 expression was evident on the B1 populations of the *Cr2KO* mice but at levels reduced comparably to those of the other B cell populations in the *Cr2KO* animal (data not shown). Therefore, the deletion of Cr2 in the *Cr2KO* animal did not alter the numbers or type of peritoneal B1 cells.

B cells in the spleen can be segregated by their varied expression of IgM and IgD. By gating on total splenic $B220^{+}$ cells, the marginal zone and transitional 1 B cells are identified as IgD^{LO} IgM^{HI} cells, while follicular mature B cells are identified by the marker profile IgD^{HI} IgM^{LO} (Loder et al., 1999). A transitional 2 immature subset can also be identified by this strategy as IgD^{HI} and IgM^{HI}. Flow cytometric analysis of splenic B cells, identified by expression of the B cell marker B220, did not identify any significant effects on frequency or total number of cells from the transitional 1, transitional 2, marginal zone, or follicular B cell populations (Figure 2.6a and b). Therefore, similar to the *Cr1/2KO* mouse, the *Cr2KO* mouse has normal B2 populations of splenic B cells.

Cr2 gene product expression on follicular dendritic cells of Cr2KO mice

As described above, the expression of the Cr1 protein is reduced on the surface of the *Cr2KO* B cells compared to WT B cells. Previously, we have shown that FDCs do not produce the Cr2 protein but instead primarily express Cr1 (Donius et al., 2013). To determine if FDC expression of Cr1 was also depressed in the *Cr2KO* animals, we first

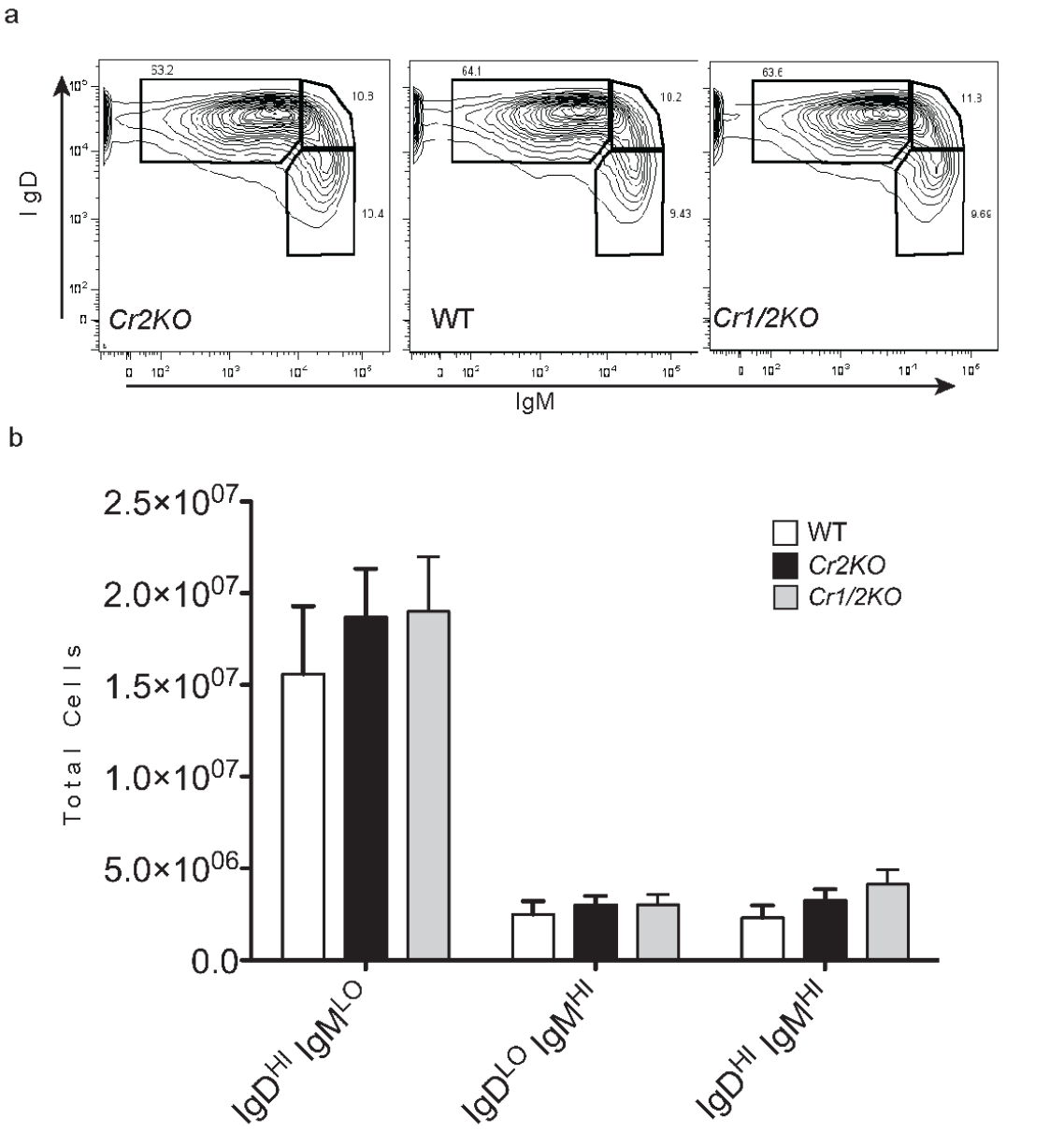

Figure 2.6. Splenic B cell populations are fully represented in *Cr2KO* mice. (a) Representative plots of $B220^{+}$ B cells from total live splenocytes isolated from WT, *Cr2KO*, and *Cr1/2KO* mice. Gates represent follicular B cells (IgD^{HI} IgM^{LO}), transitional 2 B cells (IgD^{HI} IgM^{HI}), and the marginal zone, B1, and transitional 1 B cell populations (IgD^{LO} IgM^{HI}). (b) The total number of cells from each population were calculated using gate percentages for $B220^{+}$ and IgM IgD parameters and the initial number of splenocytes counted using trypan blue. No significant differences were seen between any genotypes for any populations by ANOVA.

analyzed Cr1-specific transcripts in FDCs relative to that of total spleen. Irradiation treatment of mice is very effective at removing virtually all B cells from the spleen, leaving behind the radiation-resistant stromal cells and FDCs. As shown (Figure 2.7a), the level of Cr1-specific transcripts was depressed in the total spleen samples (containing both B cells and FDCs) as well as the irradiated samples (highly enriched for FDCs), indicating that FDC expression of Cr1 in the *Cr2KO* mouse is also reduced. Western blot analysis of spleen lysates from these B cell depleted mice further demonstrated that Cr1 is not expressed by FDCs, at least not at a detectable level (Figure 2.7b). Splenic cross-sections from WT and *Cr2KO* mice analyzed by immunohistochemistry using the anti-Cr1 antibody clone 8C12 labels *Cr2KO* spleens but in a considerably reduced pattern compared to WT (Figure 2.7c).

Discussion

The generation of a mouse specifically and singularly deficient in the Cr2 protein has been a sought-after tool for the study of the effects of the complement system on humoral immunity. A similar goal was advanced recently by the creation of a transgenic *Cr1/2KO* mouse line expressing human CR1/CD35 (Pappworth et al., 2011). However, in addition to the expression of human CR1 in a nonautochthonous environment, these mice possess other disadvantages, including premature expression of CR1 during B cell development, a broader cell specific expression pattern than murine Cr1, and the absence of the CD19 co-association exhibited by mouse Cr1. Therefore, to create a *Cr2KO* animal without these limitations, we adopted the strategy of modifying the endogenous *Cr2* gene via homologous recombination with a construct that would block Cr2 protein production

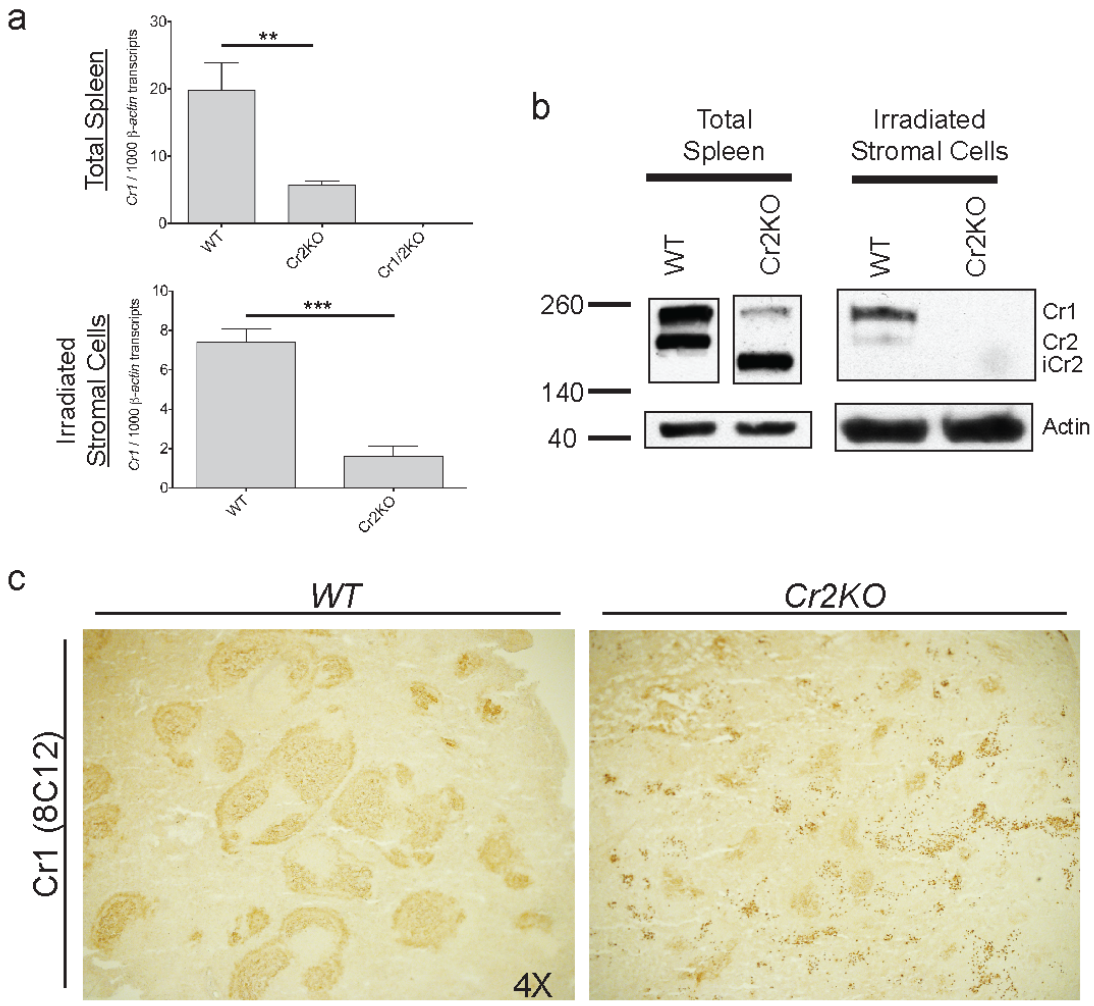

Figure 2.7. Follicular dendritic cell *Cr2* gene expression. (a) Quantitative PCR measurement of Cr1 transcripts per 1000 β-actin transcripts in cDNA samples generated from either total splenic RNA or stromal isolations from irradiated mice (B cell depleted). Black lines denote statistical analysis by the t-test. (b) Western blot analysis of Cr1, Cr2, and iCr2 in lysates isolated from spleens using the same methods as in (a). (c) Detection of Cr1 utilizing antibody clone 8C12 in splenic cross-sections from naive WT and *Cr2KO* mice. All images obtained at a magnification of 4X. (**p<0.01, ***p<0.001, and ns=not significant; total spleen graphs in (a) n=6, n=3 for *Cr1/2KO*; irradiated stromal cells n=4)

but leave intact those coding sequences required for the Cr1 protein.

This strategy of specifically manipulating the endogenous *Cr2* gene was designed to leave *Cr2* under the transcriptional control of its endogenous promoter in an approach nearly identical to that taken in the creation of the *Cr1KO* mouse (Donius et al., 2013). Creation of the *Cr2KO* mouse and the biological assessments of the animal described here, however, uncovered the importance of the intronic sequence and/or the alternative splice site in promoting overall expression of the *Cr2* gene.

Both the *Cr1KO* and *Cr2KO* mice were designed to maintain the normal positioning of the *Cr2* promoter, first exon encoding the signal sequence, and much of the first intron of the gene, especially the regions that are rich in transcription factor binding sites (Figure 2.8). While the *Cr1KO* mouse lacks the exons encoding the Cr1-specific exons encoding SCRs 1-6 (and the intervening introns), the *Cr2KO* animal, is primarily lacking only the intronic sequences between the exons encoding the first 8 SCR domains. There was no indication of a "new" alternative splice in the *Cr1KO* animal, suggesting that sequences that prompt the alternative splice are somewhere within the exons encoding the first 6 SCRs of the protein. The concept that coding exons could influence such a splicing event is not new. Recent studies on alternative splicing of CD45 in T and B cells have identified specific residues within coding exons of that gene that are recognized by the HnRNP L and L-like proteins that help facilitate the complex alternative splicing of CD45 transcripts (Oberdoerffer et al., 2008; Preussner et al., 2012; Rothrock et al., 2005; Tong et al., 2005). These target sequences that facilitate constitutive and inducible alternative exon splicing are comprised of CA rich sequences that are specifically bound by members of the HnRNP L family. Exons encoding the

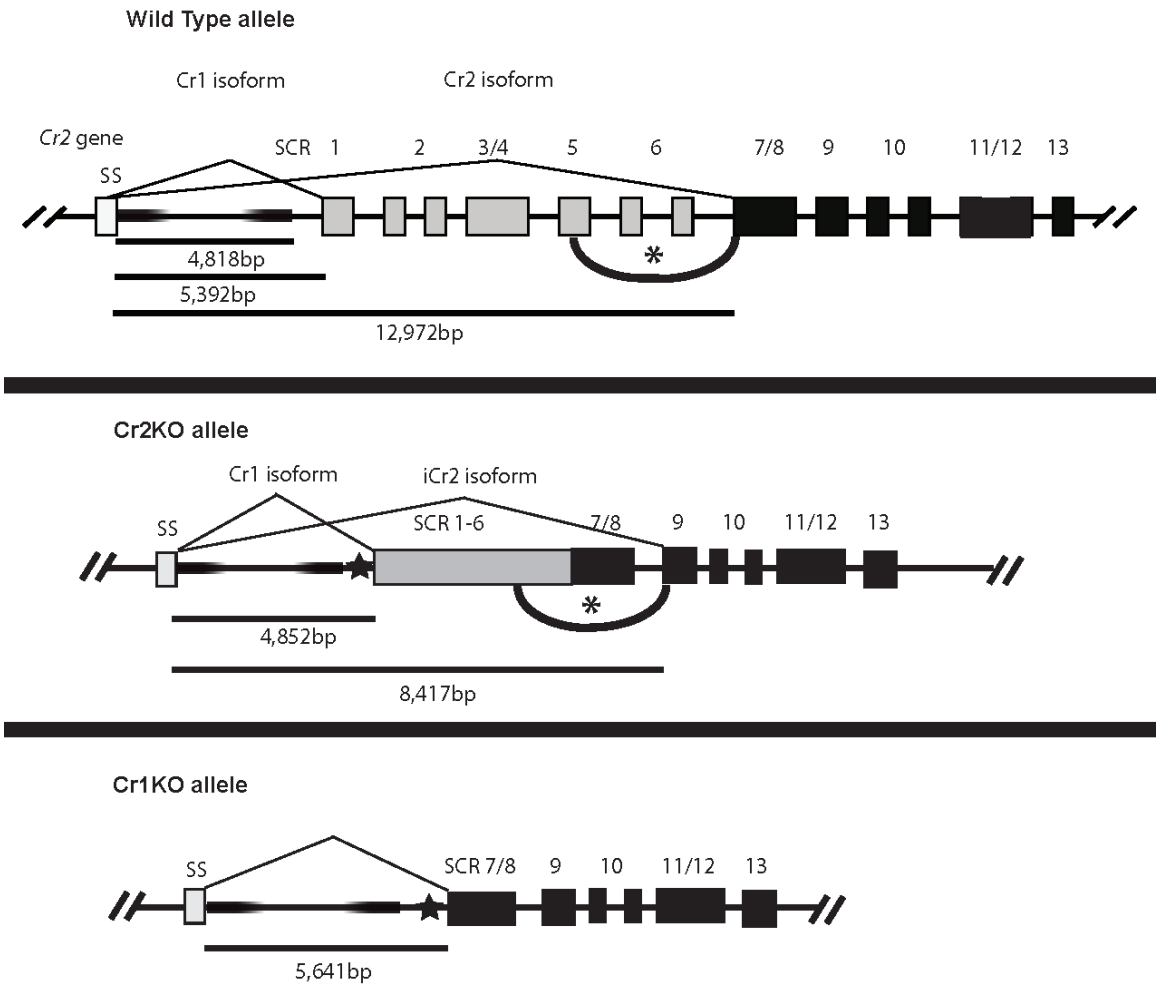

Figure 2.8. Schematic representation of the alternative splicing of the *Cr2* gene seen in WT and *Cr2KO* animal lines. The first intron sequence of 4,818bp in the WT *Cr2* gene is present in both the *Cr2KO* and *Cr1KO* lines (denoted by shaded black box). The genomic span between the signal sequence (SS) exon and that encoding SCR1 is 5,392bp and SS to that encoding SCR7/8 is 12,972bp in the WT gene. The star in the *Cr2KO* and *Cr1KO* alleles denotes the insertion site of the *Neo* gene sequence which, during germline propagation, resolves to a single *Lox* site. The *Cr1KO* allele does not demonstrate any alternative splice, suggesting the alternative splicing target sequence(s) is within coding sequences for SCRs 1-6, not the promoter or first intron of the *Cr2* gene. The position of the hypothetical location within the exons for SCRs 1-6 is indicated by the black arc and asterisk.

SCRs 4-6 of the *Cr2* gene would be the likely site for such sequences and CA-rich HnRNP L-binding regions can be identified *in silico* in these coding exons (data not shown). Future experiments using *Cr2* minigenes (similar to the minigenes constructed for the alternatively spliced exons of the CD45 gene) will be required to definitively identify sites and mechanisms controlling this alternative splicing pathway.

Although our goal was to create a mouse that only expressed the Cr1 protein from native *Cr2* gene transcripts, the creation of such a mouse would have provided for much higher Cr1 surface expression than WT. Instead we found the iCr2 protein was the major product from the targeted *Cr2KO* allele and the Cr1 protein was expressed below WT levels. The production of this iCr2 protein is nevertheless a positive outcome of the *Cr2KO* mouse since iCr2 occupies a B cell surface niche vacated in the absence of Cr2. The iCr2 protein lacks the sequences encoding the SCR7/8 domains which include the iC3b and C3d(g) binding site, but still maintains a membrane localization with full availability for CD19 association. The potential of iCr2 to associate with CD19 is especially important in light of the effects that complement receptor surface expression is proposed to have on CD19 expression (Haas et al., 2009). Haas et al. have shown that overexpression of CD19 is correlated with reduced B cell responsiveness and is controlled by Cr1/2 expression (Haas et al., 2005). The *Cr2KO* mice express an intermediate level of CD19 compared to WT and the *Cr1/2KO* mice (Figure 2.4b), suggesting that the *Cr2KO* mouse may avoid the complications associated with aberrant CD19 expression.

The most unexpected effect of deletion of the *Cr2* alternative splice site is the reduction of Cr1 expression. This reduction is especially surprising in the FDC

compartment where a strong preference for Cr1 is observed (Donius et al., 2013). Instead of remaining the same or becoming enhanced compared to WT (which would be expected since the alternative splice to create the Cr2 protein is not evident in FDCs), Cr1 was found to be reduced in FDCs at the transcriptional level and could not be detected by western blot (Figure 2.7a and b). The promoter and first intronic sequences of the *Cr1KO*, *Cr2KO*, and WT strains are virtually identical, yet the production of Cr1 in FDCs from the *Cr2KO* animal is dramatically reduced.

The *Cr2KO* animals will provide us with a unique strain with which to trace B cell activation within germinal centers. *C3KO*, *Cr1KO*, and *Cr1/2KO* animals are all deficient in the generation of activated germinal centers following immunization with sheep red blood cells (Donius et al., 2013; Wu et al., 2000). By creating bone marrow chimeras of *Cr2KO* marrow into a WT animal, we will be able to determine if B cell expression of the Cr2 protein is required for appropriate B cell activation in the germinal centers. Similarly, by creating bone marrow chimeras of WT bone marrow into *Cr2KO* animals, we will be able to determine if the reduced level of expression of Cr1 on FDC seen in the *Cr2KO* mouse is still sufficient for appropriate germinal center B cell activation.

In total, this work describes the generation of a mouse deficient in the Cr2 isoform of *Cr2*. Surprisingly, this mouse illustrates a dominant alternative splicing event that creates a novel iCr2 protein product that is expressed on the cell surface yet lacks the critical complement binding domains. The *Cr2KO* mice are thus functionally deficient in Cr2 but not Cr1; however, the effects of hypomorphism for Cr1 expression by B cells and FDCs are yet to be determined. Intriguingly, the human *CR2* homolog lacks a direct

mouse Cr1 homolog, but maintains noncoding pseudoexons with sequence conservation to mouse (Holguin et al., 1990). It is tempting to speculate that these pseudoexons of the human *CR2* gene contain regulatory sequences for splicing and *CR2* expression. In humans, *CR2* produces a long and short isoform with a strong preference for the long isoform of CR2 on FDCs (Liu et al., 1997). Understanding the splicing control mechanism disrupted in the *Cr2KO* mouse may elucidate the mechanism behind *CR2* isoform preference in humans.

Acknowledgment

The authors would like to thank the members of the Weis' laboratories for their insight and advice during the course of this investigation. We thank the Utah Transgenic and Knockout Mouse Core facility for helping with the creation of the *Cr2KO* animal. We also thank core facilities at this university for oligonucleotide preparation and DNA sequencing. This work was supported by the NIH (AI-24158 to JHW, and AI-32223 and AI-43521 to JJW), by the Weber Presidential Endowed Chair (JHW) and by the Training Program in Microbial Pathogenesis 5T32-AI-055434 (LRD).

References

Ahearn, J.M., M.B. Fischer, D. Croix, S. Goerg, M. Ma, J. Xia, X. Zhou, R.G. Howard, T.L. Rothstein, and M.C. Carroll. 1996. Disruption of the Cr2 locus results in a reduction in B-1a cells and in an impaired B cell response to T-dependent antigen. *Immunity* 4(3):251-262.

Bunting, M., K.E. Bernstein, J.M. Greer, M.R. Capecchi, and K.R. Thomas. 1999. Targeting genes for self-excision in the germ line. *Genes & Development* 13(12):1524-1528.

Carter, R.H., M.O. Spycher, Y.C. Ng, R. Hoffman, and D.T. Fearon. 1988. Synergistic interaction between complement receptor type 2 and membrane IgM on B lymphocytes. *J Immunol* 141(2):457-463.

Debnath, I., K.M. Roundy, J.J. Weis, and J. Weis. 2007. Defining in vivo transcription factor complexes of the murine CD21 and CD23 genes. *J Immunol* 178(11):7139-7150

Donius, L.R., J.M. Handy, J.J. Weis, and J. Weis. 2013. Optimal Germinal Center B Cell Activation and T-Dependent Antibody Responses Require Expression of the Mouse Complement Receptor Cr1. *J Immunol* 191(1):434-447.

Haas, K.M., M. Hasegawa, D.A. Steeber, J.C. Poe, M.D. Zabel, C.B. Bock, D.R. Karp, D.E. Briles, J. Weis, and T.F. Tedder. 2002. Complement receptors CD21/35 link innate and protective immunity during Streptococcus pneumoniae infection by regulating IgG3 antibody responses. *Immunity* 17(6):713-723.

Haas, K.M., J. Poe, and D. Steeber. 2005. B-1a and B-1b cells exhibit distinct developmental requirements and have unique functional roles in innate and adaptive immunity to S. pneumoniae. *Immunity* 23(1):7-18.

Haas, K.M., J. Poe, and T.F. Tedder. 2009. CD21/35 promotes protective immunity to Streptococcus pneumoniae through a complement-independent but CD19-dependent pathway that regulates PD-1 expression. *J Immunol* 183(6):3661-3671.

Holguin, M.H., C.B. Kurtz, C.J. Parker, J.J. Weis, and J. Weis. 1990. Loss of human CR1- and murine Crry-like exons in human CR2 transcripts due to CR2 gene mutations. *J Immunol* 145(6):1776-1781.

Jacobson, A., J.J. Weis, and J. Weis. 2008. Complement receptors 1 and 2 influence the immune environment in a B cell receptor-independent manner. *J Immunol* 180(7):5057-5066.

Krop, I., A.L. Shaffer, D.T. Fearon, and M.S. Schlissel. 1996. The signaling activity of murine CD19 is regulated during cell development. *J Immunol* 157(1):48-56.

Liu, Y.J., J. Xu, O. de Bouteiller, C.L. Parham, G. Grouard, O. Djossou, B. de Saint-Vis, S. Lebecque, J. Banchereau, and K.W. Moore. 1997. Follicular dendritic cells specifically express the long CR2/CD21 isoform. *J Exp Med* 185(1):165-170.

Loder, F., B. Mutschler, R.J. Ray, C.J. Paige, P. Sideras, R. Torres, M.C. Lamers, and R. Carsetti. 1999. B cell development in the spleen takes place in discrete steps and is determined by the quality of B cell receptor-derived signals. *J Exp Med* 190(1):75-89.

Matsumoto, A., D. Martin, R.H. Carter, L. Klickstein, J. Ahearn, and D. Fearon. 1993. Functional dissection of the CD21/CD19/TAPA-1/Leu-13 complex of B lymphocytes. *J Exp Med* 178(4):1407-1417.

Matsumoto, A.K., J. Kopicky-Burd, R.H. Carter, D.A. Tuveson, T.F. Tedder, and D.T. Fearon. 1991. Intersection of the complement and immune systems: a signal transduction complex of the B lymphocyte-containing complement receptor type 2 and CD19. *J Exp Med* 173(1):55-64.

Molina, H., V.M. Holers, B. Li, Y. Fung, S. Mariathasan, J. Goellner, J. Strauss-Schoenberger, R.W. Karr, and D.D. Chaplin. 1996. Markedly impaired humoral immune response in mice deficient in complement receptors 1 and 2. *Proc Natl Acad Sci USA* 93(8):3357-3361.

Molina, H., T. Kinoshita, C.B. Webster, and V.M. Holers. 1994. Analysis of C3b/C3d binding sites and factor I cofactor regions within mouse complement receptors 1 and 2. *J Immunol* 153(2):789-795.

Molina, H., S.J. Perkins, J. Guthridge, J. Gorka, T. Kinoshita, and V.M. Holers. 1995. Characterization of a complement receptor 2 (CR2, CD21) ligand binding site for C3. An initial model of ligand interaction with two linked short consensus repeat modules. *J Immunol* 154(10):5426-5435.

Oberdoerffer, S., L.F. Moita, D. Neems, R.P. Freitas, N. Hacohen, and A. Rao. 2008. Regulation of CD45 alternative splicing by heterogeneous ribonucleoprotein, hnRNPLL. *Science* 321(5889):686-691.

Pappworth, I.Y., C. Hayes, J. Dimmick, B.P. Morgan, V.M. Holers, and K.J. Marchbank. 2011. Mice expressing human CR1/CD35 have an enhanced humoral immune response to T-dependent antigens but fail to correct the effect of premature human CR2 expression. *Immunobiology* 217(2):147-157.

Pepys, M.B. 1974. Role of complement in induction of antibody production in vivo. Effect of cobra factor and other C3-reactive agents on thymus-dependent and thymus-independent antibody responses. *J Exp Med* 140(1):126-145.

Pramoonjago, P., J. Takeda, Y.U. Kim, K. Inoue, and T. Kinoshita. 1993. Ligand specificities of mouse complement receptor types 1 (CR1) and 2 (CR2) purified from spleen cells. *Int Immunol* 5(4):337-343.

Preussner, M., S. Schreiner, L.H. Hung, M. Porstner, H.M. Jack, V. Benes, G. Ratsch, and A. Bindereif. 2012. HnRNP L and L-like cooperate in multiple-exon regulation of CD45 alternative splicing. *Nucleic Acids Res* 40(12):5666-5678.

Rothrock, C.R., A.E. House, and K.W. Lynch. 2005. HnRNP L represses exon splicing via a regulated exonic splicing silencer. *EMBO J* 24(15):2792-2802.

Roundy, K.M., J.J. Weis, and J. Weis. 2009. Deletion of putative intronic control sequences does not alter cell or stage specific expression of Cr2. *Mol Immunol* 47(2):517-525.

Seregin, S.S., Y.A. Aldhamen, D.M. Appledorn, N.J. Schuldt, A.J. McBride, M. Bujold, S.S. Godbehere, and A. Amalfitano. 2009. CR1/2 is an important suppressor of Adenovirus-induced innate immune responses and is required for induction of neutralizing antibodies. *Gene Ther* 16(10):1245-1259.

Tan, S.S., and J.H. Weis. 1992. Development of a sensitive reverse transcriptase PCR assay, RT-RPCR, utilizing rapid cycle times. *PCR Methods Appl* 2(2):137-143.

Tong, A., J. Nguyen, and K.W. Lynch. 2005. Differential expression of CD45 isoforms is controlled by the combined activity of basal and inducible splicing-regulatory elements in each of the variable exons. *J Biol Chem* 280(46):38297-38304.

Wu, X., N. Jiang, Y.-F. Fang, C. Xu, D. Mao, J. Singh, Y.-X. Fu, and H. Molina. 2000. Impaired affinity maturation in Cr2-/- mice is rescued by adjuvants without improvement in germinal center development. *J Immunol* 165(6):3119-3127.

Zabel, M.D., J.J. Weis, and J. Weis. 1999. Lymphoid transcription of the murine CD21 gene is positively regulated by histone acetylation. *J Immunol* 163(5):2697-2703.

CHAPTER 3

OPTIMAL GERMINAL CENTER B CELL ACTIVATION AND T-DEPENDENT ANTIBODY RESPONSES REQUIRE EXPRESSION OF THE MOUSE COMPLEMENT RECEPTOR Cr1

Reprint of: Luke R Donius, Jennifer M Handy, Janis J Weis, and John H Weis. 2013. Optimal Germinal Center B Cell Activation and T-Dependent Antibody Responses Require Expression of the Mouse Complement Receptor Cr1. *The Journal of Immunology* 191(1):434-447.

The Journal of Immunology

Optimal Germinal Center B Cell Activation and T-Dependent Antibody Responses Require Expression of the Mouse Complement Receptor Cr1

Luke R. Donius, Jennifer M. Handy, Janis J. Weis, and John H. Weis

Follicular dendritic cells (FDCs) and complement receptor (Cr)1 and complement receptor (Cr)2 are important for the generation of humoral immunity. Cr1/2 expression on B cells and FDCs was shown to provide a secondary signal for B cell activation, to facilitate transport of Ag in immune follicles, and to enhance retention of immune complexes by FDCs. We show in this study that murine B cells predominantly express the Cr2 product from the *Cr2* gene, whereas FDCs almost exclusively express the Cr1 isoform generated from the *Cr2* gene. To define the specific role of Cr1, we created an animal that maintains normal cell-restricted expression of Cr2 but does not express Cr1. Cr1-deficient (*Cr1KO*) mice develop normal B1 and B2 immature and mature B cell subsets and have normal levels of naive serum Abs but altered levels of natural Abs. Immunization of the *Cr1KO* animal demonstrates deficient Ab responses to T-dependent, but not T-independent, Ags. Germinal centers from the immunized *Cr1KO* animal possess a deficiency in activated B cells, similar to that seen for animals lacking both Cr1 and Cr2 or C3. Finally, animals lacking only Cr1 respond similarly to wild-type animals to infections with *Streptococcus pneumoniae*, a pathogen to which animals lacking C3 or both Cr1 and Cr2 are particularly sensitive. Altogether, these data suggest that the production of Cr1, primarily by FDCs, is critical in the generation of appropriately activated B cells of the germinal center and the generation of mature Ab responses. ***The Journal of Immunology*****, 2013, 191: 434–447.**

Antibodies (Igs) are the major effectors of the adaptive immune response, and different isotype classes of Ab are produced to achieve different effects with Ab of the same specificity. Ig class-switch recombination is a hallmark of B cell responses to T-dependent (TD) Ags (1). These reactions occur within immune follicles of secondary immune structures, such as the spleen and lymph nodes (2). Central to follicles are follicular dendritic cells (FDCs), which establish the zonal identity (3) and act as a concentrated depot of Ag. In the course of an immune challenge, Ag is trafficked to the FDCs (4–6), where follicular B cells are recruited for surveillance of retained Ag. BCR specificity for an Ag retained on an FDC results in internalization and processing for presentation to T cells. The B cell then migrates to the T cell zone and presents the processed peptide to Th cells in the context of class II MHC. Upon a secondary signal from a peptide-specific Th cell, this B cell undergoes somatic hypermutation and isotype switch. These activated germinal center (GC) B cells must then retest their new Ig before undergoing clonal expansion and differentiation to either a plasma or memory cell. FDCs play an integral role in retention of Ag for this test of the new Ig, as well. Transport to and capture of Ag by FDCs in a primary immune response uses the protein products of the mouse *Cr2* gene: complement receptor (Cr)1 and complement receptor (Cr)2 (4).

The predominant role of the complement cascade is detection of danger signals via the classical, mannose-binding lectin and alternative pathways and targeting of bound cells for lytic killing by the membrane attack complex (7–9). However, in addition to targeting foreign cells for membrane attack complex lysis, opsonization by the protein C3 can be used in transport to an FDC, phagocytosis, secondary signals through various complement receptors, and activation of more complement. These outcomes are dependent on the cleavage fragment of C3 and the corresponding cell receptor that they encounter. C3 is central to all three complement pathways; upon activation, it is cleaved into C3b and C3a. C3a is a potent anaphylatoxin that diffuses away to recruit and activate cells, whereas C3b remains bound to the foreign molecule and forms a C3 convertase complex that cleaves more C3. Alternatively, in the presence of the complement regulator, factor I, and one of the cofactors—factor H, Crry, or Cr1—C3b can be cleaved into one of the enzymatically inactive fragments: iC3b or C3d(g). Activation of the complement pathway can modulate humoral immunity (10) through the complement receptors 1 and 2 (Cr1 and Cr2) (11–14). Both Cr1 and Cr2 can bind the terminal cleavage products of C3: iC3b, and C3d(g). In addition, Cr1 is capable of binding the enzymatically active C3 convertase subunit C3b and acting as a cofactor for factor I cleavage of C3b to iC3b or C3d(g) (15).

The mouse differs from the human in that the single mouse *Cr2* gene encodes both Cr1 and Cr2 via alternative splicing, whereas primates use distinct genes for the CR1 and CR2 proteins (16). Expression of the mouse *Cr2* gene by B cells and FDCs has long been held under the assumption that the two different isoforms, Cr1 and Cr2, are produced equally in both of these distinct cell

Division of Cell Biology and Immunology, Department of Pathology, University of Utah School of Medicine, Salt Lake City, UT 84112

Received for publication November 19, 2012. Accepted for publication May 5, 2013.

This work was supported by Public Health Service Grants AI-24158 and AI-088451 (to J.H.W.) and AI-32223 and AI-43521 (to J.J.W.), Training Program in Microbial Pathogenesis 5T32-AI-055434 (to L.R.D.), and funds from the George J. Weber Presidential Endowed Chair (to J.H.W.).

Address correspondence and reprint requests to Dr. John H. Weis, Division of Cell Biology and Immunology, Department of Pathology, University of Utah School of Medicine, Salt Lake City, UT 84112. E-mail address: john.weis@path.utah.edu

The online version of this article contains supplemental material.

Abbreviations used in this article: *C3KO*, complement component C3 knockout; Cr1, complement receptor 1; Cr2, complement receptor 2; *Cr1KO*, complement receptor 1 knockout; *Cr1/2KO*, complement receptor 1 and 2 knockout; dpi, days postinfection; DZ, dark zone; FDC, follicular dendritic cell; FOB, follicular mature B cell; GC, germinal center; KLH, keyhole limpet hemocyanin; LZ, light zone; MFI, mean fluorescent intensity; MZB, marginal zone B cell; PBT, 0.1% Tween-20 in 1× PBS; T1, transition 1; T2, transition 2; TD, T dependent; TI, T independent; TNP, trinitrophenyl; WT, wild-type.

 0022-1767/13/$16.00

www.jimmunol.org/cgi/doi/10.4049/jimmunol.1203176

types. Functionally, mouse knockout models addressed the loss of both Cr1 and Cr2 when critical sequences of the *Cr2* gene were deleted (12, 13). These studies did not delineate the specific functions of the Cr1 and Cr2 proteins on B cells and FDCs, and elevated surface expression of CD19 on Cr1/2-deficient (*Cr1/2KO*) B cells was proposed to lead to B cell anergy (17). Additional studies also used *Cr1/2KO* animals to examine the function of human CR1 or CR2 via transgenic-expression models of these proteins using Ig gene promoters (18, 19). In these studies, however, premature expression of the transgenes (compared with native *Cr2*), lack of FDC expression, expression in inappropriate cell types (e.g., T cells), and the structural distinctness of human CR1 compared with the mouse Cr1 protein introduces critical variables. In light of these variables, neither of the human CR1 or CR2 transgenic models elucidates the individual functions of the Cr1 and Cr2 proteins (mouse or human) in the context of their autochthonous immune response.

To directly assess the phenotype of an animal lacking Cr1, but expressing Cr2 under the endogenous transcriptional controls of the *Cr2* gene, we created a novel mouse Cr1 knockout model (*Cr1KO*) in which the exons encoding the domains unique to the Cr1 protein were removed, forcing *Cr2* gene transcripts to splice from the exon encoding the signal sequence to the exon encoding the first domain of the Cr2 protein. The validation of the *Cr1KO* animal showed a complete lack of that protein. Comparison of this animal with wild-type (WT) mice demonstrated the Cr1 protein on FDCs and Cr2 protein on B cells as the dominant *Cr2* gene isoforms on these cell types in the native animal. *Cr1KO* mice display numerous phenotypes that are different from WT and *Cr1/2KO* mice. *Cr1KO* mice do not exhibit the Ab response deficiencies to T-independent (TI) and low-dose TD Ags that are hallmarks of *Cr1/2KO* mice. *Cr1KO* mice also do not produce WT levels of Ab against a high dose of TD Ag, and they generate fewer activated B cells in response to TD Ags. Additionally, *Cr1KO* mice do not suffer from the reduced immunity to the bacterial pathogen *Streptococcus pneumoniae* like *Cr1/2KO* mice do. Altogether, these studies describe a new mouse strain specifically deficient in Cr1, but not Cr2; demonstrate a novel Cr1 expression preference by FDCs compared with Cr2; and further support that Cr1 is an important surface protein required for the generation of an optimal humoral immune response.

Materials and Methods

Generation of Cr1KO *mice*

A 21-kb construct was built in the pBluescriptII KS+ vector. Homologous recombination was targeted to the intronic EcoRV restriction fragment of the *Cr2* gene 5′ to exon 2 and the NheI restriction fragment 3′ to exon 8 to delete exons 2 through 8 while leaving the sequence for splicing of *Cr2* (Fig. 1A). These fragments were fused to the germline self-deleting neomycin-containing pACN positive-selection vector (20). Targeted homologous recombination was enhanced by the flanking TK1TK2 thymidine kinase–expressing negative-selection vector. The pACN and TK1TK2 vectors were obtained from the University of Utah Transgenic and Gene Targeting Mouse Core. The linearized construct was targeted to mouse strain 129–derived embryonic stem cells by electroporation, and 192 clones were screened by Southern blot for homologous recombination of the *Cr1KO* construct. Chimeras were generated via injection of a positive clone into blastocyst and surrogate implantation. Electroporation, blastocyst injection, and chimera generation were performed by the University of Utah Transgenic and Gene Targeting Mouse Core. The *Cr1KO* construct insertion was tracked via PCR of DNA isolated from tail biopsies. Primers flanking exon 2, upstream of the EcoRV site (#4150 5′-TAGTGTGAGACGGAATCTTAACAC-3′), and exon 8, downstream of the NheI site (#4316 5′-GCAGGTAGCACAGTTACATTAGATAC-3′), were designed to amplify a 483-bp fragment upon recombination for identification of the *Cr1KO* condition. The WT allele was identified with a primer from coding sequences in exon 8 (#4404 5′-TGGAATAATAAGTTTCCTGTCT-GTG-3′) and a primer in the adjacent intron between exons 8 and 9 but upstream of the NheI site (#4422 5′-AGAACTCTTCAGTAAAAGGCATG-AC-3′) that generated a 350-bp product. All experiments were carried out using *Cr1KO* mice backcrossed to C57BL/6 or BALB/C mice for at least five generations. WT C57BL/6 and BALB/C mice, as well as complement component 3–deficient (*C3KO*) mice, were purchased from The Jackson Laboratory (Bar Harbor, ME) or obtained from colonies bred on location. C57BL/6-derived (*Cr1KO*, *Cr1/2KO*, *C3KO*, and WT) (12) 8–16-wk-old male and female mice were used in all experiments, unless otherwise specified. Mice were sex matched across genotypes. All mice were housed at the Comparative Medicine Center (University of Utah Health Sciences Center) in accordance with the National Institutes of Health guidelines for the care and use of laboratory animals. Mice were housed in an Animal Biosafety Level 2 protocol–approved area for all *Streptococcus pneumoniae* infection experiments.

Total splenic protein isolation

Splenic protein isolation, with FDCs included, was performed by extracting approximately two thirds of a spleen (RNA was isolated from the remaining third using the method described above) from a mouse and disrupting it with a razor blade in 5 ml ice-cold PBS. The dissociated spleen was then pipetted into a 15-ml conical tube and centrifuged at 300 × *g*, and the supernatant was discarded. The dissociated spleen was resuspended in 300 μl RIPA buffer containing protease inhibitors (complete, mini, EDTA-free, ultra tablets; Roche Diagnostics, Indianapolis IN), transferred to a 1.5-ml microcentrifuge tube, and placed in a rotator at 4°C for 45 min. The solubilized protein was isolated by centrifuging the lysate at high speed (4°C) in a microcentrifuge for 10 min and collecting the supernatant. The resulting protein isolate was stored at −70°C until Western blot analysis.

Bone marrow transplantation

Transplant recipients were lethally irradiated 24 h prior to transplantation with two doses of 500 cGy with an x-ray irradiator. Bone marrow donor mice were sacrificed, and marrow was isolated from the femurs and tibias. RBCs were lysed with ACK lysis buffer, and the remaining cells were washed, strained through 100-μm mesh, and resuspended in ~300 μl PBS/mouse. Each recipient mouse was anesthetized with isoflurane and given 100 μl sex-matched bone marrow retro-orbitally. One donor's marrow was transplanted into up to three recipients. Mice were maintained on antibiotic water, and engraftment was allowed for 6 wk.

Quantitative RT-PCR

Total spleen RNA was isolated using the CsCl centrifugation method, as described previously (21). Briefly, spleens were isolated from mice, homogenized using a tissuemizer in 4 M guanidine isothiocyanate solution, and centrifuged at 30,000 rpm overnight on a 5.7-M CsCl gradient. The RNA pellet was recovered and resuspended in 400 μl nuclease-free water with 0.2 M NaCl, and ethanol was precipitated for 3 h. The RNA was pelleted at high speed in a microcentrifuge, washed with 70% ethanol, and resuspended in 50 μl nuclease-free water. cDNA was generated as previously described (22). Quantification of transcript levels for *Cr1*, *Cr2*, *Cr1/2*, *Alox5*, *Dbp*, *Ctsg*, *Fv*, *Lcn2*, *Klra18*, and *β-actin* was measured using a Roche LightCycler, as described previously (21, 23). Primers for PCR of total *Cr1/2* transcript were #4824 5′-AAGGAAGCAAAACTGTCTGGTGC-3′ and #4825 5′-CCCG-CAACAAACTGGTCAAC-3′. Primers for PCR of *Cr1*- and *Cr2*-specific transcripts were as previously published (22, 24, 25). PCR primers for quantification of *Alox5*, *Dbp*, *Ctsg*, *Fv*, *Lcn2*, *Klra18*, and *β-actin* were as previously published (25).

Western blot analysis

Western blot analysis was performed as previously described (22). For Cr1/2 protein detection, the membrane was blocked in 5% milk 0.2% Tween-20 in 1× TBS. Cr1/2 were detected with goat polyclonal anti-CD21 (Santa Cruz Biotechnology; #sc-7027) and visualized with the HRP-conjugated secondary Ab bovine anti-goat IgG (Jackson ImmunoResearch; #805-035-180).

Immunohistochemistry

Spleens were prepared by fixing in 4% paraformaldehyde and dehydrating in 5, 15, and 30% sucrose in PBS. Spleens were then frozen on dry ice in OCT embedding medium (Sakura Finetek USA, Torrance, CA) and stored at −70°C. Frozen spleens were sectioned on a cryostat at a thickness of 10–12 μm. Spleen sections were rehydrated in 0.1% Tween-20 in 1× PBS (PBT), treated with H_2O_2 in PBT, washed three times with PBT, and blocked with 1% BSA 1:50 anti-CD16/32 (Fc Block; eBioscience clone #93) for 1 h. Blocking buffer was discarded, and the sections were incubated overnight with biotinylated primary Ab at 4°C (anti-Cr1/2 clone 7E9 or anti-Cr1 clone 8C12). Sections were rinsed once with PBT and then

washed three times with PBT. Sections were then incubated with a 1:1000 dilution of streptavidin conjugated to HRP in 1% BSA PBT for 1 h at room temperature. Sections were washed with PBT, stained with 3, 3′-diaminobenzidine (Vector Laboratories, Burlingame, CA) per the manufacturer's protocol, and counterstained with hematoxylin QS (Vector Laboratories). Sections were then overlaid with VectaMount AQ (Vector Laboratories) preservation reagent, cover slipped, and sealed with fingernail polish.

ELISA

ELISAs to determine total serum Ab titers and Ag-specific Ab titers were performed using the same basic blocking, washing, and detection protocol. ELISA plates were prepared as follows for Ag-specific Ab quantification: 5 μg/ml trinitrophenyl (TNP)-BSA (TNP-LPS and TNP-keyhole limpet hemocyanin [KLH] Ab-response measurement), 5 μg/ml DNP-BSA (DNP–AECM–Ficoll Ab response measurement), 5 μg/ml phosphorylcholine-BSA (phosphorylcholine natural Ab quantification) (all conjugates from Biosearch Technologies), or 5 μg/ml KLH (Sigma-Aldrich) in 1× PBS was prepared and dispensed in volumes of 100 μl/well onto Immulon 4 HBX (Thermo Scientific) plates. Sandwich ELISA plates for total serum Ab quantification were prepared by incubating plates with 5 μg/ml anti-mouse IgM–IgG–IgA Ab (Pierce #31171) in carbonate buffer (15 mM Na_2CO_3, 35 mM $NaHCO_3$, 3.1 mM NaN_3). Polysorp plates (Thermo Scientific) for detection of chitin/chitosan-specific Ab were prepared as described (26). Maxisorp plates (Thermo Scientific) for dsDNA-specific Ab were coated overnight with 10 μg/ml calf thymus DNA in 1× PBS at 4°C. Plates were covered and incubated overnight at 4°C. Solution was discarded, and all wells were blocked with 200 μl 5% BSA 0.1% Tween-20 in 1× PBS blocking buffer for 1 h at room temperature. Blocking buffer was discarded, and wells were washed three times with 0.1% Tween-20 in 1× PBS (ELISA wash buffer). Serum samples were then applied serially to wells in 5% BSA in 1× PBS as follows: natural Ab detection, 1:50, 1:100, 1:200, and 1:400; total serum Ig IgM, 1:4,000, 1:8,000, 1:16,000, and 1:32,000; IgG subclasses, 1:2,000, 1:4,000, 1:8,000, and 1:16,000; and Ag-specific Ig, 1:200, 1:400, 1:800, and 1:1,600. Serum was incubated in wells at room temperature for 1.5 h. Serum was discarded, and all wells were washed three times with ELISA wash buffer. Secondary Ab was diluted 1:2000 in 5% BSA in 1× PBS, and 100 μl was distributed to each well and incubated for 1.5 h at room temperature. All secondary Abs were conjugated to HRP: rabbit anti-mouse IgM (Jackson ImmunoResearch #315-035-049), rabbit anti-mouse IgG1 (Zymed #61-0120), rabbit anti-mouse IgG2b (Zymed #61-0320), goat anti-mouse IgG2c (Jackson ImmunoResearch #115-035-208), and goat anti-mouse IgG3 (AbD Serotec #STAR6P). The secondary solution was then discarded, and the wells were washed six times with ELISA wash buffer. Bound secondary Ab was then detected by exposing to 100 μl *o*-phenylenediamine solution (8 mg *o*-phenylenediamine and 6.6 μl H_2O_2 in 20 ml citrate buffer) and stopped with 100 μl 1 N HCl, and the absorbance was read at 490 nm with a BioTek plate reader. The absorbance values were calculated by subtracting the absorbance reading at 490 nm of a well without serum treatment. Positive control Abs used were mouse IgM (eBioscience clone #11E10), purified mouse myeloma IgG1 (Invitrogen #026100), mouse IgG2b (eBioscience clone #eBMG2b), mouse IgG2c (Southern Biotech #0122-01), and mouse IgG3 (eBioscience #14-4742-85).

ELISA detection of SRBC-specific Ab was done using a variation of methods described above and elsewhere (27, 28). Immulon 4HBX plates were precoated overnight at 4°C with 5×10^7 SRBCs/100 μl PBS/well. Following overnight incubation, the SRBCs were fixed to the plate by adding 20 μl 1.8% glutaraldehyde to each well (taking care not to disturb the SRBC layer), bringing the final concentration of glutaraldehyde to 0.3%. After a 30-min incubation with glutaraldehyde at room temperature, the contents of each plate were discarded, and the wells were washed four times with 100 μl PBS. Wells were blocked with 200 μl 1% BSA in PBS for 1 h at room temperature. Blocking buffer was discarded, and serum samples were distributed to plates in 0.05% Tween 1% BSA PBS. All serum samples were diluted serially (1:50–1:400 for IgM and 1:200–1:1600 for IgG) and tested in duplicate. Nonspecific IgM or IgG samples were included as negative controls. Serum samples were incubated for 2 h at room temperature. Wells were then washed three times with PBS and 100 μl 1:2000 rabbit anti-mouse IgM, Fc μ chain specific, conjugated to HRP (Jackson ImmunoResearch #315-035-049) or 1:2000 sheep anti-mouse IgG, Fc γ-chain specific, conjugated to HRP (Jackson ImmunoResearch #515-035-071) in 0.05% Tween 1% BSA PBS. After a 1.5-h incubation at room temperature, the plates were washed three times with PBS, and incubation with *o*-phenylenediamine solution was used for visualization, as above.

FACS

Bone marrow, peritoneal cells, or splenocytes were isolated from isoflurane-anesthetized and cervically dislocated mice. Bone marrow was obtained by dissecting the femurs and tibias of mice, slicing the ends of the bones off with a razor blade, and flushing the cells from the bone with 5% BSA (Sigma-Aldrich A7906) in PBS using a 23-gauge needle. Peritoneal cells were obtained by injecting 5 ml 5% BSA PBS into the peritoneal cavity, massaging the mouse's abdomen, and retrieving the fluid from the peritoneal cavity, as described in detail by Ray and Dittel (29). Splenocytes were obtained by dissecting the spleen and mashing it through a 100-μm cell strainer. The RBCs were lysed with ACK buffer (0.15 M NH_4Cl, 1 mM $KHCO_3$, 0.1 mM Na_2EDTA). Cells were washed with 5% BSA PBS, and 2×10^6 cells were stained in 100 μl Ab or streptavidin-conjugated fluorophore staining mix. Incubations were 20 min on ice, followed by a 5% BSA PBS wash and resuspension in 500 μl 5% BSA PBS or secondary incubation. Abs used for FACS were as follows: anti-CD19 (clone 1D9; eBioscience), B220 (clone RA3-6B2; BioLegend), anti-CD21/35 (clones 7G6, BD Pharmingen; 7E9, BioLegend; eBio8D9, eBioscience), anti-CD35 (clone 8C12; BD Pharmingen), anti-CD11b (clone M1/70; BioLegend and eBioscience), anti-CD5 (clone 53-7.3; eBioscience), anti-CD23 (clone B3B4; BioLegend and eBioscience), anti-IgM (clone eB121-15F9; eBioscience), anti-CD24 (clone M1/69; BioLegend and eBioscience), anti-IgD (clone 11-26c.2a; BioLegend), anti-GL7 (clone GL7; eBioscience), anti-CD16/32 (FcR block, clone 93; eBioscience), and rat IgM–Alexa Fluor 488 isotype control (eBRM; eBioscience). Cells were strained through 100-μm mesh to disrupt cell clumps, vortexed gently with 1.5 μl 1 mM DAPI for live/dead discrimination, and analyzed using a FACSCanto II (BD Biosciences). FACS data were quantified using FlowJo software, version 8.8.7 (TreeStar).

S. pneumoniae *culture and preparation*

S. pneumoniae was generously provided by Kristina Pierce (University of Utah Medical Technology Laboratory). It was presumptively reconfirmed via exhibition of α-hemolysis and optochin sensitivity (Taxo P Discs; BD Biosciences). The isolate was determined to be serotype 3 by the Statens Serum Institute (Copenhagen, Denmark). *S. pneumoniae* was passaged once through mice by isolating viable *S. pneumoniae* from the spleen of a lethally infected C57BL/6 mouse. Isolation was performed by straining the spleen through a 100-μm strainer into sterile 5% BSA PBS and growing serial dilutions on 5% Sheep Blood Columbia Agar plates (BD Biosciences) in a candle jar (~5% CO_2) at 37°C. Five milliliters of 0.5% yeast–supplemented Todd Hewitt Broth (BD Biosciences) was inoculated with one colony *S. pneumoniae* and incubated for 3 h at 37°C in a candle jar. A total of 750 μl inoculum was transferred to 70 ml yeast-supplemented Todd Hewitt Broth and incubated for 5.5 h (adapted from Ref. 30). Twenty-five milliliters of culture was diluted to 10% glycerol and frozen in 1-ml aliquots in cryovials at −70°C. An additional 30 ml was heat killed at 60°C for 2 h, aliquoted in 1-ml volumes, and frozen at −70°C. Serial dilutions were plated on 5% Blood Columbia Agar plates for quantification, and heat-killed *S. pneumoniae* was plated to confirm inactivation.

Immunizations and S. pneumoniae *infections*

All immunizations and infections were given i.p. to 2–3-mo-old mice. Doses for TI and TD Ag-specific Ig response curves were 50 μg TNP-LPS, 25 μg DNP–AECM–Ficoll, 10 μg TNP-KLH, and 100 μg TNP-KLH (all from Biosearch Technologies, Novato, CA). Serum for Ig titering was obtained by collecting tail vein blood into heparinized capillary tubes, centrifuging at 13,000 rpm in a microcentrifuge for 6 min, and collecting the supernatant. Serum was collected every 7 d for 21 d. The low- and high-dose (10 and 100 μg) TD primary immunizations were followed 21 d later by a secondary boost of the same quantity, and an additional 28 d serum collection was done to measure the secondary Ig response.

For GC B cell–activation experiments, mice were injected with 2×10^8 SRBCs (Innovative Research, Novi, MI). Seven days later the mice were sacrificed, and splenocytes were analyzed via FACS.

Mice in *S. pneumoniae* experiments were injected with 1×10^5 heat-killed *S. pneumoniae*, followed 10 d later by infection with 1000 CFU *S. pneumoniae*. Mice were monitored daily for survival.

Results

Creation and characterization of a Cr1-deficient mouse

The functions of Cr1/2 have been well established to be important in humoral immunity. To investigate the independent roles of Cr1 and Cr2 in a cell- and stage-specific manner for the generation of functional Ab responses, we generated a Cr1-deficient, but Cr2-sufficient, *Cr1KO* mouse line. To delete *Cr1*-specific transcripts from *Cr2* without disrupting the *Cr2* locus, a construct was produced in which DNA from the Cr2 gene promoter, transcription start site, and the

first coding exon (encoding the signal sequence) was fused to the germline sequences possessing the C-terminal exons specific for the Cr2 protein (Fig. 1A). Care was taken to include flanking intronic DNA so as not to disrupt sequences required for the appropriate splicing of *Cr2* transcripts. The region between these two genomic sequences (occupied by Cr1-encoding exons in the native gene) was replaced with a neomycin selection cassette that would self-delete in the sperm of targeted animals, leaving behind a single Lox site. Analysis of *Cr1* and *Cr2* splenocyte transcripts in the *Cr1KO* animal was performed by quantitative RT-PCR using oligonucleotide sets specific for the *Cr1*-encoding transcript, a second set specific for the *Cr2* product, and a third set that includes sequences common to both *Cr1* and *Cr2* products. As expected, *Cr1KO* mice lacked Cr1-specific transcripts and expressed higher levels of Cr2-encoding transcripts than did WT mice (data not shown).

The absence of the Cr1 protein in the *Cr1KO* animal was verified by immunoblot analysis of total splenocytes and $B220^+$ splenocytes (Fig. 1B) using a polyclonal Ab with specificity for Cr1 and Cr2. The WT samples showed higher quantities of Cr2 compared with Cr1, whereas the *Cr1KO* animal only expressed Cr2 protein. FACS analysis of the expression of the Cr1 and Cr2 proteins on splenic $B220^+$ B cells was done using the Cr1-specific Ab 8C12 and the 7G6 Ab, which recognizes both the Cr1 and Cr2 proteins (Fig. 1C). These data demonstrate the absence of the Cr1 protein (8C12) and the elevated surface expression of the Cr2 protein (7G6) on the *Cr1KO* cells compared with WT cells. Similar data were obtained using the anti-Cr1/Cr2 Abs eBio8D9 and 7E9 (data not shown), indicating that Cr1 deletion results in a filling of the Cr1/2 niche with Cr2. It should be noted that the preparation of isolated splenocytes for analysis in Fig. 1B and 1C was accomplished by straining mechanically disrupted spleens through 100-μm cell strainers prior to analysis, which results in the loss of FDCs from these cell populations.

Phenotypic analysis of the Cr1KO *mouse*

The mouse Cr1 and Cr2 proteins form complexes with CD19 on the surface of mouse B cells. The absence of Cr2 gene products on the surface of *Cr1/2KO* B cells was linked to the elevated expression of CD19 that is proposed as one mechanism leading to reduced B cell responses to Ag (17). To determine whether Cr2 sufficiency returned CD19 expression on B cells to normal in *Cr1KO* mice, we measured the mean fluorescent intensity (MFI) of CD19 staining on live $B220^+$ cells from the spleen (Supplemental Fig. 1B). The MFI of CD19 staining on the *Cr1KO* cells was somewhat

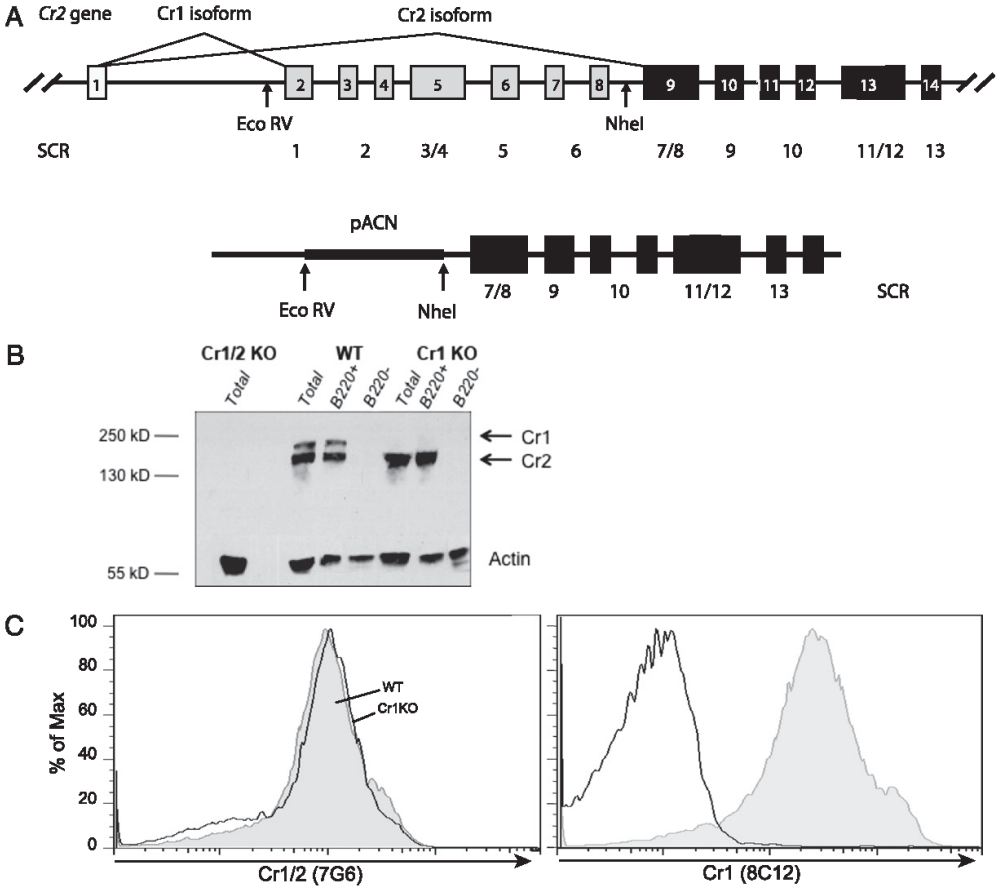

FIGURE 1. Cr1-specific deletion by targeted homologous recombination. (**A**) Diagram of the *Cr2* gene and the construct used for targeted deletion of the Cr1-specific exons. Exons are denoted 1–14 and are not inclusive of all of the 3′ *Cr2* gene exons. The coding sequences for the amino terminal SCR domains are also noted, with the *Cr1KO* deletion resulting in the deletion of exons encoding the first six SCRs of the Cr1 protein. (**B**) Western blot analysis of strained spleen lysates (no FDCs) from $B220^+$-sorted, $B220^-$-sorted, or total spleen cells. (**C**) FACS analysis of $CD19^+B220^+$ mature splenic B cells for the expression of Cr1 and Cr2 (*left panel*; 7G6 Ab) and Cr1 (*right panel*; 8C12 Ab).

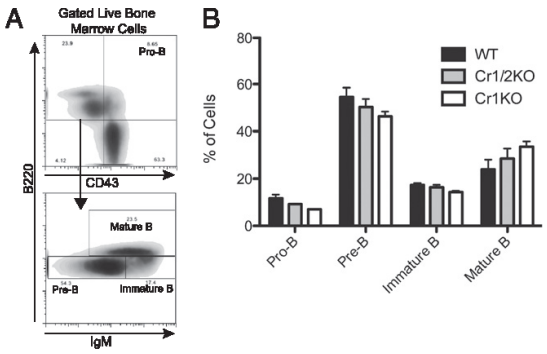

FIGURE 2. Analysis of bone marrow B cell populations from WT, *Cr1KO*, and *Cr1/2KO* mice. (**A**) Representative gating for delineating pro-B cells ($B220^+$ $CD43^+$), pre-B cells ($CD43^-$ IgM^{lo} $B220^{lo}$), immature B cells ($CD43^-$ IgM^{hi} $B220^{lo}$), and mature ($CD43^-$ IgM^{hi} $B220^{hi}$) B cells. All cells were first segregated as live ($DAPI^-$). (**B**) Quantification of the frequency of pro-, pre-, immature, and mature B cells from WT, *Cr1/2KO*, and *Cr1KO* bone marrow, as defined by the gating strategy in (A). Pre, immature, and mature B cell populations were not significantly different by ANOVA. $n = 3$; age- and sex-matched 8–12-wk-old mice; C57BL/6 background.

less than that of WT cells and substantially less than that seen on the surface of *Cr1/2KO* B cells.

Analysis of B cell subsets from *Cr1KO* mice identified no significant differences compared with WT mice. B cells in the marrow of adult mice were examined (Fig. 2) based upon the differential expression of B220, CD43, and IgM (Fig. 2A) to delineate pro-B, pre-B, immature, and mature B cells. The frequencies of each of these B cell subsets in *Cr1KO* and *Cr1/2KO* mice were not altered compared with WT mice based on ANOVA (Fig. 2B). The expression level of CD19 was also quantified on these B cell subsets (Supplemental Fig. 1A) and was shown to be identical for the four subsets of B cells, with the exception of mature B cells, which displayed a significant ($p < 0.01$) reduction in the expression of surface CD19 in *Cr1KO* mice and a significantly ($p < 0.01$) increased expression in *Cr1/2KO* mice.

FACS analysis of the $B220^+$ $CD11b^+$ and $CD5^+$ (B1a) and $CD5^-$ (B1b) cells of the peritoneal cavity revealed that they were not present at different frequencies in *Cr1KO* mice compared with WT mice (Fig. 3). Interestingly, a significant ($p < 0.001$) reduction in the frequency of B1a cells in *Cr1/2KO* mice was observed (Fig. 3B). This decrease in B1a B cells had not been documented in *Cr1/2KO* animals (12, 13), but it was described for the hypomorphic Cr1/2-deletion animal (31, 32). A decrease in B1a cells in *Cr1KO* mice was not observed. Quantification of the MFI of CD19 on the surface of the B1a and B1b cells from *Cr1KO* animals did not show any significant difference compared with WT or *Cr1/2KO* animals (Supplemental Fig. 1B).

The numbers of mature B cell subsets in the spleen of *Cr1KO* mice were also analyzed based upon differential staining of B220, CD23, CD24, and CD21/35 (Cr1/2) (Fig. 4). Comparable transition 1 (T1), transition 2 (T2), follicular mature B cell (FOB), and marginal zone B cell (MZB) subset frequencies were found in the spleens of *Cr1KO* mice as in WT and *WT/Cr1KO* heterozygote animals (ANOVA). The expression of Cr2 in the *Cr1KO* animal was consistent with the generation of T2 B cells at the same point in B cell maturation as WT B cells. Therefore, the loss of Cr1 on the surface of murine B cells did not alter their development or their localization within the splenic B cell populations.

We showed previously that the spleens of *Cr1/2KO* animals displayed signatures of a more highly inflamed environment than did WT mice, presumably due to the lack of control of complement convertases in immune complexes within immune follicles (25). The analysis of total splenic transcripts for inflammatory response genes also demonstrated altered expression of inflammatory mediator genes in the *Cr1KO* spleen compared with WT and *Cr1/2KO* animals (Supplemental Fig. 2).

The Cr1 isoform is the dominant Cr2 *gene product on FDCs*

The two major cell types of the mouse that express the *Cr2* gene are the B cell and the FDC. As described above, the Cr1 and Cr2 proteins are generated from alternative splice isoforms from the *Cr2* gene. As shown previously (Fig. 1B), immunoblot analysis of total splenic cell populations (isolated by straining free cells away from the FDC-enriched stromal matrix) for the total *Cr2* gene

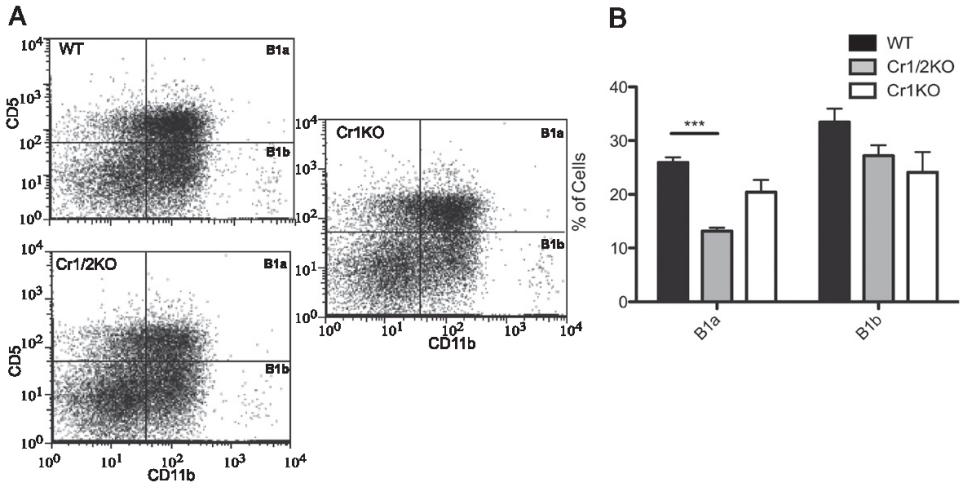

FIGURE 3. Analysis of *Cr1KO* peritoneal B1a and B1b populations by FACS. (**A**) Representative plots of B1a ($CD5^+$ $CD11b^+$) and B1b ($CD5^-$ $CD11b^+$) cell population frequency in WT, *Cr1KO*, and *Cr1/2KO* mice. All cells shown were first segregated as live ($DAPI^-$) and $B220^+$. (**B**) Quantification of B1a and B1b population frequency (one-way ANOVA, $p < 0.05$ for B1a; B1b, not significantly different). $n = 4$ WT and *Cr1KO*, $n = 3$ *Cr1/2KO*; age- and sex-matched 8–12-wk-old mice; C57BL/6 background. $^{***}p < 0.001$, Student t test.

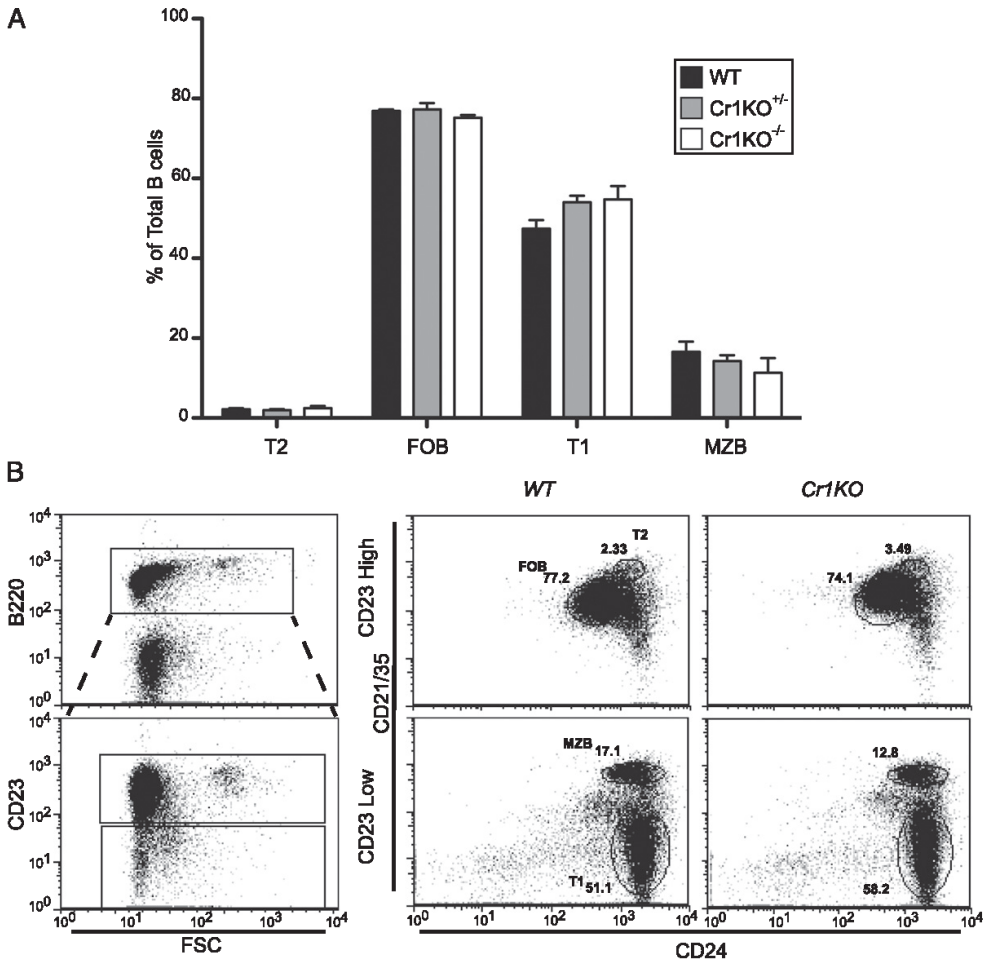

FIGURE 4. Analysis of *Cr1KO* splenic B cell populations. (**A**) Quantification of T1, T2, FOB, and MZB population frequencies in homozygous and heterozygous *Cr1KO* mice compared with WT mice. Populations were determined by segregating all $B220^+$ splenocytes into $CD23^{hi}$ and $CD23^{lo}$ populations and defining the T1, T2, FOB, and MZB populations by differential expression of CD24 and CD21/35. (**B**) Representative plots of WT and *Cr1KO* mice (n = 3 littermates, C57BL/6 background; one-way ANOVA performed on each population set).

products using a polyclonal rabbit anti-Cr1/2 Ab demonstrated a much higher quantity of Cr2 versus Cr1. A similar pattern is also obtained from the analysis of purified $B220^+$ B cells. FACS analysis of B cells with saturating levels of the Cr1-specific Ab (8C12) in contrast to Abs recognizing both Cr1 and Cr2 (7G6, 7E9, eBio8D9) also demonstrates that the MFI of Cr2 staining is much higher than that of Cr1 (data not shown). Altogether, these data suggest that the predominant isoform of the *Cr2* gene expressed by B cells is the Cr2 protein. Additionally, immunohistochemical staining for Cr1 (Cr1-specific Ab clone 8C12) of splenic or lymph node cross-sections has been used by many investigators to definitively mark FDCs. This suggested to us that FDC expression of Cr1 is not equal to B cell expression and that the Cr1/Cr2 ratio may not be equal in these two cell types. In light of these observations, we chose to definitively delineate *Cr1/2* expression in FDCs and B cells.

Initially, we used the same immunohistochemical staining strategy as other investigators to screen splenic cross-sections from *Cr1KO* mice. As shown in Fig. 5A, staining WT, *Cr1KO*, and *Cr1/2KO* spleen sections with the anti-Cr1 (CD35) Ab 8C12 demonstrates strong Cr1 expression on the FDCs of WT mice but an absence of Cr1 expression on the two mouse mutant strains. Thus, the *Cr1KO* mouse also shows the expected loss of Cr1 expression by FDCs. Staining of parallel sections with an Ab that recognizes both Cr1 and Cr2 (CD21/35; Ab 7E9) demonstrated a virtually identical pattern of B cell staining evident in WT and *Cr1KO* sections that was absent from the *Cr1/2KO* section (Fig. 5B). However, this staining did not highlight the FDCs in the WT sample in a similar fashion as did that with the anti-Cr1 Ab.

To further evaluate this question, quantitative RT-PCR and immunoblot analysis were performed on dissociated total unstrained spleen samples from bone marrow–transplant experiments in which hematopoietic cells from *Cr1/2KO* mice were transplanted into lethally irradiated WT host mice (*Cr1/2KO*→WT), as well as WT→WT, WT→*Cr1/2KO*, and *Cr1/2KO*→*Cr1KO*. Total replacement of the hematopoietic lineage of host mice, with or without donor *Cr1/2KO* B cells, was confirmed by FACS, and all mice had <1% of B cells expressing the host Cr1/2 phenotype (Fig. 6A). Transcript analysis from these chimeric mice revealed that the *Cr1* isoform is more highly expressed than is that of *Cr2*

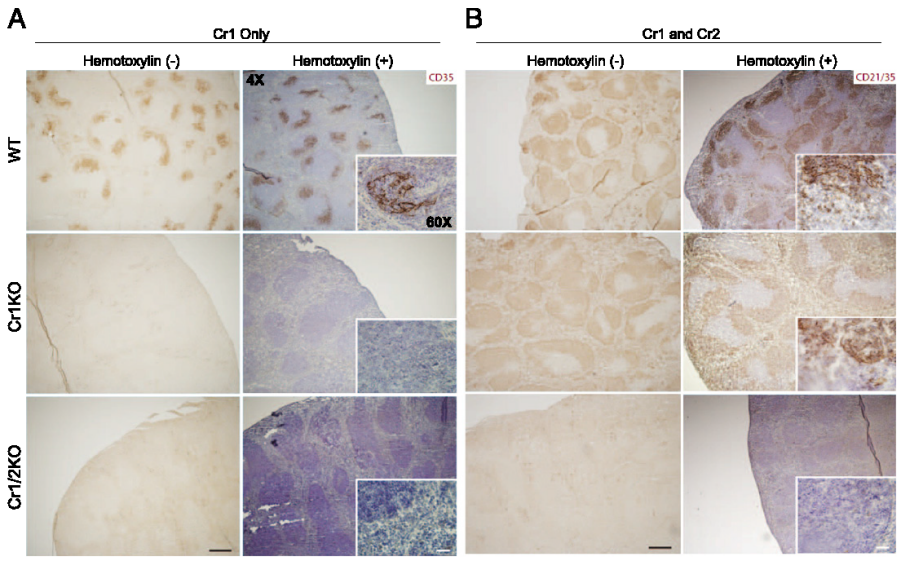

FIGURE 5. Immunohistochemistry of Cr1 (CD35) and Cr1/2 (CD21/35) in splenic cross-sections. Cr1 (CD35) was detected with the mAb 8C12 (**A**), and Cr1/2 (CD21/35) were detected using the mAb 7E9 (**B**). Ab-bound Cr1 and Cr1/2 were visualized by HRP reactivity with 3, 3′-diaminobenzidine (brown). Hematoxylin counterstaining for enhanced visualization of the splenic architecture is shown in blue. Original magnification of all images, ×4; *insets*, ×60. Example is from a single mouse but is representative of multiple similar analyses.

in the *Cr1/2KO*→WT chimera ($p < 0.001$, Fig. 6B). This was in contrast to WT→*Cr1/2KO* and WT→WT mice, neither of which displayed a significant difference in the expression of *Cr1* versus *Cr2*. It should be noted that, although some *Cr1/2* transcript is detected in *Cr1/2KO* mice using primers common to both *Cr1/2*, this is a distal portion of the transcript (3′) that cannot be translated into any portion of Cr1 or Cr2 (12). Comparison of the ratio of relative *Cr1* transcript/*Cr2* transcript demonstrated that the *Cr1/2KO*→WT chimera, in which only FDCs transcribe the *Cr2* locus, expresses *Cr1* at an ~3.5-fold greater level than *Cr2*. This is in contrast to the significantly lower 1:1 ratio displayed by the WT→*Cr1/2KO* and WT→WT chimeras, in which B cells are the most common cell type expressing the *Cr2* locus ($p < 0.001$ and $p < 0.01$, respectively, Fig. 6C). Western blot analysis of total spleen lysate (inclusive of both B cells and FDCs) from the same reconstituted mice revealed that Cr1 is nearly the exclusive product of the *Cr2* gene by FDCs, because WT irradiated mice reconstituted with *Cr1/2KO* bone marrow primarily express the Cr1 protein (Fig. 6D, *left panel*). In contrast, Western blot analysis of total spleen lysates from either irradiated WT or *Cr1/2KO* hosts given WT bone marrow transplants shows that the Cr2 protein is the predominant product of B cells (Fig. 6D, *left panel*). Interestingly, although *Cr1* and *Cr2* transcript data suggest that FDCs in the *Cr1/2KO*→*Cr1KO* chimeras produce only the *Cr2* transcript, this transcript was not translated by FDCs into appreciable levels of Cr2 protein, in contrast to the Cr2 protein produced by *Cr1KO* B cells (Fig. 1B, 1C). Total splenic lysates from *Cr1/2KO* and WT animals are shown for comparison (Fig. 6D, *right panel*).

Immunoblot analysis for Cr1/2 was also performed on lymph node and spleen lysates from mice 2 d postirradiation. Such peripheral immune organs are virtually devoid of B cells 2 d after irradiation (data not shown). Spleens were disrupted, single cells were strained away from the splenic matrix, and the resulting matrix material was solubilized in RIPA detergent for immunoblot analysis. As shown in Fig. 6D (*center panels*), the irradiated splenic tissue matrix was highly enriched for the Cr1 protein, as opposed to the Cr2 protein seen in the samples enriched for B cells.

Altogether, the data detailed above describe the *Cr1KO* mouse as lacking Cr1 expression on B cells and FDCs. However, Cr2 expression on mouse B cells is very similar to that seen for WT B cells. Additionally, although the Cr2 gene is still transcriptionally active in the FDCs of *Cr1KO* mice, as measured by the production of transcripts specific for *Cr2*, there is little to no Cr2 protein expression by these cells (as is also shown for WT FDCs, which do possess Cr1 protein but not Cr2). These findings suggest that the effect of losing the Cr1 protein in the *Cr1KO* animal is likely to be most pronounced for functions of the FDCs and not the B cells, for which the major *Cr2* gene product is Cr2 protein.

Ab deficiencies of Cr1KO *mice*

To identify possible effects of Cr1 deficiency on humoral immunity, we measured the quantities of total and Ag-specific Abs of IgM, IgG1, IgG2b, IgG2c, and IgG3 in naive and immunized mice. The levels of circulating Abs in naive *Cr1KO* animals were compared with that of WT and *Cr1/2KO* animals. As shown in Fig. 7, the levels of circulating IgGs and IgM in *Cr1KO* mice are not significantly different from those of WT mice. However, *Cr1KO* mice (as well as WT mice) have statistically higher levels of IgG2b, IgG2c, and IgG3 than do *Cr1/2KO* mice ($p < 0.01$, $p < 0.001$, and $p < 0.001$, respectively).

Within the naive Ab repertoire is a collection of Igs (IgM isotype), known as natural Abs, which is specific for conserved epitopes often found on apoptotic cells and pathogens. Many epitopes recognized by natural Abs have been identified, such as phosphorylcholine, chitosan/chitin, and dsDNA. To test the effect of Cr1 deficiency on the production of natural Abs, we quantified the titers of IgM specific for phosphorylcholine, chitosan/chitin, or dsDNA in the serum of naive mice. Anti-phosphorylcholine Ab was found at significantly reduced titers in *Cr1KO* mice compared with WT mice ($p < 0.05$), with a magnitude similar to the reduction seen in *Cr1/2KO* mice ($p < 0.001$, Fig. 8A). This pattern of

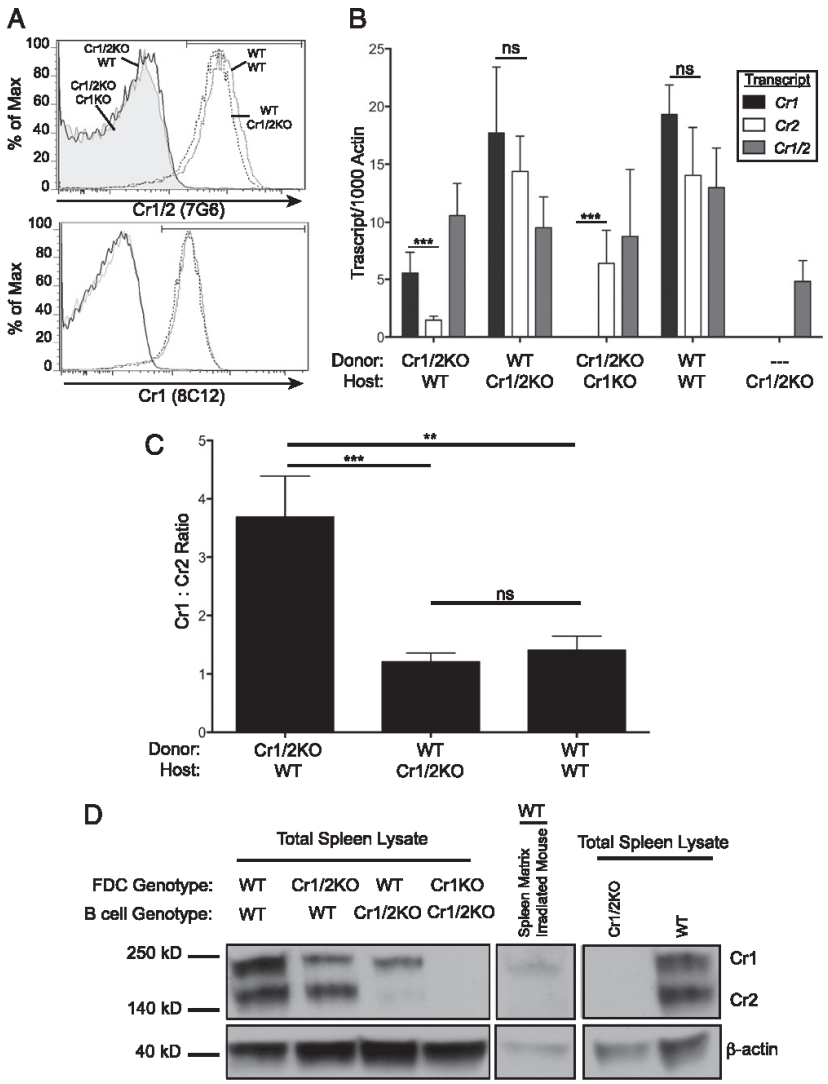

FIGURE 6. Quantitative RT-PCR and immunoblot analysis of Cr1 and Cr2 expression on FDCs and B cells. (**A**) Representative graphs of surface CR1 and CR1/2 on live peripheral blood $B220^+$ cells—from WT (donor)→WT(host) (gray line), WT→*Cr1/2KO* (dotted line), *Cr1/2KO*→WT (black line), and *Cr1/2KO*→*Cr1KO* (gray shading) mice—demonstrating full engraftment 6 wk after bone marrow transplant into lethally irradiated mice. (**B**) Quantitative RT-PCR analysis of *Cr1*, *Cr2*, and *Cr1/2* transcript in total spleen cDNA isolates from bone marrow chimeras. (**C**) Ratio of *Cr1/Cr2* transcripts quantified in (B) from *Cr1/2KO*→WT, WT→*Cr1/2KO*, and WT→WT chimeras. (**D**) Immunoblot analysis of the 190-kDa Cr1 and 140-kDa Cr2 proteins in total spleen lysates from chimeras (*left panels*), a mouse 2 d postlethal irradiation (*center panels*), and control *Cr1/2KO* and WT mice (*right panels*). $n = 8$ *Cr1/2KO*→WT; $n = 3$ WT→*Cr1/2KO*; $n = 9$ *Cr1/2KO*→*Cr1KO*; $n = 2$ WT→WT; $n = 4$ *Cr1/2KO*. Error bars represent SEM. $^{**}p < 0.01$, $^{***}p < 0.001$, Student *t* test; β-actin was used as a loading control (40 kDa). ns, Not significant.

natural Ab deficiency was not the same for anti-chitosan/chitin and anti-dsDNA natural Abs. Anti-chitosan/chitin Abs from *Cr1KO* animals were equivalent to WT levels (but statistically significantly reduced in *Cr1/2KO* mice) (Fig. 8B), whereas natural Abs specific for dsDNA were statistically significantly reduced in *Cr1KO* mice compared with WT and *Cr1/2KO* mice (Fig. 8C).

Ags are generally split into three categories defined by the secondary signal that tunes B cell activation upon BCR cross-linking: TI-1, provided by TLR ligands; TI-2, provided by large repetitive Ags, such as polysaccharides; and TD, provided by coincident recognition of protein Ag by CD4 T cells. To test the contribution of Cr1 in Ab responses to such Ags, we immunized *Cr1KO*, WT, and *Cr1/2KO* mice with the model Ags TNP-LPS (TI-1), DNP-Ficoll (TI-2), or TNP-KLH (TD) and quantified the Ag-specific response of different isotypes of Ig.

Cr1KO mice generated similar Ab responses to TI-1, TI-2, and low-dose TD Ag relative to WT mice (Fig. 9A, Supplemental Fig. 3). In contrast, *Cr1/2KO* mice were generally determined to have lower detectable levels of Ig against TI-2 and low-dose TD Ag than were WT mice, as previously observed. A similar reduction for *Cr1KO* and *Cr1/2KO* animals was observed for the Ag-specific IgG3 isotype in response to high-dose TNP-KLH immunization (days 7, 14, and 21). Intriguingly, both *Cr1KO* and *Cr1/2KO* mice displayed a significant decrease in Ag-specific IgM following high-dose TNP-KLH for days 7, 14, and 21 but a significant expansion of Ag-specific IgM (compared with WT mice) following the day-21 boost with TNP-KLH.

Follow-up analysis of Ig produced against the KLH carrier of the TNP-KLH hapten-carrier conjugate demonstrated a reduction in Ag-specific IgM produced by *Cr1KO* and *Cr1/2KO* mice, although the levels of Ag-specific IgG to KLH in *Cr1KO* mice was very similar to that of WT mice (Fig. 9B). *Cr1KO* animal responses to immunization with whole SRBCs also tracked similarly to WT animals (both IgM and IgG), whereas the SRBC-specific IgG response of *Cr1/2KO* mice was significantly less than that of WT mice (Fig. 9C).

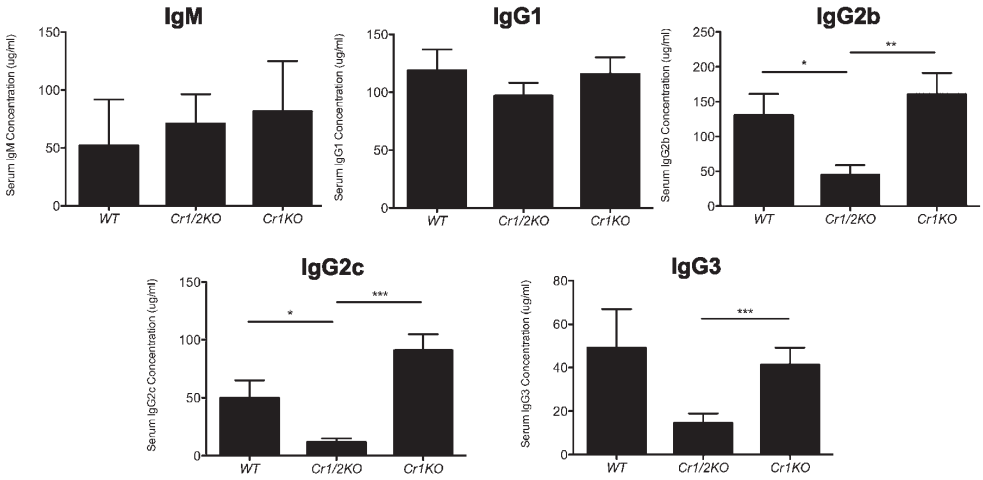

FIGURE 7. ELISA quantification of naive serum Ig. Concentration of total IgM, IgG1, IgG2b, IgG2c, and IgG3 Ig isotypes from serum of naive WT, *Cr1KO*, and *Cr1/2KO* mice ($n = 11$; 8–16-wk-old sex-matched mice). Error bars represent SEM. $*p < 0.05$, $**p < 0.01$, $***p < 0.001$, Student t test.

The generation of activated GC B cells is reduced in Cr1KO *mice*

Because of the altered response to the T cell–dependent Ag in Cr1KO mice, we questioned whether GC B cells were effectively activated in such mice. To test this, we immunized mice with 2×10^8 SRBCs and used FACS to assay splenic B cells for activated GC B cell markers. Activated GC B cells are identified by the increased expression of Fas and reduced expression of IgD, as well as increased expression of the glycan epitope recognized by the Ab clone GL7 (3, 33–35). *Cr1KO*, WT, and *Cr1/2KO* mice were immunized with SRBCs, and their spleens were isolated 7 d later. Splenocytes were $B220^+$ FACS sorted for B cells and then identified as GC B cells by IgD^{int} Fas^+. Similar to *Cr1/2KO* mice, *Cr1KO* mice consistently possessed a significantly ($p < 0.001$) reduced population of GC B cells in response to SRBC immunizations compared with WT mice (Fig. 10). GL7 expression was equivalent in the various IgD^{int} Fas^+ populations, indicating that when GC cells were activated in the *Cr1KO* mouse (and *Cr1/2KO* animal), the level of activation was equivalent to WT mice (data not shown). To determine whether the lack of activated GC B cells in *Cr1KO* (and *Cr1/2KO*) animals was complement (C3) dependent, we analyzed the generation of GC B cells in SRBC-immunized C3-deficient animals. As shown in Supplemental Fig. 4, *C3KO* mice generated significantly reduced GC B cell populations. However, the small subset of cells from the *C3KO* animal that did gate in the activated GC population also expressed elevated levels of GL7 (data not shown). Therefore, the full activation of GC B cells requires C3 in addition to expression of the Cr1 protein.

Cr2 sufficiency rescues Cr1KO *mortality during* S. pneumoniae *infection*

Cr1/2KO mice generate a deficient primary immune response to the pathogen *S. pneumoniae* and a subsequent poor secondary immune response to infection. To determine whether the susceptibility of *Cr1KO* mice to *S. pneumoniae* was similar to that of the *Cr1/2KO* animal (along with WT controls), mice were immunized with 10,000 heat-killed *S. pneumoniae* and infected 10 d later with 1000 CFU of live bacteria. Survival of *Cr1KO*, *Cr1/2KO*, *C3KO*, and WT mice was analyzed using the log-rank test ($p < 0.01$); survival of *Cr1KO* mice (85%, 2 d postinfection [dpi]) was not significantly less than the 100% survival of WT mice (Fig. 11). In contrast to *Cr1KO* animals, *Cr1/2KO* mice were significantly ($p < 0.05$, 55%, 3 dpi) more susceptible to mortality from the infection. Consistent with the critical role for the complement cascade in control of *S. pneumoniae* infections, none of the *C3KO* mice survived beyond 3 dpi.

Discussion

The complement pathway is a critical component of the innate and acquired immune response. The generation of Ab responses, both T cell dependent and independent, was demonstrated to be influenced by complement products and their cellular receptors. Animals lacking the *Cr2* gene products, the Cr1 and Cr2 receptors, have defined deficiencies in Ab responses (both natural and as the result of specific immunizations), heightened sensitivity to bacterial pathogens (e.g., *S. pneumoniae*), and a lack of optimal B cell activation (12, 13). The *Cr2* gene is transcriptionally active in B cells and FDCs and, via alternative splicing, creates the transcripts specific for Cr1 and Cr2. Gene-knockout strategies in the past eliminated the ability of B cells and FDCs to make any of the Cr2 gene products; thus, it has been impossible to delineate the specific functions of either of the individual proteins. In this study, we describe the creation of a new mouse line, the *Cr1KO* mouse, in which the exons unique to the Cr1 protein have been deleted by targeted homologous recombination, creating a gene very similar to that of human CR2, which possesses the vestiges of the Cr1-like exons but only produces the CR2 protein (36).

Characterization of the *Cr1KO* animal led us to focus upon Cr1 and Cr2 protein production by B cells and FDCs. It had always been a question why immunostaining of splenic GCs with an Ab specific for Cr1 identified FDCs, whereas similar staining with an Ab that recognizes both Cr1 and Cr2 (there are no specific anti-Cr2 Abs) primarily identifies B cells (Fig. 5). By teasing apart the protein contributions of the *Cr2* gene in B cells and FDCs, we found that the *Cr2* gene product produced in FDCs is almost exclusively that of Cr1, whereas B cells primarily splice to form the Cr2 protein (Fig. 6). Even when the *Cr2* gene is forced to only splice to the Cr2 isoform in the *Cr1KO* animal, the quantity of Cr2 produced by FDCs is minimal (*Cr1/2KO*→*Cr1KO* bone marrow chimera), whereas that of B cells is normal (Fig. 6D). Thus, the deficiency of the *Cr1KO* animal could be expected to have a greater impact upon FDC functions compared with B cell activation/Ag acquisition.

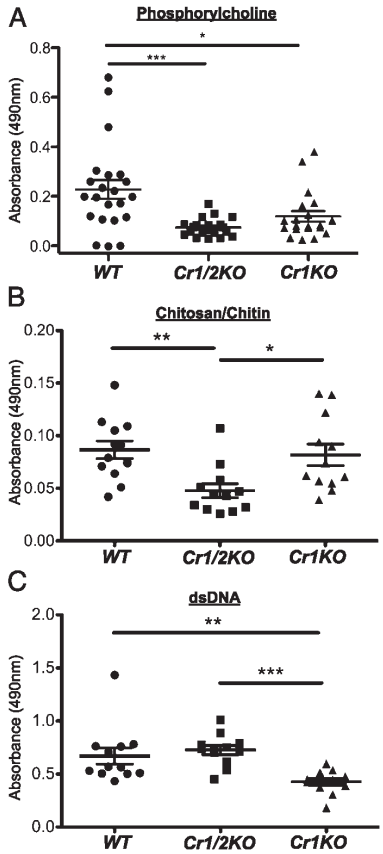

FIGURE 8. Circulating natural Ab quantification. Detection of natural Ab (IgM) specific for phosphorylcholine (**A**), chitosan/chitin (**B**), and dsDNA (calf thymus DNA) (**C**) determined (see *Materials and Methods*) from serum of WT, *Cr1KO*, and *Cr1/2KO* mice. n = 12–22, 8–16-wk-old sex-matched mice. Error bars represent SEM. $^{*}p < 0.05$, $^{**}p < 0.01$, $^{***}p < 0.001$, Student t test.

Fang et al. (37) reported that the *Cr1/2KO* animal reconstituted with bone marrow from either a WT or *Cr1/2KO* animal would not reconstitute immune complex binding to the GCs, suggesting that the *Cr2* gene–encoded proteins expressed by FDCs are critical in immune complex retention.

The comparison of Ab titers in naive and immunized *Cr1KO* and *Cr1/2KO* mice demonstrated a more dramatic deficiency when both Cr1 and Cr2 are absent (Figs. 7–9). Although the naive *Cr1/2KO* animal has depressed circulating levels of total IgG2b, IgG2c, and IgG3, the *Cr1KO* titers for these Ab types are virtually identical to those in WT mice. The responses to both TI and TD immunizations generally demonstrated a greater defect for the *Cr1/2KO* mouse than for the *Cr1KO* mouse. This is particularly true for the TI-2 Ag, DNP-Ficoll, which induced a response equal to WT mice in *Cr1KO* mice.

The greatest variation from WT for the *Cr1KO* animal was evident in the high dose (100 μg TNP-KLH) when anti-TNP titers were analyzed (Fig. 9A). *Cr1KO* mice exhibited a reduced production of TNP-specific IgM during the primary immune response, which was similar to the reduction seen in *Cr1/2KO* mice. Intriguingly, both *Cr1KO* and *Cr1/2KO* animals exhibited significantly elevated levels of TNP-specific IgM compared with WT mice following the boost of Ag (day 21) in the high-dose immunization experiment. The analysis of IgG isotypes from such immunized *Cr1KO* animals was less dramatic. Anti-TNP IgG3 was found to be significantly reduced during the primary response of the *Cr1KO* mouse, whereas the IgG1, IgG2b, and IgG2c isotypes were not significantly reduced compared with WT mice. In general, the Ab-response data for TD Ags from the *Cr1KO* animal suggest a deficiency (compared with WT mice) in primary activation (demonstrated by the reduced IgM/IgG3 responses) and decreased levels of isotype switching (evidenced by the enhanced production of IgM following the secondary boost).

The generation of Ag-specific IgM and IgG responses to the KLH carrier protein or to immunizations with SRBCs were intermediate for the *Cr1KO* animal compared with the responses of WT and *Cr1/2KO* mice, suggesting that the presence of the Cr2 protein on B cells in the *Cr1KO* animal partially mitigated the Cr1 deficiency (Fig. 9B, 9C). These results may vary from the anti-TNP responses noted above, because the population of responding B cells is much more limited for the TNP response than for the response to the many epitopes provided by the KLH protein and SRBCs. Clearly, the lack of both Cr1 and Cr2 proteins dramatically decreased the IgG anti-SRBC response in the *Cr1KO* mouse, which was virtually identical to that for WT mice. However, the decreased anti-KLH and anti-SRBC IgM responses in both the *Cr1KO* and *Cr1/2KO* animal lines, compared with WT, suggest that Cr1, expressed by either B cells or FDCs, may be playing a role in this initial Ag response. Previous work on an independently generated Cr1 and Cr2–deficient mouse by Molina et al. (13) described SRBC-specific IgM primary responses that were very similar to those demonstrated in this study.

Our IgG analysis of the *Cr1KO* animal may also be compared with bone marrow chimera studies in which Ab responses were analyzed in animals lacking functional *Cr2* gene expression in either bone marrow lineages or FDCs.

One such study analyzed responses to immunization with SRBCs and KLH; it showed that, although the absence of *Cr2* gene products expressed by FDCs had a profound impact upon Ab generation, the generation of an optimal response also needed B cell *Cr2* gene products (37). The demonstration of the predominance of expression of Cr1 on FDCs suggest that the IgG response to SRBCs or KLH in *Cr1KO* mice should mirror those of bone marrow chimeras in which complement receptor expression is limited to B cells, as described in that report. Our data on the IgG responses to SRBC immunization demonstrate there is not a significant difference in response to these immunogens, suggesting that bone marrow chimeras may not precisely define the phenotype of Cr1 deficiency. Furthermore, despite the lack of significance between the *Cr1KO* and WT IgG responses to SRBCs, the similarity of the pattern of IgG responses to KLH by *Cr1KO* mice relative to WT and *Cr1/2KO* mice (Fig. 9B, 9C, *right panels*) suggests that these differences are more than random variation. A more recent bone marrow chimera analysis (using Cr1/2 deficiency bred upon a BALB/c background) demonstrated that the presence or absence of *Cr2* gene products on B cells did not alter the generation of various IgG isotypes to immunizations with SRBCs; instead, *Cr2* gene expression by FDCs was critical for such responses (14). Intriguingly, this study also demonstrated that immunization with IgM–SRBC complexes required *Cr2* gene products on both B cells and FDCs for optimal Ab responses. Our data generated using the *Cr1KO* animal fundamentally agrees with the conclusions reached by Rutemark et al. (14); the ability of B cells to efficiently class switch from IgM to IgG isotypes (whether they express *Cr2* gene products or not) is compromised in the absence of the Cr1 protein expressed by the FDCs. However, there are specific points of variance between our studies and those using bone marrow chimera models that may be

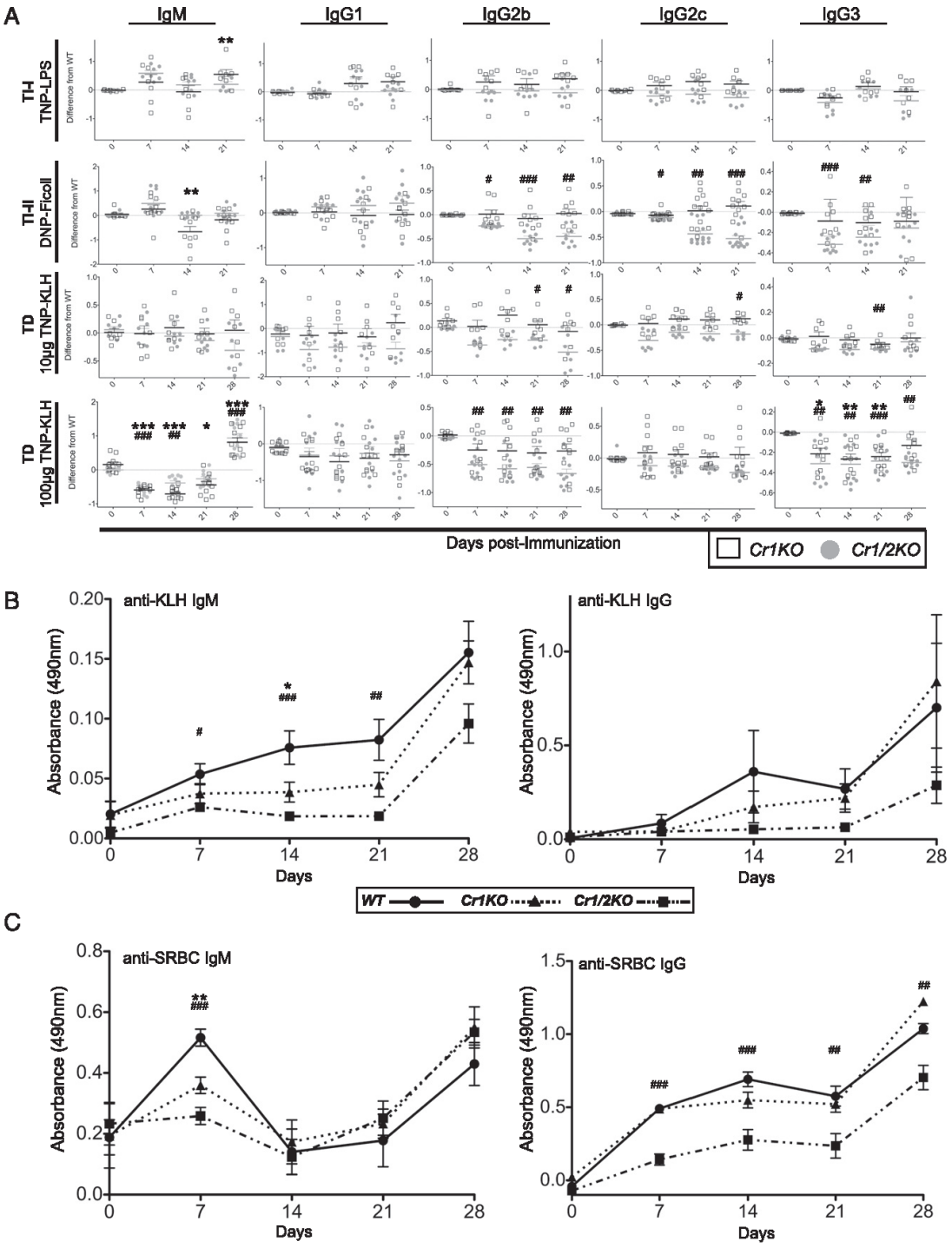

FIGURE 9. TI-1, TI-2, and TD Ag-specific Ig response. (**A**) Deviation from WT in production of Ag-specific Ig of the isotypes IgM, IgG1, IgG2b, IgG2c, and IgG3 by *Cr1KO* and *Cr1/2KO* mice. Ig in response to DNP or TNP after immunization with the model immunogens TNP-LPS (TI-1), DNP-Ficoll (TI-2), TNP-KLH (10 μg), or TNP-KLH (100 μg) was measured at 0, 7, 14, and 21 d after primary immunization. Secondary immunizations were given to TNP-KLH–immunized mice at 21 d, and 28-d serum samples were also measured. Graphs show difference in absorbance of each mouse from the average WT absorbance at 490 nm for each day. TI-1, $n = 7$–10; TI-2, $n = 9$; TD (low), $n = 7$; TD (high), $n = 10$; 8–12-wk-old sex-matched mice; all data represent a composite of two independently performed immunizations; see Supplemental Fig. 3. (**B**) ELISA analysis of KLH-specific IgM (*Figure legend continues*)

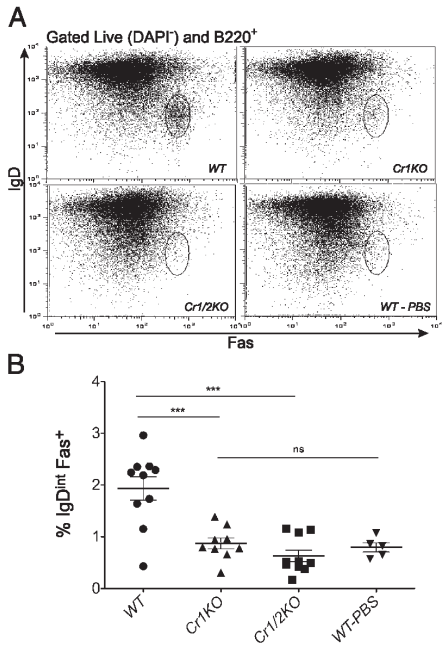

FIGURE 10. FACS analysis of GC B cell frequency after SRBC immunization. WT, *Cr1KO*, and *Cr1/2KO* mice were immunized with 2×10^8 SRBCs, and isolated splenocytes were analyzed 7 d later. The IgD^{int} Fas^+ cells were gated from the total live $B220^+$ cells (**A**), and the average population percentage was graphed (**B**). Error bars represent SEM. $n = 9$–10 from three independent replicates of $n = 3$–4; $n = 5$ WT PBS treated; sex-matched 8–12-wk-old mice. $***p < 0.001$, pairwise Student t test. ns, Not significant.

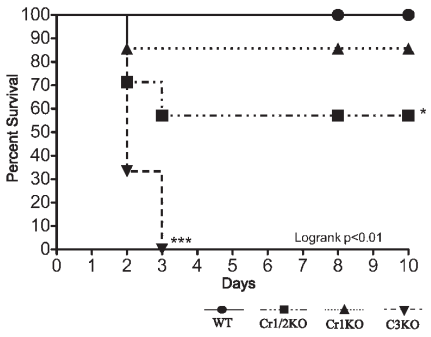

FIGURE 11. Survival curve of *Cr1KO*, *Cr1/2KO*, *C3KO*, and WT mice postinfection with *S. pneumoniae*. Mice were immunized with 1×10^5 heat-killed *S. pneumoniae*, followed 10 d later (0 d on graph) by infection with 1000 CFU of live *S. pneumoniae*. *Cr1KO* mice (dotted line) survive infection with *S. pneumoniae* at the same rate as do WT mice. *Cr1/2KO* and *C3KO* mice survive for a significantly shorter amount of time. WT, $n = 11$; *Cr1/2KO*, $n = 7$; *Cr1KO*, $n = 7$; *C3KO*, $n = 3$. $*p < 0.05$, $***p < 0.001$.

a consequence of the experimental procedures. For example, bone marrow chimera studies require irradiation and bone marrow reconstitution that may result in an immune environment that is not functionally equivalent to the environment found in a nonirradiated animal (in our case, the *Cr1KO* line). Additionally, in removing the ability of B cells to produce the Cr1 protein in the *Cr1KO* animal, all *Cr2* gene transcripts are committed to producing the Cr2 protein, which is evidenced by the increased MFI of Cr2 expression by B cells of the *Cr1KO* mouse compared with WT mice. This increase in Cr2 protein may heighten the sensitivity of the activation of B cells, reducing the difference between *Cr1KO* and WT mice. Alternatively, Cr1 expressed by B cells may suppress B cell activation. Mouse strain differences may also play a role; our Ab analyses, as well as those of Fang et al. (37), used the C57BL/6 background, whereas those of Rutemark et al. (14) used the BALB/c background. Previously, we found that *Cr1/2KO* deficiency on a BALB/c background created a more inflamed splenic environment than did the same deficiency on a C57BL/6 background that may also alter Ab responses (25). Finally, a previous report suggested that some of the functional defects in B cell responses in the *Cr1/2KO* animal were due to the elevated surface expression of CD19, usually found in a complex with Cr1/2, CD81, and Ifitm1/3 (17), leading to anergic responses. Thus, the bone marrow chimera models described above using marrow reconstitution from the *Cr1/2KO* mouse possess B cells expressing increased levels of CD19. However, the analysis of B cells obtained from the *Cr1KO* animal showed a lower level of CD19 than did those from WT mice, thus mitigating the concerns about CD19-dependent B cell anergy in the *Cr1KO* mouse.

The generation of activated GC B cells requires the interaction of the Ag-specific B cell with Ag and the cognate T cell. It was shown that the number of GC B cells after immunization was reduced in *Cr1/2KO* mice (38); this was presumed to be due, in part, to the loss of Cr2 signaling on the B cell as part of the BCR coreceptor complex. Interestingly, we found that the *Cr1KO* animal also does not generate activated B cells (Fig. 10) based upon the IgD and Fas expression status (Fig. 10). Indeed, the immunized *Cr1KO* and *Cr1/2KO* animals had the equivalent percentages of activated B cells as did the unimmunized WT control. The movement of B cells from the region of high B cell proliferation, known as the dark zone (DZ), to the FDC-localized light zone (LZ) of the GC (interzonal migration), has been defined as "cyclic re-entry"; Ag-specific B cells are selected for by binding to Ag held by the FDCs, followed by encounter with Ag-specific T cells and migration to the DZ for proliferation (39–41). After activation and proliferation in the DZ (accompanied by somatic hypermutation and isotype switching), the Ag-specific B cells then cycle back into the LZ for another round of positive Ag selection on the FDC. The absence of such activated B cells in the *Cr1KO* animal suggests that Ag bound by the FDC Cr1 protein is critical for this pathway to proceed in an optimal manner, and C3 is a required ligand. Further analysis of bone marrow chimera animals, as well as characterization of DZ- and LZ-associated B cells (via differential expression of CXCR4 and CD83) (42), will help us to determine the specific signaling defect associated with the absence of Cr1.

Functions associated with the *Cr2* gene products have also been implicated in the development and progression of systemic lupus erythematosus, although the specific pathway(s) of Cr1/Cr2 control have not been described (43, 44). The loss of Cr1 on the surface of FDCs, resulting in the loss of positive selection of ac-

and IgG from TNP-KLH (100 μg)–immunized mice shown in (A) ($n = 10$; 8–12-wk-old sex-matched mice). (**C**) ELISA analysis of SRBC-specific IgM and IgG from mice immunized i.v. with 1×10^8 SRBCs on days 0 and 21 ($n = 6$; sex-matched 8–10-wk-old mice). *WT versus *Cr1KO*, #WT versus *Cr1/2KO*, $*/\#p < 0.05$, $**/\#\#p < 0.01$, $***/\#\#\#p < 0.001$; one-way ANOVA was performed for each day, and Tukey multiple-comparison posttest results are shown for all time points for which $p \leq 0.05$ by ANOVA.

tivated B cells, may allow such cells to escape into the periphery. The mutations in the VDJ region associated with the presence of the B cell in the DZ is random, such that the generation of autoreactive B cells could easily proceed. In fact, the Ig genes obtained from autoreactive B cells demonstrate a high level of VDJ somatic hypermutation (43–46). If the absence of Cr1 expression by the FDCs allows such cells to exit the GC without selection, then the dissemination of autoreactive B cells into the periphery of the animal may be enhanced. Experiments to test this hypothesis are underway.

In summary, these data provide two new findings in support of the model that expression of *Cr2* gene products by FDCs and B cells is required for optimal Ag-specific B cell activation and Ab production to TD Ags: the novel discovery that Cr1 is preferentially expressed by FDCs, whereas Cr2 is preferentially expressed by B cells, and the fact that Cr1 is more integral to GC B cell activation and response to TD Ags than TI responses. The similarity and differences between deletion of Cr1 alone or Cr1/2 together highlight the importance and functional independence of these similar proteins and emphasize the significance of the new *Cr1KO* mouse line. These findings are relevant for the optimization of adjuvants targeted to FDCs for the enhancement of humoral immunity (47).

Acknowledgments

We thank the members of the combined Weis laboratories for helpful discussions and critical review of the data and specifically thank Peter Pioli for assistance with Western blots. We thank the Utah Transgenic and Knockout Core facility (Dr. Susan Tomowski) for assistance with generating the *Cr1KO* animal and the Flow Cytometric Core facility for assistance with cell analysis.

Disclosures

The authors have no financial conflicts of interest.

References

1. Xu, Z., H. Zan, E. J. Pone, T. Mai, and P. Casali. 2012. Immunoglobulin class-switch DNA recombination: induction, targeting and beyond. *Nat. Rev. Immunol.* 12: 517–531.
2. Vinuesa, C. G., M. A. Linterman, C. C. Goodnow, and K. L. Randall. 2010. T cells and follicular dendritic cells in germinal center B-cell formation and selection. *Immunol. Rev.* 237: 72–89.
3. Wang, X., B. Cho, K. Suzuki, Y. Xu, J. A. Green, J. An, and J. G. Cyster. 2011. Follicular dendritic cells help establish follicle identity and promote B cell retention in germinal centers. *J. Exp. Med.* 208: 2497–2510.
4. Ferguson, A. R., M. E. Youd, and R. B. Corley. 2004. Marginal zone B cells transport and deposit IgM-containing immune complexes onto follicular dendritic cells. *Int. Immunol.* 16: 1411–1422.
5. Gonzalez, S. F., S. E. Degn, L. A. Pitcher, M. Woodruff, B. A. Heesters, and M. C. Carroll. 2011. Trafficking of B cell antigen in lymph nodes. *Annu. Rev. Immunol.* 29: 215–233.
6. Suzuki, K., I. Grigorova, T. G. Phan, L. M. Kelly, and J. G. Cyster. 2009. Visualizing B cell capture of cognate antigen from follicular dendritic cells. *J. Exp. Med.* 206: 1485–1493.
7. Walport, M. J. 2001. Complement. First of two parts. *N. Engl. J. Med.* 344: 1058–1066.
8. Ricklin, D., G. Hajishengallis, K. Yang, and J. D. Lambris. 2010. Complement: a key system for immune surveillance and homeostasis. *Nat. Immunol.* 11: 785–797.
9. Walport, M. J. 2001. Complement. Second of two parts. *N. Engl. J. Med.* 344: 1140–1144.
10. Pepys, M. B. 1974. Role of complement in induction of antibody production in vivo. Effect of cobra factor and other C3-reactive agents on thymus-dependent and thymus-independent antibody responses. *J. Exp. Med.* 140: 126–145.
11. Carroll, M. C., and D. E. Isenman. 2012. Regulation of humoral immunity by complement. *Immunity* 37: 199–207.
12. Haas, K. M., M. Hasegawa, D. A. Steeber, J. C. Poe, M. D. Zabel, C. B. Bock, D. R. Karp, D. E. Briles, J. H. Weis, and T. F. Tedder. 2002. Complement receptors CD21/35 link innate and protective immunity during *Streptococcus pneumoniae* infection by regulating IgG3 antibody responses. *Immunity* 17: 713–723.
13. Molina, H., V. M. Holers, B. Li, Y. Fung, S. Mariathasan, J. Goellner, J. Strauss-Schoenberger, R. W. Karr, and D. D. Chaplin. 1996. Markedly impaired humoral immune response in mice deficient in complement receptors 1 and 2. *Proc. Natl. Acad. Sci. USA* 93: 3357–3361.
14. Rutemark, C., A. Bergman, A. Getahun, J. Hallgren, F. Henningsson, and B. Heyman. 2012. Complement receptors 1 and 2 in murine antibody responses to IgM-complexed and uncomplexed sheep erythrocytes. *PLoS ONE* 7: e41968 10.1371/journal.pone.0041968.
15. Molina, H., T. Kinoshita, C. B. Webster, and V. M. Holers. 1994. Analysis of C3b/C3d binding sites and factor I cofactor regions within mouse complement receptors 1 and 2. *J. Immunol.* 153: 789–795.
16. Jacobson, A. C., and J. H. Weis. 2008. Comparative functional evolution of human and mouse CR1 and CR2. *J. Immunol.* 181: 2953–2959.
17. Haas, K. M., J. C. Poe, and T. F. Tedder. 2009. CD21/35 promotes protective immunity to *Streptococcus pneumoniae* through a complement-independent but CD19-dependent pathway that regulates PD-1 expression. *J. Immunol.* 183: 3661–3671.
18. Marchbank, K. J., C. C. Watson, D. F. Ritsema, and V. M. Holers. 2000. Expression of human complement receptor 2 (CR2, CD21) in Cr2 $^{/}$ mice restores humoral immune function. *J. Immunol.* 165: 2354–2361.
19. Pappworth, I. Y., C. Hayes, J. Dimmick, B. P. Morgan, V. M. Holers, and K. J. Marchbank. 2012. Mice expressing human CR1/CD35 have an enhanced humoral immune response to T-dependent antigens but fail to correct the effect of premature human CR2 expression. *Immunobiology* 217: 147–157.
20. Bunting, M., K. E. Bernstein, J. M. Greer, M. R. Capecchi, and K. R. Thomas. 1999. Targeting genes for self-excision in the germ line. *Genes Dev.* 13: 1524–1528.
21. Zabel, M. D., J. J. Weis, and J. H. Weis. 1999. Lymphoid transcription of the murine CD21 gene is positively regulated by histone acetylation. *J. Immunol.* 163: 2697–2703.
22. Debnath, I., K. M. Roundy, J. J. Weis, and J. H. Weis. 2007. Defining in vivo transcription factor complexes of the murine CD21 and CD23 genes. *J. Immunol.* 178: 7139–7150.
23. Morrison, T. B., Y. Ma, J. H. Weis, and J. J. Weis. 1999. Rapid and sensitive quantification of *Borrelia burgdorferi*-infected mouse tissues by continuous fluorescent monitoring of PCR. *J. Clin. Microbiol.* 37: 987–992.
24. Roundy, K. M., J. J. Weis, and J. H. Weis. 2009. Deletion of putative intronic control sequences does not alter cell or stage specific expression of Cr2. *Mol. Immunol.* 47: 517–525.
25. Jacobson, A. C., J. J. Weis, and J. H. Weis. 2008. Complement receptors 1 and 2 influence the immune environment in a B cell receptor-independent manner. *J. Immunol.* 180: 5057–5066.
26. Rapaka, R. R., D. M. Ricks, J. F. Alcorn, K. Chen, S. A. Khader, M. Zheng, S. Plevy, E. Bengtén, and J. K. Kolls. 2010. Conserved natural IgM antibodies mediate innate and adaptive immunity against the opportunistic fungus *Pneumocystis murina*. *J. Exp. Med.* 207: 2907–2919.
27. Koganei, A., T. Tsuchiya, K. Samura, and M. Nishikibe. 2007. Use of whole sheep red blood cells in ELISA to assess immunosuppression in vivo. *J. Immunotoxicol.* 4: 77–82.
28. Carlsson, F., A. Getahun, C. Rutemark, and B. Heyman. 2009. Impaired antibody responses but normal proliferation of specific CD4+ T cells in mice lacking complement receptors 1 and 2. *Scand. J. Immunol.* 70: 77–84.
29. Ray, A., and B. N. Dittel. 2010. Isolation of mouse peritoneal cavity cells. *J. Vis. Exp.* pii: 1488.
30. Romero-Steiner, S., D. Libutti, L. B. Pais, J. Dykes, P. Anderson, J. C. Whitin, H. L. Keyserling, and G. M. Carlone. 1997. Standardization of an opsonophagocytic assay for the measurement of functional antibody activity against *Streptococcus pneumoniae* using differentiated HL-60 cells. *Clin. Diagn. Lab. Immunol.* 4: 415–422.
31. Ahearn, J. M., M. B. Fischer, D. Croix, S. Goerg, M. Ma, J. Xia, X. Zhou, R. G. Howard, T. L. Rothstein, and M. C. Carroll. 1996. Disruption of the Cr2 locus results in a reduction in B-1a cells and in an impaired B cell response to T-dependent antigen. *Immunity* 4: 251–262.
32. Hasegawa, M., M. Fujimoto, J. C. Poe, D. A. Steeber, and T. F. Tedder. 2001. CD19 can regulate B lymphocyte signal transduction independent of complement activation. *J. Immunol.* 167: 3190–3200.
33. Yoshino, T., E. Kondo, L. Cao, K. Takahashi, K. Hayashi, S. Nomura, and T. Akagi. 1994. Inverse expression of bcl-2 protein and Fas antigen in lymphoblasts in peripheral lymph nodes and activated peripheral blood T and B lymphocytes. *Blood* 83: 1856–1861.
34. Cervenak, L., A. Magyar, R. Boja, and G. László. 2001. Differential expression of GL7 activation antigen on bone marrow B cell subpopulations and peripheral B cells. *Immunol. Lett.* 78: 89–96.
35. Naito, Y., H. Takematsu, S. Koyama, S. Miyake, H. Yamamoto, R. Fujinawa, M. Sugai, Y. Okuno, G. Tsujimoto, T. Yamaji, et al. 2007. Germinal center marker GL7 probes activation-dependent repression of N-glycolylneuraminic acid, a sialic acid species involved in the negative modulation of B-cell activation. *Mol. Cell. Biol.* 27: 3008–3022.
36. Holguin, M. H., C. B. Kurtz, C. J. Parker, J. J. Weis, and J. H. Weis. 1990. Loss of human CR1- and murine Crry-like exons in human CR2 transcripts due to CR2 gene mutations. *J. Immunol.* 145: 1776–1781.
37. Fang, Y., C. Xu, Y. X. Fu, V. M. Holers, and H. Molina. 1998. Expression of complement receptors 1 and 2 on follicular dendritic cells is necessary for the generation of a strong antigen-specific IgG response. *J. Immunol.* 160: 5273–5279.
38. Wu, X., N. Jiang, Y. F. Fang, C. Xu, D. Mao, J. Singh, Y. X. Fu, and H. Molina. 2000. Impaired affinity maturation in Cr2 $^{/}$ mice is rescued by adjuvants without improvement in germinal center development. *J. Immunol.* 165: 3119–3127.

39. Kepler, T. B., and A. S. Perelson. 1993. Cyclic re-entry of germinal center B cells and the efficiency of affinity maturation. *Immunol. Today* 14: 412–415.
40. Oprea, M., and A. S. Perelson. 1997. Somatic mutation leads to efficient affinity maturation when centrocytes recycle back to centroblasts. *J. Immunol.* 158: 5155–5162.
41. Victora, G. D., and M. C. Nussenzweig. 2012. Germinal centers. *Annu. Rev. Immunol.* 30: 429–457.
42. Victora, G. D., D. Dominguez-Sola, A. B. Holmes, S. Deroubaix, R. Dalla-Favera, and M. C. Nussenzweig. 2012. Identification of human germinal center light and dark zone cells and their relationship to human B-cell lymphomas. *Blood* 120: 2240–2248.
43. Boackle, S. A., K. K. Culhane, J. M. Brown, M. Haas, L. Bao, R. J. Quigg, and V. M. Holers. 2004. CR1/CR2 deficiency alters IgG3 autoantibody production and IgA glomerular deposition in the MRL/lpr model of SLE. *Autoimmunity* 37: 111–123.
44. Boackle, S. A., V. M. Holers, X. Chen, G. Szakonyi, D. R. Karp, E. K. Wakeland, and L. Morel. 2001. Cr2, a candidate gene in the murine Sle1c lupus susceptibility locus, encodes a dysfunctional protein. *Immunity* 15: 775–785.
45. van Es, J. H., F. H. Gmelig Meyling, W. R. van de Akker, H. Aanstoot, R. H. Derksen, and T. Logtenberg. 1991. Somatic mutations in the variable regions of a human IgG anti-double-stranded DNA autoantibody suggest a role for antigen in the induction of systemic lupus erythematosus. *J. Exp. Med.* 173: 461–470.
46. Mietzner, B., M. Tsuiji, J. Scheid, K. Velinzon, T. Tiller, K. Abraham, J. B. Gonzalez, V. Pascual, D. Stichweh, H. Wardemann, and M. C. Nussenzweig. 2008. Autoreactive IgG memory antibodies in patients with systemic lupus erythematosus arise from nonreactive and polyreactive precursors. *Proc. Natl. Acad. Sci. USA* 105: 9727–9732.
47. Mattsson, J., U. Yrlid, A. Stensson, K. Schön, M. C. I. Karlsson, J. V. Ravetch, and N. Y. Lycke. 2011. Complement activation and complement receptors on follicular dendritic cells are critical for the function of a targeted adjuvant. *J. Immunol.* 187: 3641–3652.

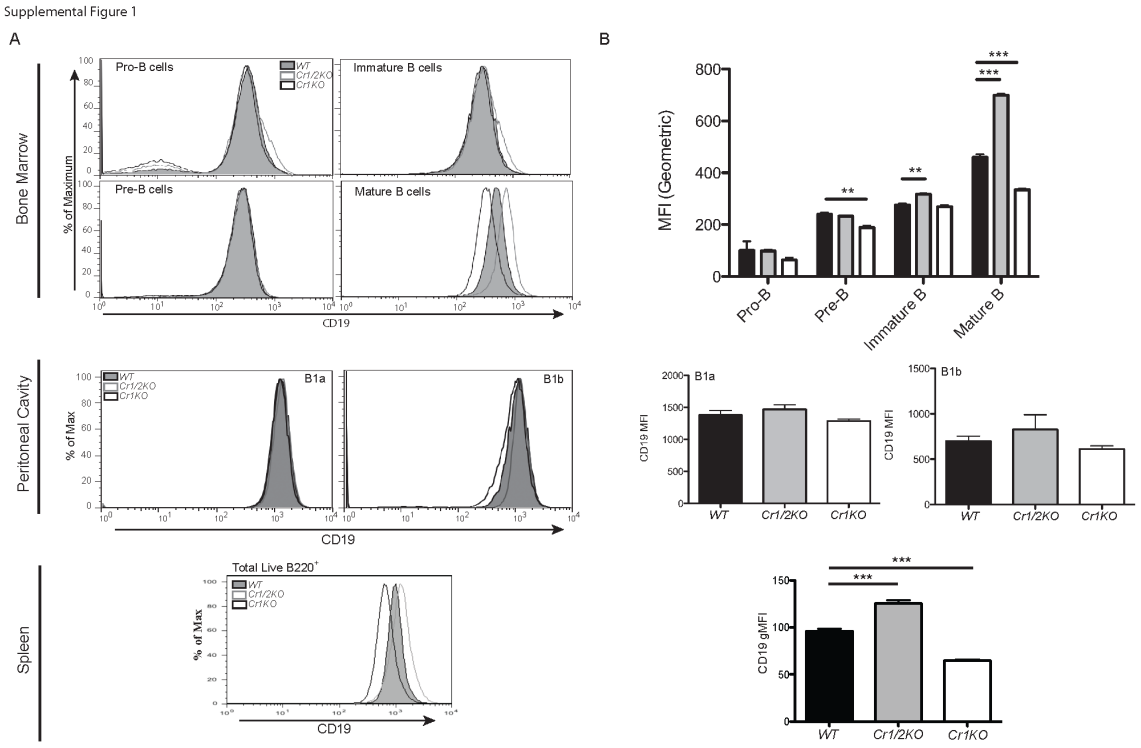

Figure 3.S1. Representative histograms of CD19 expression on bone marrow, peritoneal, and splenic B cells. *A* and *B*, Total bone marrow, peritoneal cavity, or splenic cells were isolated from naïve WT (filled histogram/black bars), Cr1/2KO (gray line histogram/gray bars), and Cr1KO (black line histogram/white bars) mice and surface CD19 expression was analyzed by FACS. *A*, Representative histograms of CD19 expression on pro-B, pre-B, immature, and mature B cells (top four plots); B1a and B1b cells from the peritoneal cavity (middle two plots); and total splenic B cells (bottom plot). *B*, Quantification of the geometric mean fluorescent intensity (gMFI) of CD19 staining by FACS analysis on B cell populations from the bone marrow, peritoneal cavity, and total splenic B cells. Bars represent the average gMFI for each genotype. CD19 gMFI was analyzed by ANOVA for each population and determined to be at least $p<0.05$ where significance is shown pairwise (* =$p<0.05$, ** = $p<0.01$, and ***=$p<0.001$ by the student's t-test; n=3; sex matched 8-12 week old mice).

Supplemental Figure 2

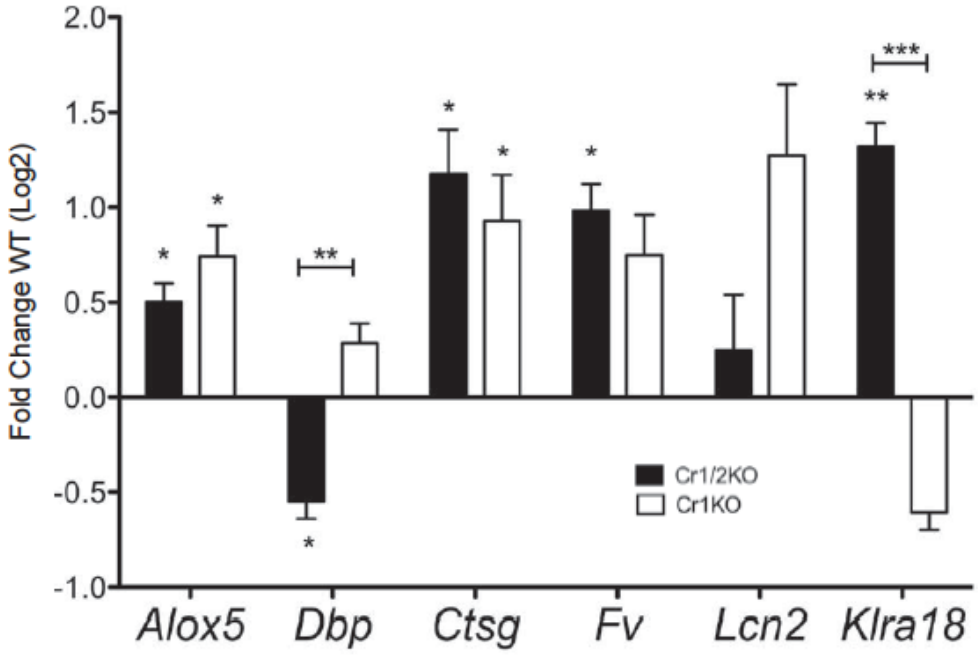

Figure 3.S2. RT-PCR quantification of splenic inflammatory gene expression. Intron spanning primer sets specific for arachidonate 5-lipoxygenase (*Alox5)*, D site albumin promoter binding protein (*Dbp)*, cathepsin G (*Ctsg)*, coagulation factor V (*Fv)*, lipocalin 2 (*Lcn2),* and killer cell lectin-like receptor, subfamily A, member 18 (*Klra18)* were used to quantify gene expression in mRNA obtained from total splenic extracts. All sample quantifications were normalized to 1000 β-actin transcripts. Bars represent the mean fold change from WT (center line) for *Cr1/2KO* (black) and *Cr1KO* (white). (WT n=3, *Cr1KO* and *Cr1/2KO* n=4; 12-16 week old female mice; BALB/C background; Error bars represent SEM; *=$p<0.05$, **=$p<0.01$, ***=$p<0.001$ by student's t-test).

Supplemental Figure 3

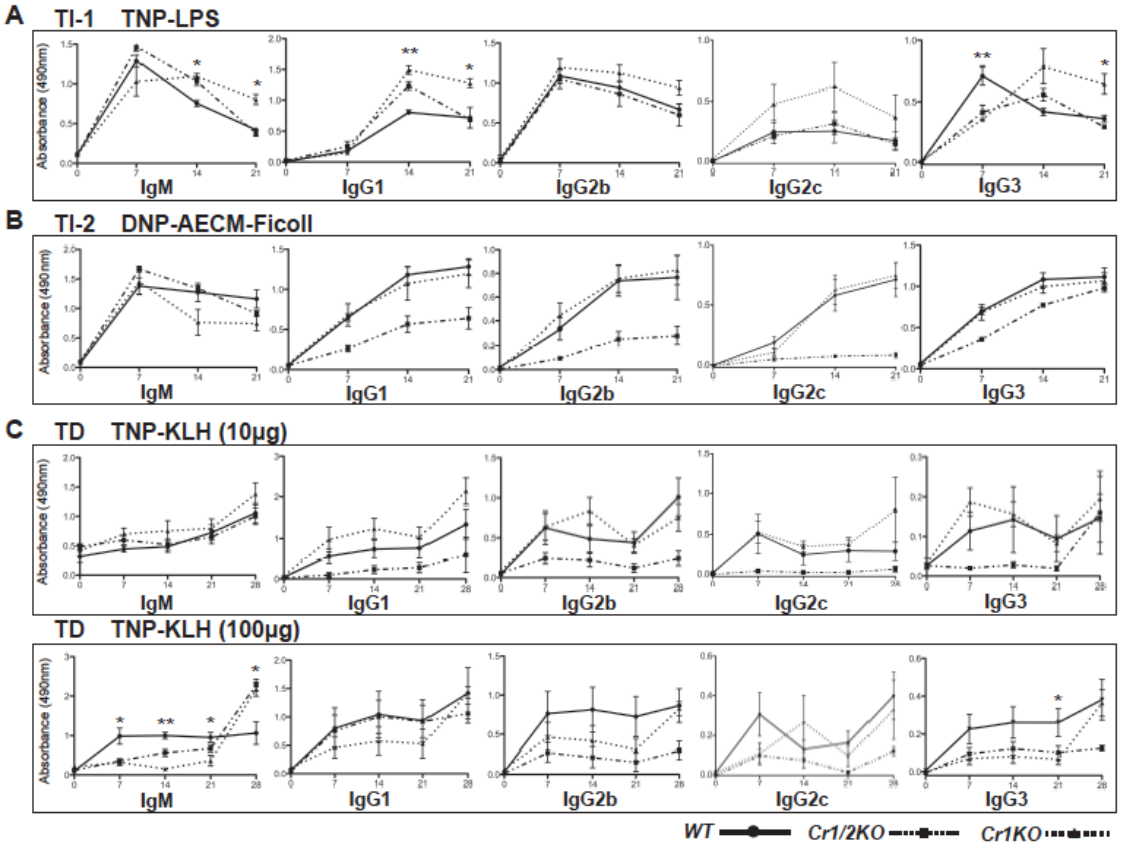

Figure 3.S3. TI-1, TI-2, and TD antigen specific immunoglobulin responses. Experiments were performed in which WT, *Cr1/2KO*, and *Cr1KO* mice were immunized with the model antigens (*A*) TNP-LPS (TI-1) and (*B*) DNP-AECM-Ficoll (TI-2), as well as (*C*) TNP-KLH (TD) at both a low dose immunization (10µg) and high dose immunization (100µg). All mice that were immunized with TNP-KLH were administered a secondary immunization at 21 days. Serum samples were collected at seven day intervals post-immunization, and antigen specific immunoglobulin (IgM, IgG1, IgG2b, IgG2c, and IgG3) abundance was measured by ELISA. All data graphed here are included in the larger data set shown in **Fig.9**. (TI-1 n=4-7; TI-2 n=6; TD (low) n=4; TD (high) n=5; 8-12 week old sex matched mice; * = $p<0.05$; ** = $p<0.01$ significance between WT and Cr1KO by student's t-test).

Supplemental Figure 4

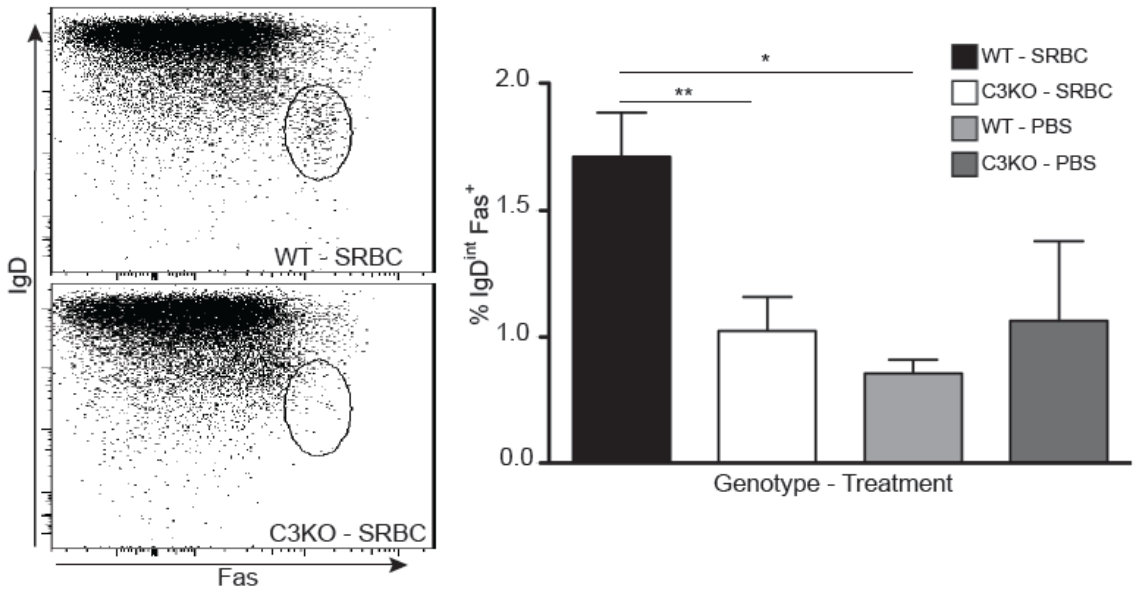

Figure 3.S4. FACS analysis of C3KO GC B cells following SRBC immunization. Percentage of live $B220^{+}$ splenocytes that are IgD^{int} Fas^{+} in SRBC immunized WT and C3KO mice compared to mock PBS immunized mice and representative dot plots. (n=8 immunized, n=2 PBS; Error bars represent SEM; ns=not significant; *=$p<0.05$, **=$p<0.01$, ***=$p<0.001$ by student's t-test)

CHAPTER 4

MURINE COMPLEMENT RECEPTOR 1 IS REQUIRED FOR GERMINAL CENTER B CELL MAINTENANCE AND THE GENERATION OF MEMORY B CELLS BUT NOT LONG-TERM IMMUNOGLOBULIN PRODUCTION

Abstract

Germinal centers are the sites of maturation for high affinity immunoglobulin switch expressing plasma cells and memory B cells. The GC B cells that are precursors of these cells circulate between the light zone B cell population that interacts closely with antigen laden FDCs and the highly proliferative dark zone B cell population. Antigen retention by FDCs is dependent on Fc receptors as well as complement receptors and complement receptor 1 (Cr1) is the predominant complement receptor expressed by FDCs. The newly created *Cr1KO* mouse was used to test the effect of Cr1-deficiency on the kinetics of the germinal center reaction and the generation of IgM and switched memory B cell formation. Immunization of *Cr1KO* mice results in the normal expansion of B cells with a GC phenotype but these cells are not maintained at WT levels. This GC

B cell reduction is dependent on FDC expression of Cr1, and although it does not affect antigen-specific IgG titers after 37 days, memory B cell numbers are reduced.

Introduction

B cells specific for any given antigen are found in modest numbers. For large multi-epitope proteins mice have been shown to contain thousands of antigen-specific cells (1). Immunization with these antigens can produce tens of thousands of long-term memory B cells from this pool. Phenotypically, these cells are nearly indistinguishable from naïve cells by markers, but they consist of a heterogeneous population of various immunoglobulin classes, enhanced immunoglobulin affinity, and heightened antigen sensitivity. Conventionally, memory B cells have been described as emerging from the follicular (FO) B cell subset (B2 B cells); however, memory has also been shown to be generated from the B1b pool (2) and presumably from the marginal zone (MZ) B cell pool as well (3). Despite the considerable work being done on B cell responses and generation of immunological memory, the mechanistic details of these functions are still not fully understood. Two impediments have slowed the progress in the advance of memory B cell research. The first is the inherently small number of memory cells residing after an immune response. The second is that despite an accepted marker for memory B cells in humans, CD27, a similar marker has not been defined in the murine system. Support has been provided for the use of some markers such as CD35 (Cr1), CD80, and CD73 (4, 5) to delineate unswitched immunoglobulin from switched immunoglobulin and GC-derived from non-GC-derived but memory B cells still must be tracked by other means. Recently, however, B cells' characteristic of binding the antigen

for which they are specific and the immunogenic nature of the fluorophore allophycocyanin (APC) has been utilized to track memory B cells (1, 5, 6).

Research has implicated the complement system and complement receptors (Cr) 1 and 2 in the generation of memory B cell responses. Studies directly assessing the ability of *Cr2* hypomorphic (mice in which the *Cr2* gene produces low quantities of smaller Cr1/2 proteins (7, 8)) and *Cr2-/-* mice has supported a role for Cr1/2 in the generation of memory B cells (9-11). These effects have been attributed to the deficiency of expression of Cr1/2 in the stromal compartment, most notably the follicular dendritic cells (FDC). FDC are responsible for the trapping of antigen via Cr and Fc receptors (12, 13), and for orchestrating the GC reaction (14, 15). The recent development of a mouse specifically deficient for the Cr1 isoform of *Cr2*, the *Cr1KO* (16), and the revelation that Cr1 is the nearly exclusive isoform expressed by the stromal compartment FDCs (16) suggested that the Cr1-deficiency (*Cr1KO*) may result in a significant reduction in GC output of memory B cells. Initially, we assessed the extent of the GC B cell reduction in *Cr1KO* mice and determined that this reduction is dependent on FDC expression of Cr1. However, the reduction in GC B cells was not shown to be caused by a specific block in progression through the LZ or DZ B cell stage. It is also shown that Cr1 is required for memory B cell generation from the unswitched compartment, and to a lesser extent, the switched compartment. Intriguingly, these results were found to be independent of long-term antibody production. I propose that these data suggest a model in which Cr1 is not simply a marker of derivation but a functional receptor in the determination of memory B cells in GC independent responses, and I propose a temporal model for plasma versus

memory B cell formation in which extended antigen retention is required later in GCs for optimal memory formation.

Materials and Methods

Mice and immunizations

All mice used were six to twelve weeks of age. *Cr1KO* mice were at least N=6 generations backcrossed on C57BL6/J and derived from those described previously (16). *Cr1/2KO* mice bred on site were *Cr2*-null mice on the C57BL6 background (17). *C3KO* mice bred on site were progeny of *C3*-null mice purchased from The Jackson Laboratory (Bar Harbor, ME). All WT C57BL6/J mice were purchased from The Jackson Laboratory or bred on site.

For sheep red blood cells (SRBC) (Innovative Research Inc., Novi, MI), immunizations SRBC were washed three times with cold PBS and resuspended in PBS just before use. SRBC immunizations were $2x10^8$ SRBC delivered i.p. in 200µl. Immunization with APC was i.p. injection of 30µg APC (ProZyme Inc., Hayward, CA) in 200µl of an emulsion of 1:1 complete Freund's adjuvant. PBS controls were done identically with no APC.

Bone marrow chimera mice

Bone marrow chimera mice were generated as described previously (16). Briefly, one day prior to transplant, two doses of 550 cGy (4 hours apart) were delivered to host mice using an x-ray irradiator. Bone marrow was isolated into PBS from femurs and tibias of donor mice. WT and *Cr1KO* bone marrow was pooled respectively and split into

a ratio of one donor to three host mice. The lethally-irradiated mice were anesthetized with isoflurane (VetOne, Meridian, ID); the bone marrow transplant was administered retro-orbitally. Chimeras were administered sulfamethoxazole/trimethroprim via drinking water for 21 days and full reconstitution was allowed for six weeks.

Flow cytometry

Cell staining and flow cytometric analysis of dark zone, light zone, and total GC B cells was performed exactly as described previously (16). The following antibodies from BioLegend (San Diego, CA) were used: rat anti-CD83 Alexafluor647 (clone: Michel-19), rat anti-B220 APC/Cy7 or BV785 (RA3-6B2), rat anti-CD38 PE or PE/Cy7 (90). The following antibodies from eBioscience (San Diego, CA) were used: rat anti-GL7 Alexafluor488, rat anti-CXCR4 PerCP/Cy5.5 (2B11), rat anti-IgM PE (eB121-15F9), and purified rat anti-CD16/32 (93) as Fc block. The following antibodies from BD Biosciences (San Jose, CA) were used: rat anti-CD95 (Fas) PE/Cy7 (Jo2), rat anti-CD4 PE (GK1.5), and rat IgG2a, kappa PE (Catalog #553930) as an isotype control for anti-IgM. Rat anti-IgM was proactively determined to be negative for cross-reactivity with rat IgM anti-GL7. Data acquisition was performed on a FACS CantoII (BD Biosciences, San Jose, CA) and data analysis was performed using FlowJo version 8.8.7 (Tree Star, Inc., Ashland, OR).

APC-positive cell enrichment

The protocol for enrichment of APC^+ cells from total splenocytes was adapted from methods described by others (1, 5). Total splenocytes were isolated by straining

spleens through 100µm mesh strainers into ice cold 0.5% BSA 2mM EDTA PBS (FACS buffer), pelleted by centrifugation, and resuspended in ACK red blood cell lysis buffer. Cells were repelleted and washed with 10ml of ice cold PBS. Cells were then stained with 2.5µg/ml APC (ProZyme Inc., Hayward, CA) in 2% rat serum PBS with rat anti-CD16/32 (Fc block) for 30 minutes on ice in the dark. A 12.5ml volume of FACS buffer was added to the cell mix and the cells were pelleted by centrifugation. APC-stained cells were incubated in a 500µl volume of FACS buffer with 50µl of anti-APC microbeads (Miltenyi Biotec Inc., Auburn, CA), covered in the dark for 15 minutes. Cells were washed with an additional 12.5ml of FACS buffer and pelleted by centrifugation. The cells were then resuspended in 500µl FACS buffer and retained on a prewashed, magnetized LS column (Miltenyi Biotec Inc., Auburn, CA) followed by three washes with 3ml of FACS buffer before removing the column from the magnet and flushing the retained cells free with 5ml of FACS buffer. Total cell numbers for APC-enriched and APC^- fractions were determined by trypan blue cell counts. All APC-enriched cells (1-3x10^6 viable cells) and 2-4x10^6 viable APC^- cells were aliquotted and stained for flow cytometric analysis. Total APC^+ cell numbers were calculated after flow cytometry by determining the total APC^+ population of interest from enriched and negative (usually negligible) sorts and adding the two together. Total memory B cell numbers were determined by subtracting the average number of APC^+ cells in PBS/CFA immunized mice from APC/CFA immunized counts.

ELISA

Immulon 4HBX (Thermo Fisher Scientific Inc., Waltham, MA) plates were coated by applying 100µl of 5µg/ml APC in PBS, sealing, and incubating overnight at 4^{o}C. Plates were washed three times by flooding with 0.1% Tween/PBS (wash buffer) and discarding. Plates were blocked with 200µl volumes per well of 1% BSA/0.1% Tween/PBS for 1.5 hours at room temperature. Serial dilutions of serum were prepared in 1%BSA/PBS in 96-well polystyrene plates. For IgM, dilutions were started at 1:10 and 7 serial dilutions of 1:2 were performed to a maximum of 1:1280. IgG assessment was done identically with 8 dilutions from 1:100 to 1:12800. Plates were washed once. Diluted samples were applied to plates in 100µl volumes after blocking and incubated for 1.5 hours at room temperature. Plates were washed three times. Horseradish peroxidase conjugated sheep anti-mouse IgG (#515-035-071, Jackson ImmunoResearch, West Grove, PA) or rabbit anti-mouse IgM (#315-035-049, Jackson ImmunoResearch, West Grove, PA) was diluted 1:2000 in 1% BSA/PBS and wells were incubated with 100µl volumes for 1.5 hours at room temperature. Plates were washed six times with wash buffer and horseradish peroxidase was visualized by exposure o-Phenylenediamine solution. Reaction was stopped with 1N HCl and absorbance was measured at 490nm with a plate reader (BioTek Instruments Inc., Winooski, VT). Serial diluted standards on capture antibody were included on each plate to assure plate to plate consistency and nonspecific IgM or IgG was used to assure secondary specificity. Reciprocal titers were determined by calculating the best fit logarithmic trendline for each sample's serial dilution and calculating the reciprocal dilution necessary for a specified absorbance (OD=0.4 for IgM and OD=1 for IgG).

Statistical analysis

Statistical analysis and graphs were generated using Prism version 5.0c (GraphPad Software, Inc)

Results and Discussion

Previous work from our group characterizing the *Cr1KO* mice revealed that the most striking phenotype was a reduction in the percentage of GC B cells (16). This study also revealed the surprising finding that the Cr1 and Cr2 isoforms are differentially expressed on B cells and FDCs with a preference for Cr2 on the former and near exclusivity of Cr1 on the latter. In light of these findings we were intrigued to investigate the effects and extent of the GC B cell reduction in terms of timing and the dependence of FDC expression of Cr1. We initially designed experiments to define the extent of the previously described GC B cell deficit. B cells expressing an activated, GC B cell, phenotype are commonly seen as early as 4 days and peak at 8 to 14 days after immunization with sheep red blood cells (SRBCs) (18), a trend which is seen with most immunizations (19). Cr1-deficiency was found to result in a reduced frequency of GC B cells at 7 days postimmunization (dpi) but SRBC-specific IgG titers suggested normal plasma cell generation. We considered the possibility that GC B cells recovered after 7 days. To visualize the progression of the GC B cell response we immunized *Cr1KO*, WT, *Cr1/2KO*, and *C3KO* mice intraperitoneally (i.p.) with $2x10^8$ SRBCs and harvested spleens at 5, 7, 9, 11, and 13 dpi (Figure 4.1a and b). Intriguingly, the expansion of B cells with an activated GC phenotype appeared to be initiated equally as well as WT in the absence of Cr1, but the maintenance of GC B cells past 7 days is markedly

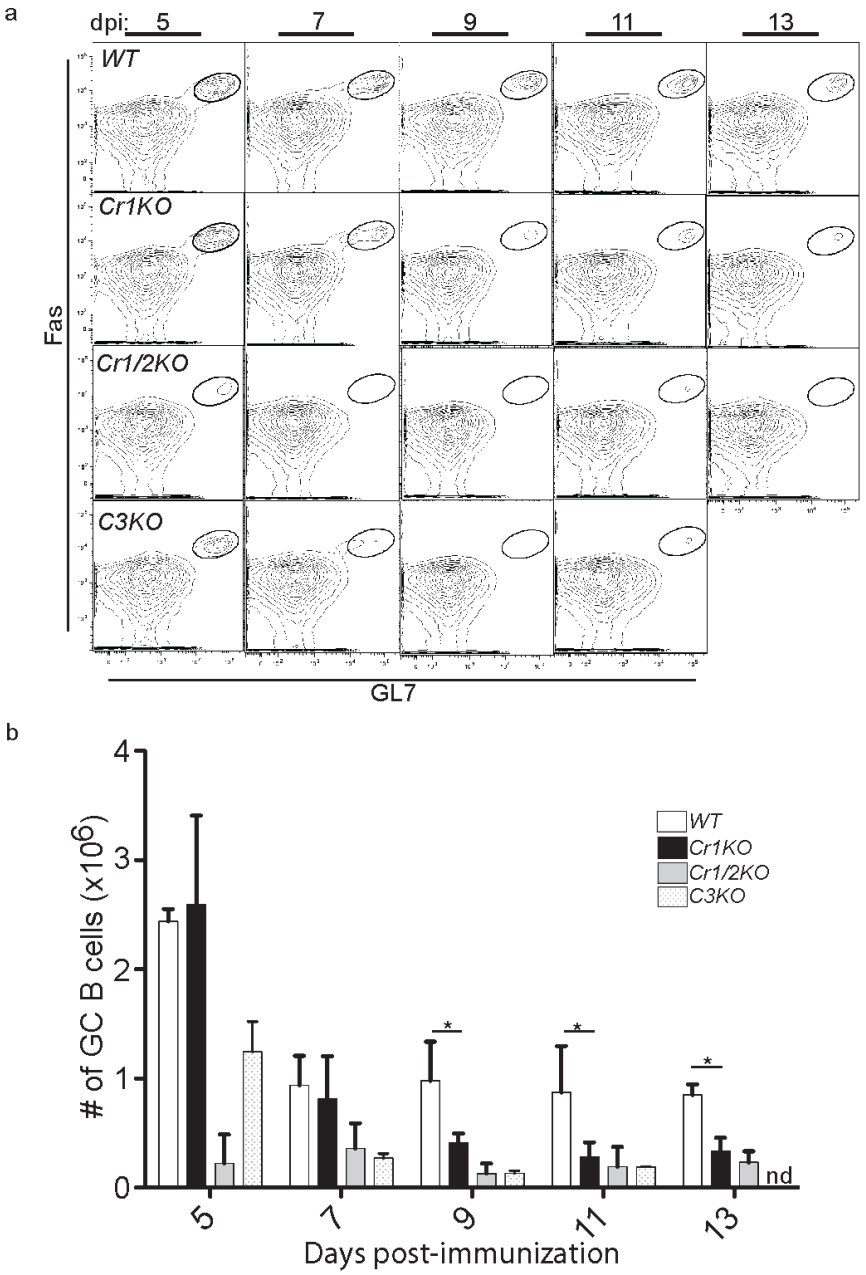

Figure 4.1. GC B cell maintenance is Cr1 dependent but C3 and Cr2 are required for their generation. (a) Representative flow cytometric analysis of GC B cells, identified as the Fas^{+} $GL7^{+}$ cells in the $B220^{+}$ subset, from mice 5, 7, 9, 11, and 13 days post-immunization (dpi) with $2x10^{8}$ SRBCs (administered i.p.). (b) Quantification of the average number of splenic GC B cells for *WT*, *Cr1KO*, *Cr1/2KO*, and *C3KO* mice represented in (a). Data represent a compilation of two independent experiments (n=4, days 7, 9 and 11; n=2, days 5 and 13 and all *C3KO*). Significance for *Cr1KO* compared to *WT* as shown *$p<0.05$ by unpaired t-test.

reduced. Besides expressing the GC B cell markers GL7 and Fas, these cells are expressed at a time consistent with their presence in GCs. It is possible, however, that these cells are in fact expressing a GC B cell phenotype but are still localized in the perifollicular region where they expand in context with T cells before transitioning to GCs. From these data, it can be concluded, however, that WT-like numbers of B cells with a GC phenotype are present early on.

The GC B cell time course data also demonstrate the importance of C3 ligands and Cr2 during B cell responses. In contrast to the normal expansion but depressed maintenance of GC B cells in the *Cr1KO* mice, the *C3KO* and *Cr1/2KO* mice exhibited significantly fewer GC B cells at all time points (Figure 4.1a and b). These findings are consistent with the hypothesis that Cr1 on FDCs retains complement bound antigen for GC B cell maturation, but Cr2 and C3 are necessary for B cell co-receptor enhancement initially. The considerable depression in *Cr1/2KO* GC B cells in comparison even to the *C3KO* supports the suggestion by others that these mice have additional C3 ligand independent deficiencies such as the subtle anergy caused by CD19 overexpression (20).

Cr2 expression in the *Cr1KO* mouse has been found to rescue many of the phenotypes of the *Cr1/2KO* mouse that are unlikely to involve an FDC component; normal response to TI antigens, normal naïve antibody levels, normal B1a population frequency, etc. Along with these data from the *Cr1KO*, the normal expansion of B cells with a GC B cell phenotype suggests that the rapid contraction of the GC B cell compartment is caused by the deficiency of Cr1 on FDCs. To test the effects of Cr1-deficiency exclusively in B cells or FDCs, we took advantage of the radioresistance of FDCs and generated bone marrow chimeras. WT bone marrow was transplanted into

Cr1KO hosts (WT-->*Cr1KO*) and *vice versa* for comparison to control WT-->WT and *Cr1KO*-->*Cr1KO* chimeras. Immunization of these mice with $2x10^8$ SRBCs revealed that GC B cells were found more frequently in WT host mice than in *Cr1KO* host mice at 9 dpi regardless of the genotype of the hematopoietic compartment (Figure 4.2a and b). These data show that expression of Cr1 on FDC is responsible for the GC B cell phenotype exhibited by *Cr1KO* mice. Additionally, these data show that Cr1 has a minimal role on B cells in GCs.

Historically, GC reactions have been defined as containing two GC B cell subsets, centroblasts and centrocytes. The highly proliferative centroblasts are found in the visibly darker "dark zone" (DZ) and the centrocytes are found in the visibly lighter "light zone" (LZ) in close interaction with antigen laden FDCs (21). Recently, the Nussenzweig group identified markers that delineate DZ and LZ B cells from within the GC B cell niche (22). It may be hypothesized that in the absence of Cr1, a reduction in antigen retention would result in an accumulation of LZ B cells unable to cycle back at normal rates to the proliferative DZ B cell stage. Assessment of the percentage of GC B cells ($CD38/CD4^-$ Fas^+) that were found in the LZ ($CXCR4^{lo}$ $CD83^{hi}$) compartment versus the DZ ($CXCR4^{hi}$ $CD83^{lo}$) compartment was not affected by Cr1 deficiency (Figure 4.3a and b). It should be noted, however, that as subsets of the total GC B cell population, the actual number of DZ and LZ B cells is reduced in the *Cr1KO* compared to WT mice (data not shown).

The previous *Cr1KO* study demonstrated that TD antigen specific IgM and IgG3 titers were significantly reduced compared to WT when mice were immunized with

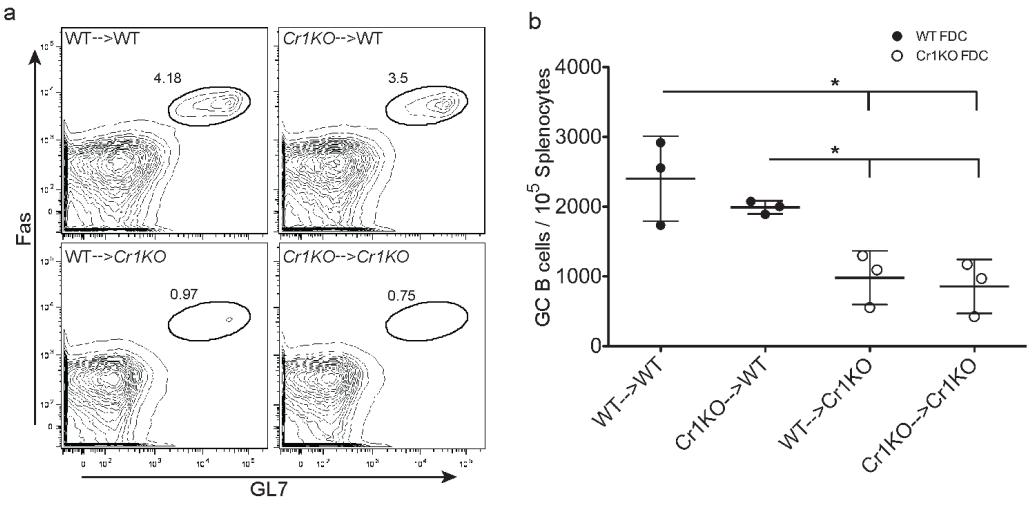

Figure 4.2. FDC but not B cell expression of Cr1 is required for GC B cell production. Bone marrow chimera mice (Donor-->Host) were generated between all possible pairings of *Cr1KO* and WT mice. SRBC immunizations ($2x10^8$) were administered i.p. six weeks following bone marrow reconstitution of lethally irradiated hosts. (a) Analysis of the Fas^+ $GL7^+$ (GC B cells) from the total $B220^+$ population of the spleen 9 days following SRBC immunization. (b) *Cr1KO*-->WT chimeras showed the same number of GC B cells per 10^5 splenocytes as WT-->WT chimeras 9 dpi with SRBCs. WT-->*Cr1KO* and *Cr1KO*-->*Cr1KO* chimeras showed significant reductions in GC B cells per 10^5 splenocytes compared to chimeras in which the hosts were WT. Closed circles denote chimeras in which FDCs are WT in contrast to open circles which represent chimeras with *Cr1KO* FDCs. Points represent individual mice with the average and standard deviation for each group shown. Brackets designate statistical analysis by unpaired t-test; *$p<0.05$. All mice were age matched female mice; n=3.

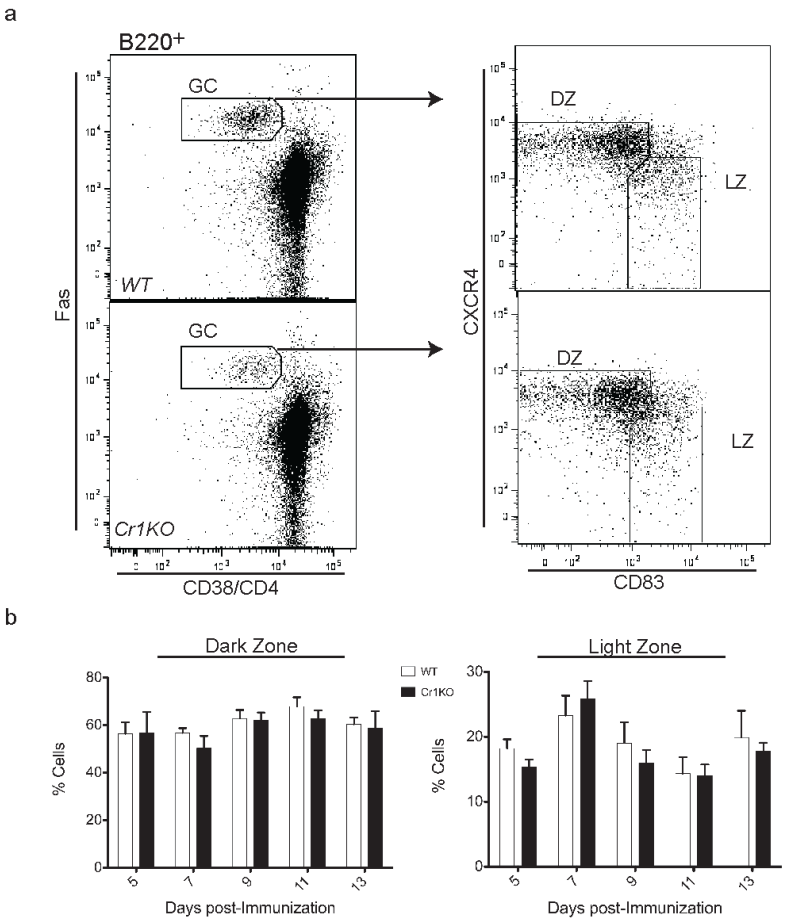

Figure 4.3. Dark zone and light zone B cells are proportionately represented in the absence of Cr1. (a) Gating example showing the strategy used to identify dark zone (DZ) versus light zone (LZ) B cells from the GC B cell compartment. Example shown is from 9 dpi. GC B cells were sorted from the total $B220^{+}$ population of splenic B cells as Fas^{+} and $CD38/CD4^{-}$. DZ B cells are characterized as $CXCR4^{hi}$ and $CD83^{lo}$ and LZ B cells are $CXCR4^{lo}$ and $CD83^{hi}$. (b) Average percent of GC B cells that are DZ or LZ B cells from *WT* and *Cr1KO* mice 5, 7, 9, 11, and 13 dpi with $2x10^{8}$ SRBCs (administered i.p.). All days and genotypes represent compilation of two independent experiments (n=4 for all days). Error bars represent SD.

soluble TNP-KLH (Figure 3.9a). In light of the large reduction in GC B cells in the *Cr1KO* mouse, it could be predicted that the effects on other IgG isotypes, especially IgG1, and on recall would be more pronounced. We considered the possibility that 21 dpi may still be too early to identify reductions in the GC-derived immunoglobulin. To investigate this possibility, we measured the total allophycocyanin (APC) specific IgM, as well as IgG, antibody titer from *Cr1KO* and WT serum samples collected 35 to 37 days after immunization with 30μg APC emulsified in complete Freund's adjuvant (CFA) (Figure 4.4). The results suggested that by 35 to 37 dpi, anti-APC IgM had retracted to the levels seen in mice immunized with a PBS/CFA emulsion (Figure 4.4a). However, there were differences between anti-APC IgM in WT and *Cr1KO* at this new baseline. This trend was seen in the PBS/CFA mice and was exacerbated significantly between the genotypes in the APC/CFA immunized mice. Anti-APC IgG titers, however, were still present at considerable levels. The anti-APC IgG titers were strikingly similar among the *Cr1KO* and WT mice (Figure 4.4b).

GC B cells are predominantly the precursors of high affinity and class-switched memory B cells. To test the effect the reduced GC B cell number in *Cr1KO* mice had on memory B cells, we used the recently described method of immunizing mice with APC and tracking the generation of APC^+ cells. The same mice from the APC-specific antibody experiment were assayed 35 to 37 dpi by incubating their splenocytes with APC and using anti-APC magnetic beads to enrich for APC^+ cells on a magnetized column. These cells were then analyzed by flow cytometry for their expression of the naïve/memory B cell phenotypic markers $CD38^+$ $GL7^-$ and the percent of APC^+ cells from the IgM^+ and IgM^- (switched) fraction was assessed (Figure 4.5a). Using the

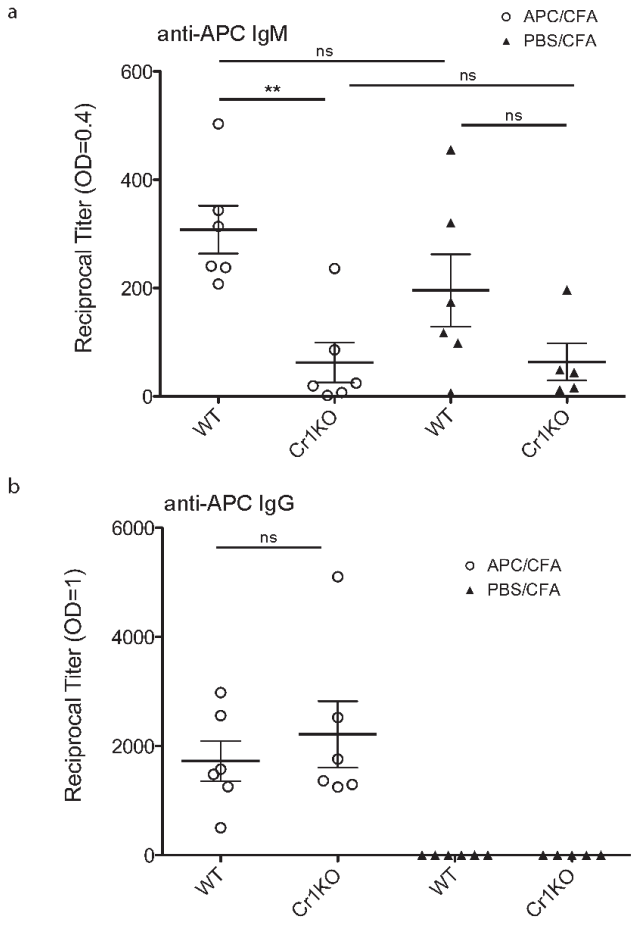

Figure 4.4. The IgG response to APC is not affected by Cr1-deficiency despite a significant reduction in anti-APC natural antibody of the IgM isotype. (a) ELISA analysis of serum from *WT* and *Cr1KO* mice 35-37 days after i.p. immunization with 30μg APC emulsified in CFA (APC/CFA) versus negative control PBS/CFA immunized mice. Reciprocal anti-APC IgM required to produce an absorbance of OD=0.4. (b) Reciprocal titers of anti-APC IgG from the same serum samples shown in (a). Each symbol represents one mouse with the mean shown by the bar. Error bars represent SEM. *$p<0.05$, **$p<0.01$, and ns=not significant by unpaired t-test.

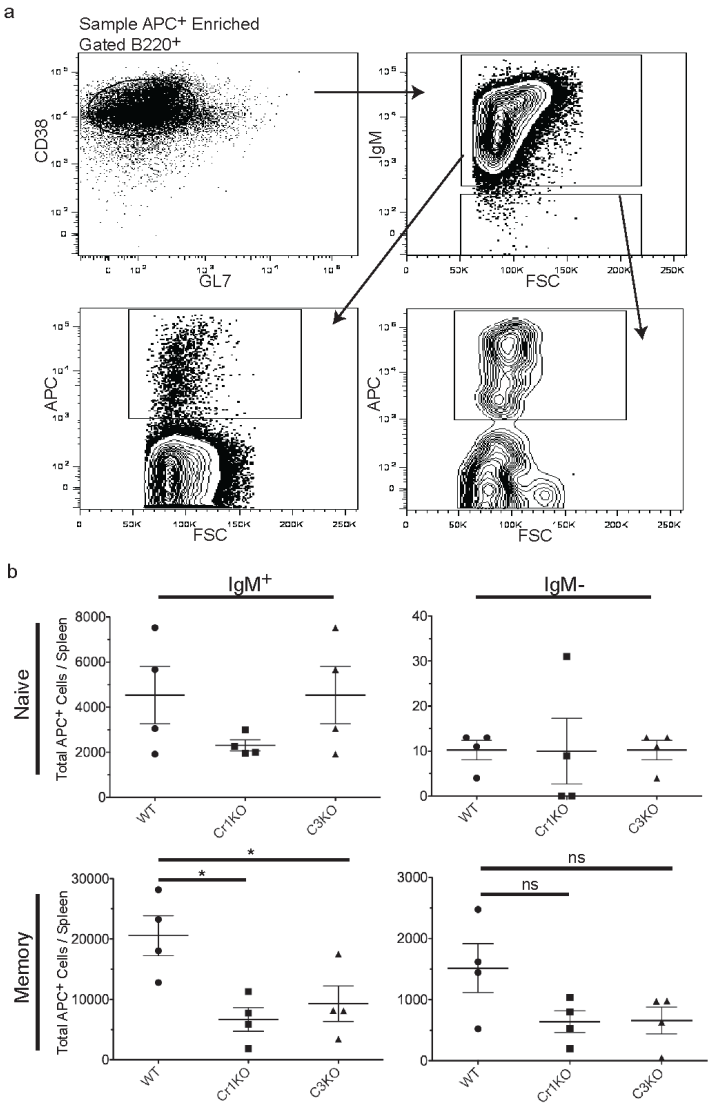

Figure 4.5. Memory B cells are reduced in the absence of Cr1. APC positive B cells from *WT*, *Cr1KO*, and *C3KO* mice were quantified 35-37 days after i.p. immunization with 30μg APC/CFA. Prior to flow cytometric analysis, total splenocytes were incubated with APC and enriched by magnetic column isolation. (a) Naïve and memory B cells were identified using flow cytometry to sort out $B220^+$ $CD38^+$ $GL7^-$ subset and to assess the IgM and APC expression. IgM- cells were considered to be Ig switched. (b) The average number of naïve IgM^+ and Ig switched APC^+ cells is shown with error bars showing SEM. The number of naïve cells was calculated by determining the number of these cells present in PBS/CFA immunized mice. Memory B cells for APC were calculated by subtracting the average number of APC+ cells from PBS/CFA immunized mice from those found in APC/CFA immunized mice. Significantly fewer IgM^+ APC^+ memory cells were generated in *Cr1KO* and *C3KO* mice compared to *WT*, while slightly fewer Ig switched memory cells were generated. Data represents one of two experimental replicates. Symbols represent individual mice; *$p<0.05$, ns=$p>0.05$ by unpaired t-test.

percentages from the enriched and depleted fractions the number of APC^+ memory B cells was calculated in comparison to the number APC^+ naïve B cells in the PBS/CFA immunized mice. The number of naïve APC^+ cells in the IgM^+ and IgM^- populations were not found to differ between the *Cr1KO*, WT, and *C3KO* mice (Figure 4.5b). As would be predicted, the APC^+ IgM^- naïve B cell population was very near to zero. Following immunization, approximately 20,000 WT APC^+ IgM^+ were generated and remained at 35-37 dpi. The *Cr1KO* and *C3KO* mice generated only about 5000-10,000 APC^+ IgM^+ B cells. A similar trend was identified in the IgM^- population of cells. 1500 APC^+ IgM^- cells were generated in WT mice while only about 500 cells were present in the *Cr1KO* and *C3KO* mice. This difference was not significantly different; however, a second replicate not shown displayed an identical trend, albeit with reduced overall numbers of cells (data not shown). Further replicates will be necessary to definitively determine if these populations are different.

Together, the data in this report support an importance for Cr1 GC B cell maintenance and memory B cells but not antigen-specific antibody. Surprisingly, the memory B cell population that is most strongly affected is the IgM^+ subset despite the minimal GC-dependence of this population. This suggests that despite the dependence of GC B cells on FDC expression of Cr1, an additional function of Cr1 on B cells is important for GC-independent responses. A function that is also suggested by the recent identification of Cr1 as a marker for unmutated memory B cells (4).

If we temporarily ignore the IgM results, which may or may not be GC-derived and focus solely on the IgM^- memory B cells and IgG antibody, a few explanations of the data exist. In the first model, I propose that switched plasma cells and memory B cells

emerge from the GC at temporally different stages. B cells with a GC B cell phenotype are generated readily early on after immunization and if these cells form most of the plasma cells, then immunoglobulin levels would be minimally affected in the *Cr1KO* mice. If the memory B cells then emerged in the later stages of the GC when *Cr1KO* GC B cells are reduced in number, then we would predict a stronger effect on the memory population. Additionally, the small population of GC B cells that does persist may be the reason for the less dramatic reduction in total IgM^- memory cells. This model is not without precedence. In humans, where memory B cells are more readily identifiable, it has been suggested that plasma cells emerge between 6 and 8 days while memory B cells are not detected until 8 days. The caveats of this study are that it followed cells responding to tetanus toxin immunization in previously vaccinated people and inferred emergence from appearance in peripheral blood samples (23). In contrast to this study and the data described in this report, it has been suggested that in mice, plasma cells emerge later and memory B cells emerge earlier during the GC reaction (24-26). Takahashi *et al.*, however, did not analyze memory B cell number or mutation content prior to 20 days. Inamine *et al.* provide the best evidence for the early emergence of highly mutated memory B cells; however, no comparisons were made to plasma cell production and memory B cells overall were normal. The most conclusive finding of these papers is that disruption of the GC B cell phenotype more strongly affects SHM than fate. It will be critical to determine the effects of Cr1-deficiency on mutation number and Ig affinity (SHM). Alternatively, it is possible that both IgM^- memory B cells and IgG secreting plasma cells are equally reduced in number but by inferring relative plasma

cell number from antibody titers, a reduced population that is producing more antibody per cell has been misrepresented.

The second explanation for the discrepancy between GC-derived antigen-specific IgG and IgM^- memory B cell differences may come from the persistence of some GC B cells in the *Cr1KO*. It is intriguing that GC B cells although significantly reduced continue to persist in the *Cr1KO*. The current understanding of Cr in FDC antigen retention and exclusivity of Cr1 on FDCs strongly suggests that antigen is not properly retained on FDCs. If antigen on FDCs is absolutely required for GC persistence, then other receptors must be playing a role. Fc receptors are known to retain immune complexes on FDCs; however, it has been determined that this is not prevalent during the early portion of the primary response. At the onset of a primary response, no antigen specific IgG is present and Fc (gamma chain specific) receptors lag a few days in expression (27). There are, however, three possibilities: one that low levels of Fc receptors are sufficient to retain some antigen and promote limited GC B cell maturation, two that the use of adjuvant results in extended exposure sufficient to foster the reduced GC reactions observed, and three that another receptor such as the recently discovered Fcμ receptor may be expressed on FDCs (28). Another option is that antigen persistence is not necessary to maintain GCs and that Cr1 provides an unidentified function on FDCs. The importance of antigen persistence in long-term memory maintenance is a hotly debated topic (29) and at least in the early stages GC reactions have been shown to proceed in the near absence of persistent antigen (30). Experiments to establish the antigen retention abilities in the absence of Cr1 and the effects on FDCs will be needed to identify the specific cause of the GC reduction.

Concluding Remarks

The data in this report suggest that Cr1 on FDCs is required for maintenance of GC B cells and for formation of memory B cells. The possibility that Cr1 has a role on B cells is not, however, ruled out and the strong reduction in IgM^+ memory B cells suggests an FDC-independent contribution. Cr1 may be important in the generation of switched memory B cells as well, but the difference is less striking. It seems that reduced GC B cell numbers can at least partially fill this compartment. In light of the demonstrated Cr1-dependent reduction in GC B cells, it is surprising that total antigen-specific IgG was not affected long-term. In context of the GC B cell data in which Fas^+ $GL7^+$ B cells in the spleen are generated at normal numbers until 7 dpi then decline relative to WT, these data suggest that plasma cells emerge very early on while memory B cells emerging later are not produced in optimal numbers. Not shown, however, is the affinity within either of these populations. It is possible that the WT IgG levels and inconclusiveness of the IgM^- memory B cell data demonstrate an ability of low affinity B cells to fill these niches when high affinity GC B cells are not being generated. In total, the data support our previous identification of the importance of Cr1 on GC B cells and provide evidence that the loss is dependent on FDC expression of Cr1. The data do not demonstrate a straight forward role for Cr1, but they do provide further evidence of the requirement for FDC expressed Cr1 in GC B cell maintenance. The *Cr1KO* is an intriguing tool for the study of suboptimal GC conditions on humoral immune outcomes.

References

1. Pape, K. A., J. J. Taylor, R. W. Maul, P. J. Gearhart, and M. K. Jenkins. 2011. Different B cell populations mediate early and late memory during an endogenous immune response. *Science* 331: 1203-1207.

2. Alugupalli, K. R., J. M. Leong, R. T. Woodland, M. Muramatsu, T. Honjo, and R. M. Gerstein. 2004. B1b lymphocytes confer T cell-independent long-lasting immunity. *Immunity* 21: 379-390.

3. Phan, T. G., S. Gardam, A. Basten, and R. Brink. 2005. Altered migration, recruitment, and somatic hypermutation in the early response of marginal zone B cells to T cell-dependent antigen. *J. Immunol.* 174: 4567-4578.

4. Anderson, S. M., M. M. Tomayko, A. Ahuja, A. M. Haberman, and M. J. Shlomchik. 2007. New markers for murine memory B cells that define mutated and unmutated subsets. *J. Exp. Med.* 204: 2103-2114.

5. Taylor, J. J., K. A. Pape, and M. K. Jenkins. 2012. A germinal center-independent pathway generates unswitched memory B cells early in the primary response. *J. Exp. Med.* 209: 597-606.

6. Taylor, J. J., M. K. Jenkins, and K. A. Pape. 2012. Heterogeneity in the differentiation and function of memory B cells. *Trends Immunol.* 33: 590-597.

7. Ahearn, J. M., M. B. Fischer, D. Croix, S. Goerg, M. Ma, J. Xia, X. Zhou, R. G. Howard, T. L. Rothstein, and M. C. Carroll. 1996. Disruption of the Cr2 locus results in a reduction in B-1a cells and in an impaired B cell response to T-dependent antigen. *Immunity* 4: 251-262.

8. Hasegawa, M., M. Fujimoto, J. C. Poe, D. A. Steeber, and T. F. Tedder. 2001. CD19 can regulate B lymphocyte signal transduction independent of complement activation. *J. Immunol.* 167: 3190-3200.

9. Brockman, M. A., A. Verschoor, J. Zhu, M. C. Carroll, and D. M. Knipe. 2006. Optimal long-term humoral responses to replication-defective herpes simplex virus require CD21/CD35 complement receptor expression on stromal cells. *J. Virol.* 80: 7111-7117.

10. Fernandez Gonzalez, S., J. P. Jayasekera, and M. C. Carroll. 2008. Complement and natural antibody are required in the long-term memory response to influenza virus. *Vaccine* 26 Suppl 8: I86-93.

11. Barrington, R. A., O. Pozdnyakova, M. R. Zafari, C. D. Benjamin, and M. C. Carroll. 2002. B lymphocyte memory: role of stromal cell complement and FcgammaRIIB receptors. *J. Exp. Med.* 196: 1189-1199.

12. Tew, J. G., J. Wu, D. Qin, S. Helm, G. F. Burton, and A. K. Szakal. 1997. Follicular dendritic cells and presentation of antigen and costimulatory signals to B cells. *Immunol. Rev.* 156: 39-52.

13. Roozendaal, R., and M. C. Carroll. 2007. Complement receptors CD21 and CD35 in humoral immunity. *Immunol. Rev.* 219: 157-166.

14. Wang, X., B. Cho, K. Suzuki, Y. Xu, J. A. Green, J. An, and J. G. Cyster. 2011. Follicular dendritic cells help establish follicle identity and promote B cell retention in germinal centers. *J. Exp. Med*. 208(12): 2487-2510.

15. Allen, C. D. C., and J. G. Cyster. 2008. Follicular dendritic cell networks of primary follicles and germinal centers: phenotype and function. *Semin. Immunol.* 20: 14-25.

16. Donius, L. R., J. M. Handy, J. J. Weis, and J. Weis. 2013. Optimal germinal center B cell activation and T-dependent antibody responses require expression of the mouse complement receptor cr1. *J. Immunol.* 191: 434-447.

17. Haas, K. M., M. Hasegawa, D. A. Steeber, J. C. Poe, M. D. Zabel, C. B. Bock, D. R. Karp, D. E. Briles, J. Weis, and T. F. Tedder. 2002. Complement receptors CD21/35 link innate and protective immunity during Streptococcus pneumoniae infection by regulating IgG3 antibody responses. *Immunity* 17: 713-723.

18. Shinall, S. M., M. Gonzalez-Fernandez, R. J. Noelle, and T. J. Waldschmidt. 2000. Identification of murine germinal center B cell subsets defined by the expression of surface isotypes and differentiation antigens. *J. Immunol.* 164: 5729-5738.

19. Shlomchik, M. J., and F. Weisel. 2012. Germinal centers. *Immunol. Rev.* 247: 5-10.

20. Haas, K. M., J. C. Poe, and T. F. Tedder. 2009. CD21/35 promotes protective immunity to Streptococcus pneumoniae through a complement-independent but CD19-dependent pathway that regulates PD-1 expression. *J. Immunol.* 183: 3661-3671.

21. MacLennan, I. C. 1994. Germinal centers. *Annu. Rev. Immunol.* 12: 117-139.

22. Victora, G. D., T. A. Schwickert, D. R. Fooksman, A. O. Kamphorst, M. Meyer-Hermann, M. L. Dustin, and M. C. Nussenzweig. 2010. Germinal center dynamics revealed by multiphoton microscopy with a photoactivatable fluorescent reporter. *Cell* 143: 592-605.

23. Odendahl, M., H. Mei, B. F. Hoyer, A. M. Jacobi, A. Hansen, G. Muehlinghaus, C. Berek, F. Hiepe, R. Manz, A. Radbruch, and T. Dörner. 2005. Generation of migratory antigen-specific plasma blasts and mobilization of resident plasma cells in a secondary immune response. *Blood* 105: 1614-1621.

24. Shlomchik, M. J., and F. Weisel. 2012. Germinal center selection and the development of memory B and plasma cells. *Immunological Reviews* 247: 52-63.

25. Inamine, A., Y. Takahashi, N. Baba, K. Miyake, T. Tokuhisa, T. Takemori, and R. Abe. 2005. Two waves of memory B-cell generation in the primary immune response. *Int. Immunol.* 17: 581-589.

26. Takahashi, Y., H. Ohta, and T. Takemori. 2001. Fas is required for clonal selection in germinal centers and the subsequent establishment of the memory B cell repertoire. *Immunity* 14: 181-192.

27. El Shikh, M. E., R. El Sayed, A. K. Szakal, and J. G. Tew. 2006. Follicular dendritic cell (FDC)-FcgammaRIIB engagement via immune complexes induces the activated FDC phenotype associated with secondary follicle development. *Eur. J. Immunol.* 36: 2715-2724.

28. Shima, H., H. Takatsu, S. Fukuda, M. Ohmae, K. Hase, H. Kubagawa, J. Y. Wang, and H. Ohno. 2010. Identification of TOSO/FAIM3 as an Fc receptor for IgM. *Int. Immunol.* 22: 149-156.

29. Haberman, A. M., and M. J. Shlomchik. 2003. Reassessing the function of immune-complex retention by follicular dendritic cells. *Nat. Rev. Immunol.* 3: 757-764.

30. Hannum, L. G., A. M. Haberman, S. M. Anderson, and M. J. Shlomchik. 2000. Germinal center initiation, variable gene region hypermutation, and mutant B cell selection without detectable immune complexes on follicular dendritic cells. *J. Exp. Med.* 192: 931-942.

CHAPTER 5

SUMMARY AND CONCLUSION

A Novel Understanding of Cr1 Expression and Cr2 Splicing

Our knowledge of the role of complement receptors in humoral immunity has expanded tremendously over the last three decades. This understanding was initiated early on by observations of the complement enhancing effects of humoral immunity and then pioneered by the detailing of the signaling mechanisms of CR2 by Douglas Fearon and colleagues (1). However, it was not determined how independent production of Cr1 and Cr2 from the murine *Cr2* gene achieved improved functionality compared to producing just Cr1. Cr1 contains all the binding domains found in both and would be predicted to function in all the roles of each. Studies suggest that using *Cr1/2KO* mice to understand the homogeneous functions of Cr1 and Cr2 may have been misleading, especially with respect to complement regulation by Cr1 (2-4). The predicted conservation of roles and sequence between Cr1/Cr2/CRRY and CR2/CR1, in mice and humans respectively, provide evolutionary evidence for the conservation of function among the three proteins (2, 5). Humans express CR2 from the *Cr2* gene homolog *CR2* while they express CR1 from a separate, *CR1*, that is more closely related to *Crry*. However, CR1 possesses similarity with Cr1 and CRRY. CR1 is similar in size to Cr1,

but sequence and expression pattern evidence suggests that it is derived from duplications of *Crry* (2). We propose that these receptors accomplish three tasks. These receptors provide an approximately 190,000 Dalton complement receptor on their B cells and FDCs with a C3 convertase regulatory function (Cr1/CR1), a C3d binding receptor on their B cells (Cr2/CR2), and general cell surface C3 convertase regulator on all cell types (CRRY/CR1). The importance of the individual activities of Cr1 and Cr2, in light of these receptor similarities, suggests important functions of each are paralleled in humans. To determine how these receptors independently function in humoral immune responses, the *Cr1KO* and *Cr2KO* mice were generated.

Characterization of the *Cr2KO* mouse in Chapter 2 revealed the presence of a previously unknown splicing control mechanism present within *Cr2*. Introduction of the SCR1-8 encoding exons into the genome without introns was meant to eliminate Cr1 expression of Cr2 and, in turn, force expression of Cr1 (Figure 2.1a). The resulting mouse no longer produced Cr2 but produced considerably less Cr1 and a new iCr2 protein as well. Immunoprecipitation of the *Cr2* gene products with antibodies that are known to block C3d binding to Cr2 were unable to bind iCr2, suggesting that iCr2 likely does not bind C3 ligands (Figure 2.3a and b). The deletion of the C3d binding site along with the maintenance of Cr1 expression means that the *Cr2KO* mouse is still functionally deficient in only Cr1. However, the loss of Cr1 expression on FDCs and reduction in overall Cr1 suggests that the strain's utility will be limited to relatively specific situations, such as analysis of *Cr2KO* B cells in the context of WT FDCs.

Analysis of *Cr2* expression in these mice did, however, demonstrate the importance of the SCR1-8 encoding exons in controlling splicing. When the introduced

sequence is viewed in the context of the genomic DNA removed in the *Cr1KO*, it seems likely that a sequence within the exons encoding SCR1-8 is the only sequence present in WT and *Cr2KO* (Figure 2.8). In the case of the *Cr2KO*, removing the introns must position splicing machinery within the region of the fusion (asterisk and arc in Figure 2.8). The machinery now splices to the next available junction and actively excises the SCR1-8 construct as a giant intron. The direct mechanism by which this is occurring is still an open question, but strongly suggests that future attempts at deletion of Cr2 from the *Cr2* gene should take into account a better understanding of the splicing control involved in generating Cr2. These data also suggest that the feasibility of generating a *Cr2KO* without causing reductions in *Cr2* expression may be significantly more difficult than predicted.

In addition to the new understanding of Cr2 expression suggested in Chapter 2 a novel Cr1 expression pattern was discovered and described in Chapter 3 (Figure 3.5 and 3.6). Despite the widely accepted use of Cr1 as an FDC-specific marker capable of defining FDCs in a field of B cells, Cr1 and Cr2 were assumed to be expressed evenly among the two cell types. I have shown here that Cr1 and Cr2 are expressed unequally on B cells and FDCs. B cell expression of Cr1 is not insignificant but they express Cr2 in excess of Cr1. FDCs on the other hand express large quantities Cr1 and hardly any Cr2 (Figure 3.6). The implications of this expression profile are tremendous considering the role of complement receptors in FDC retention of antigen. This difference in expression provides support for our hypothesis that Cr1 and Cr2 have individual roles. The predominance of Cr1 on FDCs also generated the major question for the investigation of the role of Cr1 in GC reactions in Chapters 3 and 4.

Cr1-deficiency and B Cells

Consistent with the FDC bias in Cr1 expression, the effects of Cr1-deficiency on B cells were found to be minor in most cases. In many cases, differences between *Cr1/2KO* and WT mice were ameliorated in the *Cr1KO* mouse. Among these phenotypic recoveries are the full WT expansion of B1a populations in the peritoneal cavity (Figure 3.3), the full WT production of serum immunoglobulin titers in naïve mice (Figure 3.7), a WT response to the TI-2 antigen DNP-Ficoll (Figure 3.9a), and initial GC B cell expansion (Figure 4.1). The lone results suggesting that B cells are not normal in the absence of Cr1 were found in the analysis of the titers of natural antibody. The natural antibody repertoire, as assessed by three known epitopes, was determined to be significantly reduced in two of the three (Figure 3.8). However, in total, nearly every measure of B cell function revealed a WT state or response. These data are strongly supported by the Cr1 expression data, and caused us to generate a hypothesis that Cr1 is required for proper GC formation and output.

Cr1-deficiency and GCs

The importance of *Cr2* gene products for the retention of antigen within follicles has long been known. In light of the data demonstrating the predominance of Cr1 by FDC and the minimal effects of Cr1 deficiency on B cell functions, we reasoned that the function of Cr1 is critically important for FDC function. Therefore, experiments were undertaken in order to investigate the role of Cr1 in TD B cell responses, which proceed through an FDC coordinated GC reaction. Immunizations with TD antigens demonstrated reductions in antigen-specific IgM and in one case, antigen-specific IgG3 (Figure 3.9).

These effects suggest a B cell intrinsic effect of Cr1-deficiency; however, analysis of GC B cell formation after SRBC immunization identified a reduction in the percentage of GC B cells. In order to understand the GC-independent versus GC-dependent discrepancy suggested by the antibody titer data and GC B cell reductions, a more detailed analysis of GC B cells was performed. This time course analysis of GC B cell formation revealed that GC B cells expanded normally during the initial phase up to about 7 days, but then was not maintained over the next 6 days (Figure 4.1a and b). Follow up bone marrow chimera experiments between WT and *Cr1KO* demonstrated that the GC B cell reduction was not affected by Cr1 deficiency on B cells but rather was completely dependent on FDC expression of Cr1 (Figure 4.2a and b). Together, these experiments demonstrated the importance of Cr1 on FDC for GC B cell biology. However, it is surprising that when considering the two readouts of B cell function, antibody production (Figure 3.9 and 4.4) and memory B cell generation (Figure 4.5), the former exhibits a strikingly WT phenotype across a range of immunogens. The current model does not easily describe these contrasting results. The time course data of GC B cells may provide the best insight into what may be occurring. These data suggest a model in which plasma cell versus memory B cell output is regulated temporally. I propose that early GC B cells are more frequently determined to become plasma cells while transitioning to a memory B cell differentiation pathway later. In terms of an infection, it is easy to imagine the benefits that this temporal switch would provide. Memory B cells are critical for future protection but if an organism does not survive, an initial infection memory is not necessary. I propose that it would be advantageous for the earliest GC B cells to be determined to make antibody producing plasma cells in order to most effectively neutralize an infection.

Additionally, with antigen retained by Cr1 on FDCs, the pressure to produce memory would not truly arise for a number of weeks when antibody titers had retracted. A temporal switch model is not without precedent. A study analyzing the emergence of plasma cells and memory B cells into the peripheral blood after immunization with the tetanus toxin vaccine (3-5) found that plasma cells emerged first around 6 days following immunization and were then followed by the appearance of memory cells at eight dpi. Additional studies will be necessary to fully test the temporal model of early preference for plasma cells, and the temporal differences in *Cr1KO* GC B cell reductions will provide an ideal tool for answering this question.

The significant reduction in antigen-specific IgM and IgM memory cells may be exacerbated by the reduction in GC B cells, but they are unlikely the result of the GC B cell reduction (Figure 3.9 and 4.4). Two models could explain the IgM deficiency. The first model is that strong, inappropriate complement activation on the B cell surface reduces B cell responses. The second model is that the now enhanced expression of Cr2 (Figure 3.1) on the B cell surface provides an excess of signaling that shunts the responding B cells to GCs. The first of these is an attractive explanation because it explains why Cr1 is on B cells and supports previous findings (3, 4, 6). This model inherently relies on differential complement activation of the various antigens used (TNP-LPS, DNP-Ficoll, TNP-KLH, SRBCs, and APC); or that complement activation generates products that disrupt T cell responses (such as C3a). The generally stronger complement activation generated by proteins (6-8) is in agreement with the presence of antigen-specific IgM reductions associated strongly with protein antigen immunization. In the second model, I propose that B cells receive such a strong Cr2 signal along with

BCR signaling that they are quickly recruited or differentiated into fates other than IgM secreting plasma cells. The possibilities could include becoming a GC B cell or jumping to production of antigen-specific IgG, leaving the impression of a reduction in IgM. In fact, some of the 5 dpi with SRBC GC B cell analyses revealed that the highest percentage of Fas^+ $GL7^+$ cells came from *Cr1KO* mice and not WT (data not shown). However, this trend was not reflective of an overall significant excess of total GC B cells. Additional evidence for slightly over-activated B cells was, however, suggested in some other data such as the naïve antibody titers (Figure 3.7) and TI-1 antibody responses (Figure 3.S3a). Bone marrow chimera experiments will better identify the source of these deficiencies, but the evidence supports a function for Cr1, specifically in the early B cell response to protein (TD) antigens. Simply because the most extensive B cell response effects are in the IgM population does not necessarily exclude a FDC or GC-dependent mechanism. The extent of the FDCs' contribution to initial antigen encounter by B cells is still not fully understood, and some IgM memory B cells are generated through GC-dependent mechanisms (9). In some cases, these cells even undergo some limited affinity maturation (7, 8).

Concluding Remarks

The work described here was undertaken to generate two new tools: the *Cr1KO* and *Cr2KO* mice. These mice were designed to specifically identify the necessary functions of Cr1 and Cr2, while avoiding the disadvantages of the existent *Cr1/2KO* mouse. Unforeseen changes in the expression of complement receptor products from the *Cr2* gene in the *Cr2KO* suggested that poorly understood splicing mechanisms were

inappropriately disrupted. In contrast, the *Cr1KO* mouse is not only a tool to study the roles of Cr1, but the effects seen on GC B cells suggest that it will invaluable in the investigation of GCs. In these foundational studies of murine Cr1, I have demonstrated Cr2-independent roles for Cr1. These studies include the central findings of this dissertation, the defining of the FDC preference for Cr1 expression, and the extensive data demonstrating that while *Cr1KO* B cells are generally no different than WT, FDC-dependent B cell functions were strongly affected. These data also demonstrated a role for Cr1 in the generation of IgM^+ and IgM^- memory B cells. These findings support the hypothesis that Cr1 is expressed on FDCs for the cultivation of GC B cell responses and GC output. The absence of a difference in antigen-specific IgG in response to many TD antigens suggests that the GC B cell reductions do not affect all GC-derived populations equally. These data along with GC B cell time course data suggest a temporal switch for fate determination of plasma cells and memory B cells. The *Cr1KO* will be useful in testing this hypothesis as well as the significant outstanding questions about the importance of FDC antigen retention for GC biology. Additionally, the limited but not absent nature of GC B cells raises questions about the extent to which a limited number GC B cells fill effector niches and the inhibition (or possibly enhancement) of GC B cell affinity maturation within these GCs.

Finally, I propose that Cr1 on FDCs is directly analogous to CR2L on human FDCs. Both receptors share a near exclusivity of expression on FDCs and both are the larger variant of their respective *Cr2* genes. These parallels suggest similar roles for the two in humoral immunity. Targeting of FDC expressed Cr is a strategy for enhancement of vaccines that has been previously suggested by members of the Cr field, specifically

by the Lycke group (10). The ubiquity of Cr2/CR2S expressing B cells in the vicinity of FDCs in both organisms suggests the targeting of vaccines specifically to Cr1/CR2L would produce a more specific targeting of antigen to FDCs. The use of the *Cr1KO* to elucidate the functions for which this targeting may be exploited will be invaluable.

References

1. Fearon, D. T., and R. H. Carter. 1995. The CD19/CR2/TAPA-1 complex of B lymphocytes: linking natural to acquired immunity. *Annu. Rev. Immunol.* 13: 127–149.

2. Jacobson, A. C., and J. Weis. 2008. Comparative functional evolution of human and mouse CR1 and CR2. *J. Immunol.* 181: 2953–2959.

3. Jacobson, A. C., J. J. Weis, and J. Weis. 2008. Complement receptors 1 and 2 influence the immune environment in a B cell receptor-independent manner. *J. Immunol.* 180: 5057–5066.

4. Seregin, S. S., Y. A. Aldhamen, D. M. Appledorn, N. J. Schuldt, A. J. McBride, M. Bujold, S. S. Godbehere, and A. Amalfitano. 2009. CR1/2 is an important suppressor of Adenovirus-induced innate immune responses and is required for induction of neutralizing antibodies. *Gene Ther.* 16: 1245–1259.

5. Odendahl, M., H. Mei, B. F. Hoyer, A. M. Jacobi, A. Hansen, G. Muehlinghaus, C. Berek, F. Hiepe, R. Manz, A. Radbruch, and T. Dörner. 2005. Generation of migratory antigen-specific plasma blasts and mobilization of resident plasma cells in a secondary immune response. *Blood* 105: 1614–1621.

6. Bjerre, A., B. Brusletto, T. E. Mollnes, E. Fritzsønn, E. Rosenqvist, E. Wedege, E. Namork, P. Kierulf, and P. Brandtzaeg. 2002. Complement activation induced by purified Neisseria meningitidis lipopolysaccharide (LPS), outer membrane vesicles, whole bacteria, and an LPS-free mutant. *J. Infect. Dis.* 185: 220–228.

7. Dogan, I., B. Bertocci, V. Vilmont, F. Delbos, J. Mégret, S. Storck, C.-A. Reynaud, and J.-C. Weill. 2009. Multiple layers of B cell memory with different effector functions. *Nat. Immunol.* 10: 1292–1299.

8. Taylor, J. J., K. A. Pape, and M. K. Jenkins. 2012. A germinal center-independent pathway generates unswitched memory B cells early in the primary response. *J. Exp. Med.* 209: 597–606.

9. Taylor, J. J., M. K. Jenkins, and K. A. Pape. 2012. Heterogeneity in the differentiation and function of memory B cells. *Trends Immunol.* 33: 590–597.

10. Mattsson, J., U. Yrlid, A. Stensson, K. Schön, M. C. I. Karlsson, J. V. Ravetch, and N. Y. Lycke. 2011. Complement Activation and Complement Receptors on Follicular Dendritic Cells Are Critical for the Function of a Targeted Adjuvant. *J. Immunol.* 187(7): 3641-3652.